151

Advanced Path Generator for Computer Numerical Control

by

Peter Orban

A Thesis
Submitted to the Faculty of Graduate Studies
in Partial Fulfillment of the Requirements
for the Degree of

Doctor of Philosophy

University of Manitoba
Department of Electrical and Computer Engineering
Winnipeg, Manitoba

ISBN 0-612-13422-9

Name _____

Dissertation Abstracts International is arranged by broad, general subject categories. Please select the one subject which most nearly describes the content of your dissertation. Enter the corresponding four-digit code in the spaces provided.

INDUSTRIAL ENGINEERING — SUBJECT TERM

0546 — SUBJECT CODE

U·M·I

Subject Categories

THE HUMANITIES AND SOCIAL SCIENCES

COMMUNICATIONS AND THE ARTS
Architecture 0729
Art History 0377
Cinema 0900
Dance 0378
Fine Arts 0357
Information Science 0723
Journalism 0391
Library Science 0399
Mass Communications 0708
Music 0413
Speech Communication 0459
Theater 0465

EDUCATION
General 0515
Administration 0514
Adult and Continuing 0516
Agricultural 0517
Art 0273
Bilingual and Multicultural 0282
Business 0688
Community College 0275
Curriculum and Instruction 0727
Early Childhood 0518
Elementary 0524
Finance 0277
Guidance and Counseling 0519
Health 0680
Higher 0745
History of 0520
Home Economics 0278
Industrial 0521
Language and Literature 0279
Mathematics 0280
Music 0522
Philosophy of 0998
Physical 0523
Psychology 0525
Reading 0535
Religious 0527
Sciences 0714
Secondary 0533
Social Sciences 0534
Sociology of 0340
Special 0529
Teacher Training 0530
Technology 0710
Tests and Measurements 0288
Vocational 0747

LANGUAGE, LITERATURE AND LINGUISTICS
Language
- General 0679
- Ancient 0289
- Linguistics 0290
- Modern 0291

Literature
- General 0401
- Classical 0294
- Comparative 0295
- Medieval 0297
- Modern 0298
- African 0316
- American 0591
- Asian 0305
- Canadian (English) 0352
- Canadian (French) 0355
- English 0593
- Germanic 0311
- Latin American 0312
- Middle Eastern 0315
- Romance 0313
- Slavic and East European 0314

PHILOSOPHY, RELIGION AND THEOLOGY
Philosophy 0422
Religion
- General 0318
- Biblical Studies 0321
- Clergy 0319
- History of 0320
- Philosophy of 0322

Theology 0469

SOCIAL SCIENCES
American Studies 0323
Anthropology
- Archaeology 0324
- Cultural 0326
- Physical 0327

Business Administration
- General 0310
- Accounting 0272
- Banking 0770
- Management 0454
- Marketing 0338

Canadian Studies 0385
Economics
- General 0501
- Agricultural 0503
- Commerce-Business 0505
- Finance 0508
- History 0509
- Labor 0510
- Theory 0511

Folklore 0358
Geography 0366
Gerontology 0351
History
- General 0578
- Ancient 0579
- Medieval 0581
- Modern 0582
- Black 0328
- African 0331
- Asia, Australia and Oceania 0332
- Canadian 0334
- European 0335
- Latin American 0336
- Middle Eastern 0333
- United States 0337

History of Science 0585
Law 0398
Political Science
- General 0615
- International Law and Relations 0616
- Public Administration 0617

Recreation 0814
Social Work 0452
Sociology
- General 0626
- Criminology and Penology ... 0627
- Demography 0938
- Ethnic and Racial Studies 0631
- Individual and Family Studies 0628
- Industrial and Labor Relations 0629
- Public and Social Welfare 0630
- Social Structure and Development 0700
- Theory and Methods 0344

Transportation 0709
Urban and Regional Planning 0999
Women's Studies 0453

THE SCIENCES AND ENGINEERING

BIOLOGICAL SCIENCES
Agriculture
- General 0473
- Agronomy 0285
- Animal Culture and Nutrition 0475
- Animal Pathology 0476
- Food Science and Technology 0359
- Forestry and Wildlife 0478
- Plant Culture 0479
- Plant Pathology 0480
- Plant Physiology 0817
- Range Management 0777
- Wood Technology 0746

Biology
- General 0306
- Anatomy 0287
- Biostatistics 0308
- Botany 0309
- Cell 0379
- Ecology 0329
- Entomology 0353
- Genetics 0369
- Limnology 0793
- Microbiology 0410
- Molecular 0307
- Neuroscience 0317
- Oceanography 0416
- Physiology 0433
- Radiation 0821
- Veterinary Science 0778
- Zoology 0472

Biophysics
- General 0786
- Medical 0760

EARTH SCIENCES
Biogeochemistry 0425
Geochemistry 0996
Geodesy 0370
Geology 0372
Geophysics 0373
Hydrology 0388
Mineralogy 0411
Paleobotany 0345
Paleoecology 0426
Paleontology 0418
Paleozoology 0985
Palynology 0427
Physical Geography 0368
Physical Oceanography 0415

HEALTH AND ENVIRONMENTAL SCIENCES
Environmental Sciences 0768
Health Sciences
- General 0566
- Audiology 0300
- Chemotherapy 0992
- Dentistry 0567
- Education 0350
- Hospital Management 0769
- Human Development 0758
- Immunology 0982
- Medicine and Surgery 0564
- Mental Health 0347
- Nursing 0569
- Nutrition 0570
- Obstetrics and Gynecology .. 0380
- Occupational Health and Therapy 0354
- Ophthalmology 0381
- Pathology 0571
- Pharmacology 0419
- Pharmacy 0572
- Physical Therapy 0382
- Public Health 0573
- Radiology 0574
- Recreation 0575
- Speech Pathology 0460
- Toxicology 0383

Home Economics 0386

PHYSICAL SCIENCES
Pure Sciences
Chemistry
- General 0485
- Agricultural 0749
- Analytical 0486
- Biochemistry 0487
- Inorganic 0488
- Nuclear 0738
- Organic 0490
- Pharmaceutical 0491
- Physical 0494
- Polymer 0495
- Radiation 0754

Mathematics 0405
Physics
- General 0605
- Acoustics 0986
- Astronomy and Astrophysics 0606
- Atmospheric Science 0608
- Atomic 0748
- Electronics and Electricity 0607
- Elementary Particles and High Energy 0798
- Fluid and Plasma 0759
- Molecular 0609
- Nuclear 0610
- Optics 0752
- Radiation 0756
- Solid State 0611

Statistics 0463

Applied Sciences
Applied Mechanics 0346
Computer Science 0984
Engineering
- General 0537
- Aerospace 0538
- Agricultural 0539
- Automotive 0540
- Biomedical 0541
- Chemical 0542
- Civil 0543
- Electronics and Electrical 0544
- Heat and Thermodynamics ... 0348
- Hydraulic 0545
- Industrial 0546
- Marine 0547
- Materials Science 0794
- Mechanical 0548
- Metallurgy 0743
- Mining 0551
- Nuclear 0552
- Packaging 0549
- Petroleum 0765
- Sanitary and Municipal 0554
- System Science 0790

Geotechnology 0428
Operations Research 0796
Plastics Technology 0795
Textile Technology 0994

PSYCHOLOGY
General 0621
Behavioral 0384
Clinical 0622
Developmental 0620
Experimental 0623
Industrial 0624
Personality 0625
Physiological 0989
Psychobiology 0349
Psychometrics 0632
Social 0451

Nom _____

Dissertation Abstracts International est organisé en catégories de sujets. Veuillez s.v.p. choisir le sujet qui décrit le mieux votre thèse et inscrivez le code numérique approprié dans l'espace réservé ci-dessous.

_____ ☐☐☐ U·M·I

SUJET — CODE DE SUJET

Catégories par sujets

HUMANITÉS ET SCIENCES SOCIALES

COMMUNICATIONS ET LES ARTS
Architecture 0729
Beaux-arts 0357
Bibliothéconomie 0399
Cinéma 0900
Communication verbale 0459
Communications 0708
Danse 0378
Histoire de l'art 0377
Journalisme 0391
Musique 0413
Sciences de l'information 0723
Théâtre 0465

ÉDUCATION
Généralités 515
Administration 0514
Art 0273
Collèges communautaires 0275
Commerce 0688
Économie domestique 0278
Éducation permanente 0516
Éducation préscolaire 0518
Éducation sanitaire 0680
Enseignement agricole 0517
Enseignement bilingue et multiculturel 0282
Enseignement industriel 0521
Enseignement primaire. 0524
Enseignement professionnel 0747
Enseignement religieux 0527
Enseignement secondaire 0533
Enseignement spécial 0529
Enseignement supérieur 0745
Évaluation 0288
Finances 0277
Formation des enseignants 0530
Histoire de l'éducation 0520
Langues et littérature 0279
Lecture 0535
Mathématiques 0280
Musique 0522
Orientation et consultation 0519
Philosophie de l'éducation 0998
Physique 0523
Programmes d'études et enseignement 0727
Psychologie 0525
Sciences 0714
Sciences sociales 0534
Sociologie de l'éducation 0340
Technologie 0710

LANGUE, LITTÉRATURE ET LINGUISTIQUE
Langues
- Généralités 0679
- Anciennes 0289
- Linguistique 0290
- Modernes 0291

Littérature
- Généralités 0401
- Anciennes 0294
- Comparée 0295
- Médiévale 0297
- Moderne 0298
- Africaine 0316
- Américaine 0591
- Anglaise 0593
- Asiatique 0305
- Canadienne (Anglaise) 0352
- Canadienne (Française) 0355
- Germanique 0311
- Latino-américaine 0312
- Moyen-orientale 0315
- Romane 0313
- Slave et est-européenne 0314

PHILOSOPHIE, RELIGION ET THÉOLOGIE
Philosophie 0422
Religion
- Généralités 0318
- Clergé 0319
- Études bibliques 0321
- Histoire des religions 0320
- Philosophie de la religion 0322

Théologie 0469

SCIENCES SOCIALES
Anthropologie
- Archéologie 0324
- Culturelle 0326
- Physique 0327

Droit 0398
Économie
- Généralités 0501
- Commerce-Affaires 0505
- Économie agricole 0503
- Économie du travail 0510
- Finances 0508
- Histoire 0509
- Théorie 0511

Études américaines 0323
Études canadiennes 0385
Études féministes 0453
Folklore 0358
Géographie 0366
Gérontologie 0351
Gestion des affaires
- Généralités 0310
- Administration 0454
- Banques 0770
- Comptabilité 0272
- Marketing 0338

Histoire
- Histoire générale 0578
- Ancienne 0579
- Médiévale 0581
- Moderne 0582
- Histoire des noirs 0328
- Africaine 0331
- Canadienne 0334
- États-Unis 0337
- Européenne 0335
- Moyen-orientale 0333
- Latino-américaine 0336
- Asie, Australie et Océanie 0332

Histoire des sciences 0585
Loisirs 0814
Planification urbaine et régionale 0999
Science politique
- Généralités 0615
- Administration publique 0617
- Droit et relations internationales 0616

Sociologie
- Généralités 0626
- Aide et bien-être social 0630
- Criminologie et établissements pénitentiaires 0627
- Démographie 0938
- Études de l' individu et de la famille 0628
- Études des relations interethniques et des relations raciales 0631
- Structure et développement social 0700
- Théorie et méthodes. 0344
- Travail et relations industrielles 0629

Transports 0709
Travail social 0452

SCIENCES ET INGÉNIERIE

SCIENCES BIOLOGIQUES
Agriculture
- Généralités 0473
- Agronomie. 0285
- Alimentation et technologie alimentaire 0359
- Culture 0479
- Élevage et alimentation 0475
- Exploitation des pâturages 0777
- Pathologie animale 0476
- Pathologie végétale 0480
- Physiologie végétale 0817
- Sylviculture et faune 0478
- Technologie du bois 0746

Biologie
- Généralités 0306
- Anatomie 0287
- Biologie (Statistiques) 0308
- Biologie moléculaire 0307
- Botanique 0309
- Cellule 0379
- Écologie 0329
- Entomologie 0353
- Génétique 0369
- Limnologie 0793
- Microbiologie 0410
- Neurologie 0317
- Océanographie 0416
- Physiologie 0433
- Radiation 0821
- Science vétérinaire 0778
- Zoologie 0472

Biophysique
- Généralités 0786
- Medicale 0760

SCIENCES DE LA TERRE
Biogéochimie 0425
Géochimie 0996
Géodésie 0370
Géographie physique 0368
Géologie 0372
Géophysique 0373
Hydrologie 0388
Minéralogie 0411
Océanographie physique 0415
Paléobotanique 0345
Paléoécologie 0426
Paléontologie 0418
Paléozoologie 0985
Palynologie 0427

SCIENCES DE LA SANTÉ ET DE L'ENVIRONNEMENT
Économie domestique 0386
Sciences de l'environnement 0768
Sciences de la santé
- Généralités 0566
- Administration des hôpitaux 0769
- Alimentation et nutrition 0570
- Audiologie 0300
- Chimiothérapie 0992
- Dentisterie 0567
- Développement humain 0758
- Enseignement 0350
- Immunologie 0982
- Loisirs 0575
- Médecine du travail et thérapie 0354
- Médecine et chirurgie 0564
- Obstétrique et gynécologie 0380
- Ophtalmologie 0381
- Orthophonie 0460
- Pathologie 0571
- Pharmacie 0572
- Pharmacologie 0419
- Physiothérapie 0382
- Radiologie 0574
- Santé mentale 0347
- Santé publique 0573
- Soins infirmiers 0569
- Toxicologie 0383

SCIENCES PHYSIQUES
Sciences Pures
Chimie
- Généralités 0485
- Biochimie 487
- Chimie agricole 0749
- Chimie analytique 0486
- Chimie minérale 0488
- Chimie nucléaire 0738
- Chimie organique 0490
- Chimie pharmaceutique 0491
- Physique 0494
- PolymÈres 0495
- Radiation 0754

Mathématiques 0405
Physique
- Généralités 0605
- Acoustique 0986
- Astronomie et astrophysique 0606
- Électronique et électricité 0607
- Fluides et plasma 0759
- Météorologie 0608
- Optique 0752
- Particules (Physique nucléaire) 0798
- Physique atomique 0748
- Physique de l'état solide 0611
- Physique moléculaire 0609
- Physique nucléaire 0610
- Radiation 0756

Statistiques 0463

Sciences Appliqués Et Technologie
Informatique 0984
Ingénierie
- Généralités 0537
- Agricole 0539
- Automobile 0540
- Biomédicale 0541
- Chaleur et thermodynamique 0348
- Conditionnement (Emballage) 0549
- Génie aérospatial 0538
- Génie chimique 0542
- Génie civil 0543
- Génie électronique et électrique 0544
- Génie industriel 0546
- Génie mécanique 0548
- Génie nucléaire 0552
- Ingénierie des systèmes 0790
- Mécanique navale 0547
- Métallurgie 0743
- Science des matériaux 0794
- Technique du pétrole 0765
- Technique minière 0551
- Techniques sanitaires et municipales 0554
- Technologie hydraulique 0545

Mécanique appliquée 0346
Géotechnologie 0428
Matières plastiques (Technologie) 0795
Recherche opérationnelle 0796
Textiles et tissus (Technologie) 0794

PSYCHOLOGIE
Généralités 0621
Personnalité 0625
Psychobiologie 0349
Psychologie clinique 0622
Psychologie du comportement 0384
Psychologie du développement 0620
Psychologie expérimentale 0623
Psychologie industrielle 0624
Psychologie physiologique 0989
Psychologie sociale 0451
Psychométrie 0632

ADVANCED PATH GENERATOR FOR COMPUTER NUMERICAL CONTROL

BY

PETER ORBAN

A Thesis submitted to the Faculty of Graduate Studies of the University of Manitoba in partial fulfillment of the requirements of the degree of

DOCTOR OF PHILOSOPHY

Abstract

The advent of commercially available CAD systems has provided the means for designing sophisticated parts, but producing those parts on existing machining systems is still complicated, time consuming and prone to errors.

The free-form shapes designed on CAD systems are described by higher order polynomials, but state-of-the-art controllers can generate only lines and arcs. In practice, the tool paths for sculptured surfaces are approximated by a series of lines, where the number of lines is based on the accuracy required. This method needs many steps, produces large NC programs, and the parts still need considerable hand finishing. If NC controllers could "understand" and generate motion commands for higher order curves, then parts could be produced with a better finish, less intermediate data, and fewer processing steps.

In this thesis, the design and verification of a real-time path generator module for a Computer Numerical Controller for machining sculptured surfaces is presented. The advanced path generator produces the individual axis commands directly from surface geometry descriptions for non uniform rational spline (NURBS) surfaces, from tool data, and from part set-up data. NURBS are rational generalization of piecewise polynomials hence include B-splines, Bézier curves and surfaces and Coons patches. Both the 3-axis and 5-axis versions are modeled and simulated for various types of tools. Existing speed control schemas control the speed of the tool center point, resulting in

speed variation in the contact point. In this thesis accurate speed control of the path generation has been established as well.

Acknowledgments

This thesis represents my Ph. D. dissertation and covers, in part, research supported by the National Research Council of Canada.

Beside gratefully acknowledging the support of my supervisor, Dr. M. Barakat, I would like to thank the contribution of my supervisory committee, Dr. W. Lehn and Dr. D. Walton, by their many excellent comments. Special thanks are due to Dr. D. Gospodnetic, the external examiner, who also suggested many improvements.

I also would like to recognize the help given to me by my colleagues at NRC, who contributed to the initial implementation of the results of this research.

Finally, I would like to express my appreciation to my family for their patience, understanding, and support.

Table of Contents

List of Figures

List of Tables

1 Introduction

Producing parts with sculptured surfaces in the manufacturing industry has an ever increasing importance. These parts have to satisfy several requirements beyond their functionality, such as aesthetics, shape continuity, flow characteristics, etc. The application of such parts where shape and function are so closely integrated is widespread in the aerospace, car and ship building industries as well as tool and mold making industries. Their usage in various consumer products is also increasing [Krouse-83, Rogers-83, Renner-78, Giessen-86a].

The advent of commercially available CAD/CAE systems has provided the means for designing sophisticated parts, but producing these parts on existing machining systems is still complicated, time consuming and prone to errors. When machining is used for parts manufacturing, the process from design to finished product with metal cutting processes consists of about 5 layers of information processing [Strohmer-86, Grossman-86].

The reasons for the cumbersome part production are mostly historical. Firstly, the design and production of such parts includes many disciplines. This has been hindering the efforts to look at the design and production as an integrated process, and emphasis was instead placed on the individual levels and their interfaces within the production process [Krouse-83].

Secondly, the basic principles of NC machines and their programming have not changed much since the fifties, when they were originally laid down [Noble-84]. NC machines still generate line segments, arcs in the main planes, and their combinations. When machining higher order surfaces, they are

approximated by primitives that NC machines can execute, usually only by line segments. This feature of NC controllers sets the level of abstraction of data in the production process. As a result, the intermediate data passed between the layers are huge, and parts still need significant effort in hand finishing [Broomhead-86].

If the level of data abstraction could be raised, i.e. NC controllers could "understand" and generate higher level motion commands, then parts with sculptured surfaces could be produced with fewer processing steps, less intermediate data, and a better finish.

This thesis discusses an improved path generator for NC controllers, that moves the tool directly on a sculptured surface without approximating it with line segments. By using a "more intelligent" controller in the production, the process itself could be simplified, the individual tasks redistributed more logically, the intermediate data reduced, and the part quality improved. In other words, the production of parts would be faster and cheaper with better quality.

In the second chapter the existing technology is reviewed. The current machining practices for parts with sculptured surfaces are examined. The individual steps are evaluated and their importance is analyzed. The existing architecture for the methods are discussed, and the shortcomings of the solutions are highlighted.

Having examined the state-of-art of production practices, existing solutions and research are then surveyed in Section 2 of Chapter 2. At the end of that section, the reviewed systems are evaluated, highlighting the need for further advancements in the area of real-time tool path generation.

In the third chapter, the foundations of sculptured surface machining are outlined. This includes the theory of geometric modeling, with the mathematics of different curve and surface representation, and the different machining strategies in use.

Chapter 4 discusses the advanced tool path generation in detail.

In Section 1 of Chapter 4, the mathematics of 3-axis and 5-axis machining are developed, and the calculations to control the axis coordinates for the sculpturing of free-form shapes are put forth.

The system specification and a critical evaluation thereof are discussed in Section 2 of Chapter 4.

In Section 3 of Chapter 4, the particulars of real time path generation are presented. Simulation examples are given, and the results are assessed.

The thesis finishes with a conclusion, summarizing the results and findings, outlining the direction of further research in the field, and providing the first results of an industrial implementation of the work.

2 Existing Technology

In this part of the thesis, state of the art of the technology is explored and how it relates to sculptured surface part production. This includes the discussion and evaluation of existing methodologies of producing parts with sculptured surfaces (Section 1), and a literature survey and discussion on the current research in the field (Section 2).

2.1 Sculptured Surface Part Production

Producing a part with sculptured surfaces is a complex task. However these days, the process is aided by computers at all steps of the design and production (CAD/CAM), the existing design and machining systems are still complicated, and the process is time consuming and prone to human errors.

In this chapter, current manufacturing practices are critically reviewed and evaluated.

2.1.1 Review

The procedure starts with the designed part. The geometry of parts with sculptured surfaces has to satisfy several design criteria such as functionality and aesthetics, to name a few.

Today there are a multitude of CAD/CAE systems, aiding the user in the design and analysis of a part and in the creation of the geometry of it [Daratech-89]. Proceeding with the design depends on the CAD/CAE system used. Some are general purpose, where the surfaces have to be built up hierarchically (points, curves, surfaces), while other CAD systems are application oriented, hiding some of the elementary steps from the user. Objects in a geometrical data base can be represented in several ways. The most commonly used form for free-form surfaces is piecewise patches of vector-scalar functions [Faux-79, Mortenson-85].

When the design in the CAD system is completed, the next step is to prepare for the machining of the part. This is where the CAM part of the CAD/CAM process starts.

First, the machining strategy has to be decided on. This includes the process selection (3D milling, 5D milling, turning, chemical machining, etc.), fixturing, and tool selection [Giessen-86a]. Usually a particular part can be produced in several ways. The planning of the machining strategy is heavily influenced by the existing technology and infrastructure in the machine shop.

In the conventional NC metal cutting processes, the tool path for the machining of the part has to be defined next. The machining of a part can be classified into two steps: the roughing process and the finishing. Depending on the part and the machining strategy applied, usually several set-ups are needed. Two sets of tool paths are generated to do the machining. The roughing processor generates programs to remove as much material from the block as possible in a simple and efficient way depending on the size of the

blank. Roughing programs are generally simple zig-zag motions along the main features of the part.

The finishing processor generates the tool path for the final contouring of the parts. Several main contouring methods can be distinguished for sculpting, but the most widely used are the 3-axis and 5-axis machining [Giessen-86a, Giessen-86b, Qiulin-87].

The tool paths for the machining programs are output in the language called Automatically Programmed Tools (APT). APT is a manufacturing language in which geometry and machining processes can be described [APT-77]. To generate the APT program for the machining, the tool geometry has to be given. The output tool path describes the tool end point coordinates. Though APT can describe higher order curves and surfaces, the tool motions to machine the sculptured surfaces are approximated by line segments. The resolution of the approximation depends on the machining tolerance required. There are several reasons to approximate the surface machining with line segments. The rationale is mostly historical: machine tool controllers can only generate line segments in 3D, and arc segments can only be created in the main planes. There are advantages associated with the line segment representation as well. One of them is that the output information is human readable: the basic element is a point, where the tool is supposed to go with the desired tool axis orientation. Another advantage has to do with efficiency: to display a tool path graphically on a work station geometric calculations do not have to be repeated and tool motion data can be taken directly from the APT file for display. This only had significance in the early days of CAD/CAM, when computing power for all kinds of calculations were

at a premium. Today's computers and workstations certainly would have no difficulty performing the more computationally intensive tasks.

In the next step, the high level APT program gets compiled into the Cutter Location (CL) file. The CL file is still machine tool independent. No information on the particular features of the machine tool or of its controller's are contained. The main task of the APT processor is to perform geometrical calculations related to the tool path generation [ICAM-88].

The machine tool dependent information is added to the part program at post processing time. Though the NC language is standardized, the physical features and other properties of machine tool systems differ from each other considerably [van den Berg-86]. All pertinent information on the particular machine tool and its controller is contained in the post processor. Post processors are dedicated to specific machine tools. The output from the post processor is the NC tape, which can be run on the machine tool.

The last step of the whole procedure is the actual machining. The machining includes the setting up of the part and the cutting tools and running the previously generated NC programs. Setting up the part and the tools is an important step; it inherently influences the accuracy of the produced part. When machining sculptured surfaces, the set up has to be done very accurately to the predetermined values, i.e. the values that were used for geometrical calculations during the course of the NC tape preparations [van den Berg-88]. This contrasts sharply with conventional, non free-form machining, where tool and part offset values can be entered into the NC controller before machining, and the compensation calculated and applied run-time by the NC controller [Venjara-93].

2.1.2 Evaluation

It can be seen from the description of the free-form machining process that it is complicated, the preparation for the machining is time consuming and prone to errors.

The goal in the production is to reduce costs and lead times, and to have the first finished part right, without a lot of human expertise and supervision [MOSAIC-90].

There are several problems associated with the production process described above.

First of all, the process has far too many steps, or in other words, the system which produces the parts has too many layers. The information passed between the layers is in some "standard" file format [Ogorek-85]. Difficulty arises as each vendor has its own implementation and interpretation of the various standards, requiring further customized filtering and conversion between the layers [van den Berg-86]. Debugging the production process is difficult, the source of errors is not always obvious, and it is difficult to pin down at which step the error originated.

Researchers have realized this deficiency, and called for a simpler system implementation [Greene-82, Grossman-86, Suzuki-86, Kim-88, Storr-89, Lee-91]. Most of the researchers have found that an optimal system would have three layers: the design, machining planning, and the actual machining function. Suzuki [Suzuki-86] suggested a two layer system: the design layer,

and a "super" NC controller, including all the functions for the machining planning and the metal cutting. Industry and researchers took this approach one step further and have produced systems including even the CAD functions into the controller, together with the machining preparation functions [Sharnoa-91, Yellowley-94]. Though this design and production of parts with sculptured surfaces, and doing 3D machining at the same station is impressive, the idea of using a complete machine tool for design purposes is questionable, and it is possibly worthwhile only to develop simple parts with limited design requirements or to make small changes to existing designs. The trend in today's controllers certainly points toward including the design and planning functions in to the controller of the machine tool, effectively creating a manufacturing workstation [MOSAIC-90, Bourne-92].

The information in the CL files and NC tape files, which contain the line segment approximation of the machining tool path, is very low level, and hence huge in size. Handling the huge data files is awkward, and usually special techniques have to be applied to overcome the limited storage capacity of the controllers [Orban-86].

Another problem associated with the line segment approximation is the block processing speed of NC controllers. As accuracy requirements of the parts are increasing, the number of line segments to cover the same path is increasing, and the controller has to process this increased number of line segments while executing at the same machining speed. Machining speeds are also on the increase due to better quality cutting tools, due to machine tools with good dynamic behavior at higher speeds, and due to the general demand for higher productivity. Though the block processing speeds of the

new controllers are faster and are approaching the millisecond rate [Heidenhain-91, Allen-Bradley-91], this is still a "brute force" approach. The solution would be to pass more concise, higher level information to the controller, and let the controller do the processing at run time.

Several researchers have suggested to pass geometrical information to the controller instead of passing just line segments [Greene-82, EUCLID-83a, Hermann-84a, Broomhead-86, Chen-93]. Early results of this research were included in a commercial system, the EUCLID/OZELOT. The system is a complete solution, including CAD, CAM and a modified Numatek 3000 machine tool controller for 3D free-form machining [EUCLID-83b, EUCLID-86].

Another deficiency of conventional sculptured surface part production is that tool and part set-up values for the machining have to be known in advance, well before the actual machining. There is nothing wrong with selecting the tool type and specifying the fixturing during the machining planning stage (actually, that should be part of the machining planning), but this selection should only be nominal. The actual values should be able to vary, as tools are sharpened repeatedly, inserts replaced, or different tools of the same nominal size are used, and parts fixtured on the machine tool without high precision. The minute deviations from the nominal values should be identified just before the actual cutting, and compensated for during the machining.

Many researchers have suggested and reported on moving postprocessing down to the machine tool level [Kochan-83, Pond-85, Broomhead-86]. Unfortunately, this can not be done under the present

circumstances for free-form machining, as the CL file does not have information in it on the contact point between the tool and the part. The CL file only describes the trajectory of the tool end point. When one machines parts with non sculptured surfaces, the contact point is known, and the tool compensation can be applied at the machine tool. There is an ongoing effort to overcome this problem for sculptured surface machining as well. The proposed solution is to include surface normal information in the CL file [ISO-91]. This would allow for the calculation of the contact point between the tool and the part, and hence for the run time tool offset calculation in the machine tool controller.

The sequence of line segments describing the sculptured surface tool path is only positionally continuous, the direction of the individual lines follow the surface. At the knot points, if the tool followed the path accurately, the acceleration of the motion would be infinite. In practice, this could bring about jerky motion of the machine tool, resulting in unwanted vibration, rough surface finish on the part, and excessive wear and tear in the machine tool. Machine tool operators routinely prevent this from occuring by reducing the machining speed. Realizing these problems, Qian suggests to calculate the line segments and feed speeds according to the geometry (curvature) of the tool path and dynamic features of the machine tool [Qian-93].

Yet another problem with conventional sculptured surface machining is that maintaining the machining speed accurately is a challenging task. At 3-axis machining, a ball nose cutter is employed. The contact point with the part where the actual cutting takes place, moves around the sphere end of the tool. In the NC commands, the end point of the tool is programmed and the speed

of the tool path refers to this point. When machining parts whose curvature is comparable to the radius of the tool, the speed of the contact point could change quite dramatically. With 5-axis machining, where the contact point does not change much, the speed programmed in the NC line does not represent the machining speed. Here the reason is that the part is being rotated to keep the proper tool orientation angle, and the tool has to move just to follow that point. Consequently, the programmed speed does not represent the relative, tool to part speed, i.e. the actual surface traversal (machining) speed.

In conclusion, it can be seen that the production of free-form parts would be best done in a system consisting of three layers: design, manufacturing planning and machining. For such a solution, a machine tool controller that understands surface geometric information as well as machining commands and generates the tool path directly on the surface would provide the machining layer. This would lead to an optimal task distribution among the layers with reduced amount of data. The machining would require reduced set-up time, and would result in parts with better finish than those of existing free-form machining practices.

2.2 Literature Survey

It was seen from the previous chapter, that present practices for producing parts with sculptured surface have many deficiencies. The problems are well known, and remedies are proposed from many directions.

In this Chapter, existing solutions for tool path generation for free-form shapes are reviewed and evaluated from the standpoint of addressing the previously discussed obstacles. The assessment covers commercial and experimental systems as well as research relating to individual fields of sculptured surface machining.

2.2.1 Review of Existing Solutions

There are many ways to generate trajectories for machining sculptured surfaces. The easiest approach from a system designers' standpoint is when the trajectories are approximated by line segments, and the calculations are done off-line. This is what most CAD/CAM systems do; the machining modules generate the approximating line segments for the surface machining. Alternatively, higher degree curves can be generated in the controller itself. This can be done in different ways: doing the approximation of the curves with line segments in real-time and executing them or calculating the direct movements for the curves and doing away with the run-time approximation. Existing solutions employ these techniques and their variations.

The early interpolators of numerical controllers were based on the principle of digital differential analyzers (DDA) [Sizer-68]. A DDA is basically the hardware solution of discretized differential equations. DDAs provided reasonable solutions for generating line and arc segments in the early NC controllers. Implementation was in hardware, using only ternary increments

(+1, 0, -1). Calculations such as multiplications and additions could be implemented in a very simple manner using only serial arithmetic. With increments different than ternary, more complex arithmetic is required. Theoretically curves of higher degrees could also be generated, but the DDA has its limitations which are more relevant at generating solutions for higher degree equations. DDAs are basically incremental devices, so the error accumulates during the calculations. The resolution of the data representation has to be selected in such a way that the accumulated error would still be less than the allowed value, even at the end of the longest path segment. Generating the same curve with increased resolution also meant the increase in the computational speed required. Continued development work on the DDA ensures that it still provides an attractive alternative for path generation in simple (by today's standards) machine tool controllers [Lim-92]. Qin and Bin has extended the DDA interpolator, so that it now also generates circular arcs in the space, not just in the main planes [Qin-90].

With the advent of microcomputers, designers of numerical controllers started to implement the interpolation functions in software. These solutions draw heavily from algorithms used for controlling peripheral devices for computers like plotters and displays. These algorithms focused on generating mostly arc segments and lines, and never looked at the problems of generating trajectories for sculptured surfaces [Bresenham-65, Danielsson-70, Bergren-71, Papaioannou-76, Orban-80a, Orban-80b, Okamoto-80, Masory-82, Chikurov-84]. With the arrival of digital signal processors, which brought increased computing power and floating point arithmetic, the

number of axes could be extended, and more precise control of the speed profile of the interpolation could be realized [Kim-91].

Several researchers looked at generating curves more general than the line and arc segments. Enlin describes an algorithm suitable for numerically controlled machines for higher order curve generation [Enlin-82]. The interpolation of the higher order curve is performed by the interpolation of straight lines which are in the tangential directions of the points on the curve. The algorithm is presented for third order curves. By selecting proper scaling, the calculations need only integer arithmetic. This solution lends itself well to hardware implementation. A weak point of the method is the variation of the speed along the path, depending on the trajectory. The author also described the extension of the algorithm for the generation of 4-th order curves.

Robot controllers were the first to use higher order curves for trajectory generation. For anthropomorphous robots, where the kinematics of the manipulator resembles a human arm (trunk, shoulder, elbow, wrist joints), the individual joints are controlled by complex trigonometric functions of the end coordinate. These joint coordinates are calculated according to the inverse kinematics of the manipulator [Paul-81, Snyder-85]. The joints, which have to move according to these trigonometric functions, are controlled with spline functions. The spline functions approximate the trigonometric joint trajectories. The end coordinate trajectory is divided up into segments, and at the segment points with the inverse kinematics, the individual joint coordinates are calculated. Through these joint coordinates, splines are constructed. Using third order splines, smooth acceleration of the

joints can be achieved [Lin-82, Edwall-82]. The accuracy of the trajectory generated depends on the number of intermediate points selected and on the path itself. There are two main strategies to implement the spline based path generation for the robots. In the first case, the intermediate points and the spline parameters are defined off-line, in advance, and the controller merely reproduces the trajectory. In the other strategy all the calculations are executed run-time. In this case, the trajectory can be modified on-line, adapting to the robots' changing environment. The first case requires less real-time computational efforts due to the off-line processing. The second solution provides more flexibility for the robot, allowing for real-time path modification with sensory input. Laflamme reported on a real-time implementation of the polynomial joint control for robots [Laflamme-85]. The solution used a master-slave architecture. The spline parameters were calculated in the master unit real-time and interpolating the trajectory was done by the slave processors. The robotic application was intended for polishing parts with sculptured surfaces, such as turbine blades.

Sata *et.al.* were the first to report on a system that machines sculptured surfaces with a true, real-time, higher degree interpolation method [Sata-81]. The "intelligent controller" they implemented does 3D machining on Bézier surfaces with ball nose cutters. Their solution is to implement an interpolator that generates third order Bézier curves. The control points of the curve are passed on to the controller for the path generation. The expression for the Bézier curve is turned into an incremental form. By carefully selecting the parameter step size, the expression can be calculated by simple additions and shift operations. The size of the selected step also defines the error bound for

the approximated expression. Sata uses two methods for the tool path calculation. In the first case, the tool path is generated on an offset surface. The surface machining is done along parameter lines. In this case, the tool path reduces to a simple third degree Bézier curve. This method is not feasible if the offset surface is not readily available when the shape of the part is already given. In this case, the authors prefer the tool compensation within the controller. For generating the tool offsets, they calculate the surface normals and offset points at 16 by 16 mesh points in the u, v parameter space. These points are simply connected with straight lines for the tool path. If this solution does not give the required accuracy, they suggest a hybrid method, where locally, in the region of question, a Bézier patch is constructed from the offset points, and the tool path is generated on that offset patch. Their experimental set-up consisted of a VAX 11/780 for the basic calculations for the tool path generation and an 8-bit microcomputer doing the real-time calculations and driving a conventional 3-axis machine tool with its controller in the Behind Tape Reader (BTR) mode.

In 1986, the same research group reported on the progress of the project [Haapaniemi-86]. Keeping the same principles as before [Sata-81], improvements are made in the hardware implementation, better user interface and utilities are provided for the machine tool operator. The controller implementation is a multiprocessor architecture with color monitor operator's panel. Utilities help the operator to verify the tool path by simulation and collision checking.

Researchers at the Computer and Automation Institute in Hungary have been developing and documenting an integrated system for sculptured

surface part production since the late seventies [Renner-78, Gaal-81, Varady-82, Hermann-84a, Hermann-84b, Hermann-88]. The system developed is a comprehensive CAD/CAM system with geometric design, machining planning, and optional machine tool controller modules. The CAD system is a surface based modeler, allowing for several kind of curve and surface creation methods: Ferguson, B-spline, Renner and a heuristic algorithm were implemented. The underlying uniform surface representation is done by bicubic Coons patches. The technological modules include a 2.5D roughing processor and 3-axis and 5-axis finishing processors. One of the options of the system is a CNC controller that generates higher order curves in real-time. The controller is the extension of a "conventional" CNC controller with a hardware DDA interpolator. A preprocessor is added to the system, which interprets the higher order curve descriptions and approximates them by line segments in real-time. The interpolator of the CNC executes the approximating line segments, thus generating the higher order curves. The input language of the controller was expanded, adding new G-codes for the description of B-spline vertices and knot points. The researchers demonstrated the operation of the system in 2D on a lathe machine. For the 3D milling machine controller, a multiprocessor architecture was planned. It is interesting to note that for the 3D surface machining run-time collision checking was also planned.

The first commercial offering of the sculptured surface machining technology, an integrated CAD/CAM system with a CNC controller executing higher order curves, was offered by the Swiss FIDES company [EUCLID-83a, EUCLID-83b, EUCLID-86]. Their EUCLID/OZELOT system is the product of a

consortium, the cooperation of a manufacturing research institute, a system house, and a controller manufacturer. The EUCLID CAD system provides the interactive tools for the designers to manipulate and modify the design. Internally, the system is based on Bézier curve and surface representation. The OZELOT postprocessor and controller represents the CAM part of the system. The machining module produces 3-axis tool path for the special controller. The geometric features of the patches are passed on to the controller, and the tool path is given in the parameter plane. The authors claim about 5 - 15 times reduction in NC program length, 60% NC programming time savings, including tool path verification and set-up time. The OZELOT controller itself is based on the NUMATEK 3000 CNC. The architecture includes individual bit-slice processors for each axis for positional control and fine interpolation, a processor for coordinating the work of the axis processors, and another processor with a floating point accelerator to preprocess the input commands. With this multiprocessor architecture the controller has a 0.2 msec servo sampling time, and a 10 - 40 msec block processing time.

Stripling describes the HECTRAN system for 5-axis machining of hydrodynamically engineered rotors [Stripling-81]. Though the system does all the processing off-line, it addresses all the problems associated with tool path generation for free-form shapes. The design of the shapes are based on the hydrodynamic equations of fluid flow. The digitized surface data describing the airfoil or blade sections for various types of rotor and stator configurations and for the blade tip and the hub are sorted in an orderly sequenced storage file. The cutter offset processor produces cutter offset

normal to the blade surface for the different tools. Machining can be done along or between streamlines. Optimum cutter sizes and lengths are selected from a standard cutter table while maintaining a protection or collision shield around the rotor or stator configuration. The universal post processor translates the tool path and cutter offsets to 5-axis NC tapes. With this system the authors claim that the process allows the machining of one-of-a-kind rotors at cycle times and costs normally associated with production type operations.

Duncan and Mair describe a unique method of machining sculptured surfaces [Duncan-83]. The method is called polyhedral machining, as the surface to be machined is approximated by a multifaceted non-regular polyhedron. The method of creating a faceted surface from random points was originally developed for mapping ocean floors [Taylor-71]. This also explains the shortcoming of the surface description method, where surfaces are represented as one valued functions, $z = f(x, y)$, which means, that no undercuts can be modeled with the system. The machining is done by touching the surface successively with ball nose cutters of decreasing diameters, similarly to the "pointing" sculpting method human sculptors use. The method inherently includes interference checking, the tool can sink only as deep into the part that none of the faucets would be undercut. The machining strategy includes touching all the triangles either in a zig-zag motion or along linear paths. The advantage of the system is that very simple machinery is required, only one continuous path controlled axis is needed, while the other two only need positional control. The original

implementation by the authors was an off-line solution. A PC based version of the system was commercially available.

Kochan *et al.* describe the elements of a system for designing and producing parts with sculptured surfaces [Kochan-83]. Their solution is a three layer system, consisting of design, production planning, and manufacturing. NC tape preparation for the machining is done by 2.5D roughing processor, and 2.5D, 3D and 5D contouring. The authors also suggest an improved data flow in the production by moving the postprocessing functions into the NC controller. They also propose technological and geometric input information for the controller.

Broomhead and Edkins describe the real-time generation of NC control blocks at the machine tool [Broomhead-86]. Their main motivation for the system is the reduction of paper tape (information) passed to the controller. The system developed implements 3-axis machining on surfaces described by Bézier-patches. Instead of tool path increments, the control polygon of the patches are passed to the controller. Machining is done along parameter lines. The step size in the forward direction is based on forward tolerance bands, while the sideways step size is based on the sideward tolerance, on the cusp height between the consecutive tool paths. Utilities exist to evaluate the surface beforehand for machinability, curvature, and undercut for each patch. There is also a roughing processor for machining the blanks before final contouring. The system implementation includes a microcomputer with a floating point coprocessor feeding a conventional NC controller in the BTR mode. Their actual machining tests have shown a tenfold information reduction for the surface machining.

Loney and Ozsoy describe an integrated system for machining of free-form surfaces based on CAM-I's CASPA (Computer Aided Sculptured Pre-APT) system [Loney-87]. The enhancements include an interactive front end and increased flexibility in surface machining. The machining modules include a roughing processor and a 3D contouring package. The contouring is done on parameter lines, where the forward step is based on chordal deviation and side step is based on scallop height calculations. The off-line implementation was on DEC VAX computers and graphics terminals.

Kim and Kwangsoo describe an integrated approach for sculptured surface design and manufacture [Kim-88, Kwangsoo-88]. Kim's method for machining the free-form shapes is to approximate the parametric space curves by a sequence of linear tool paths for ball nose cutters. The algorithm optimizes the cutter movements by minimizing the number of intermediate points while the approximated curves stay within the specified tolerance. The calculations are based on the normal and tangent vectors and the radius of curvature of the surface at the contact point. Their implementation of the system was on an IBM Personal Computer, running off-line.

Dean and Dow describe a versatile controller for 3D machining. [Dean-88]. The controller is distinctive in that it can produce complex lines and surfaces without a postprocessor or a computer, often from a small input. The path generator unit of the controller interpolates line segments and arcs in general orientation, not only in the main planes. The input language of the controller uses BASIC, and the arithmetic capabilities of the language can be used for calculating the tool path on complex shapes. Implementation was on an Intel single board computer enhanced with a numeric data processor.

Recently the US Government has initiated a project to develop the Next Generation machine/workstation Controller (NGC), which is part of a wider effort to revitalize the US machine tool industry [Barnes-91]. The program is to develop and validate a Specification for an Open System Architecture Standard (SOSAS) for a family of workstation/machine controllers. The specification will include system specification, module specification and a neutral manufacturing language specification. Among others, the NGC will have "advanced schemes of interpolation such as parabolic and non-uniform B-splines in addition to conventional linear and circular modes". Details are sketchy, as the project is classified.

As part of the NGC project, researchers at New York University have been working on an open architecture controller called Mosaic [MOSAIC-90]. The goal of the NYU researchers is to design a controller that even the first part produced on the machine tool would be right, without much human expertize and oversight. The system would have five software layers: machine applications at the lowest level to interface with the hardware and with dedicated controllers, control applications for motion control and sensory information processing, planning applications for motion planning of complex shapes and for providing for adaptive control in real-time, the language layer to process input information, and the graphics user interface. The system architecture of Mosaic is based on UNIX workstations running a real-time kernel system, with VME bus extensions to contain the dedicated hardware. Efforts included expert systems for part alignment and for set-up planning and fixturing. Limited adaptive machining strategies have also been

implemented. Plans included the addition of other sensors and on-line compensation for the machine dynamics.

Huang and Yang further refined the theory of parametric spline interpolators [Huang-92a, Huang-92b]. Their contribution is to develop a general methodology that eliminates the speed variation problem associated with spline interpolators based on chord length parameterization. Their solution to the speed variation question is to include the curve speed - curve parameter relationship into the calculations. They have carried out simulations and comparisons for 3-rd degree spline curves that prove the superior performance of their interpolation method compared to the others. A detailed analysis of their spline interpolator can be found in [Yang-94].

Bedi and Quan describe a B-spline interpolator for NC machines [Bedi-92]. The tool path is given as a 3-rd degree curve, with the control vertices passed to the interpolator. First the control vertices of the cubic polynomial coefficients are calculated for uniform knot sequences. Then the cubic segments are approximated by line segments with an iterative technique. The implementation is done in two stages: a rough and a fine interpolator. The solution is running on a PC - Transputer based multiprocessor platform.

Chungwatana *et. al.* present a methodology for the generation of machining instructions directly from the CAD model of the mechanical components consisting of NURBS based sculptured surfaces [Chungwatana-92]. The off-line system includes the modeler, path planner for rough cutting and finishing, module for selecting the technological parameters, and a simulator. In the process, first the sculptured surface CAD model is analyzed, using geometric reasoning algorithm, to select the proper tool for the rough

machining and finishing operations. Cutter path are then generated to ensure satisfactory surface quality while optimizing the total machining time. The machining parameters are selected based on mechanical dynamics models, analyzing vibration, chatter, and tool deflection. Before the NC code is finalized, a machining simulation model verifies the correctness of the NC commands.

Chen *et. al.* describe a system to machine sculptured surfaces [Chen-93]. Their solution is to move the planning and NC processor module into the controller. The tool path is generated for 3-axis machining in a novel way. First the tool path is generated on an offset surfaces for all patches. Then the tool paths are sorted and checked for gauging. Finally, the tool path trajectories are sent to the interpolator for execution. An interesting feature of the solution is that the part geometry is passed to the controller in IGES form. The system is implemented on a Multibus II based multiprocessor platform.

The proposed system described by Suzuk and his colleagues [Suzuk-93] generates the tool path in real-time. In fact, it also moves the complete planning tasks into the controller itself. They are using roughing and finishing processors. The tool path generation is based on the inverse offset method. The advantage of this method is the inherent collision checking in the tool path generation, and the computational efficiency [Sakuta-91]. For this processing the team used a parallel, Transputer processor based hardware architecture. The resultant 3-axis tool path is passed along to a conventional linear interpolator. Recognizing the disadvantages of the line segment approximation of the sculptured surface tool path, the researchers have also

suggested and demonstrated a spline interpolator for driving the servo amplifiers. That demonstration also utilized 3-axis machining.

Other approaches to reduce the size of the tool path data for sculptured surfaces were proposed by Piegl [Piegl-86] and Meek and Walton [Meek-93]. These solutions approximate the tool path by G^0 (Piegl) or G^1 (Meek and Walton) arc splines. G^0 arc splines are continuous curves, composed of arcs and line segments, G^1 arc splines have continuous tangents. Yeung and Walton applied the method [Yeung-94] to generate the arc splines from an overdetermined set of points and experimentally verified the improvements to the machining process as well as the surface quality of the machined part. As NC machines are able to generate arc segments directly in the main planes, this method is applicable where the tool path is given in a main plane (lathe machines, sheet metal processing, flame and laser cutters, etc.).

Shpitalni *et. al.* have studied real-time curve interpolators in their paper [Shpitalni-94]. They have proposed two curve interpolators: one for curves given in an implicit form, the other for parametric curves. For the parametric curves they proposed the same speed control method as Huang and Yang.

Kiritsis describes a parametric curve interpolator with incremental steps [Kiritsis-94]. The algorithm implements a search algorithm to find the closest neighbor on the grid (the grid representing the basic length of unit (BLU) of the machine tool). The search is guided by the direction of the curve and the distance between the curve and a grid point. The speed control is implemented by introducing delays between the calculations.

Siemens in 1994 commercially introduced their 840 series high end CNC controllers with a spline interpolator [Siemens-94]. The interpolator generates 3-rd degree NURBS curves. The tool path can be given either as a spline with the control points specified, or conventionally, as a series of line segments. Internally, the CNC only uses the NURBS based spline interpolator. In case of the line segment programming, the controller looks ahead and compresses the line segments into 3-rd degree NURBS in real-time and executes the splines. The controller itself does not have the geometrical description of the part to be machined, only the tool path, the trajectory of the tool end point is given in the NURBS form.

2.2.2 Evaluation of Existing Solutions

Section 2.2.1 is a review of the literature relevant to the path generation for NC controllers and for parts with sculptured surfaces. The citations covered solutions from methods and modules of path generators, which would be physically part of the controller, to complete systems, which prepare the data for the part production. Though the title of this research and the thesis refers to an actual path generator of a controller, the review of complete systems is well justified, as parts of the functionality of off-line systems have to be moved into or performed by the advanced path generator.

The review compiled above is mostly from research papers. The information available on the internal workings and implementation issues

of existing commercial controllers is far and few between, they are treated as trade secrets by the companies.

Current commercial and research CAD/CAM systems allow for sculptured surface machining [Stripling-81, Varady-82, Duncan-83, Kochan-83 Loney-87, Kim-88, Kwangsoo-88, Chungwatana-92]. The solutions apply off-line data processing for the tool path generation. This has all the disadvantages of being too complex and producing a huge amount of data as discussed earlier. On the other hand, there is also a tendency to move the design and planning functions into the controller, helped by the ever increasing and cheaply available computing power. Industry have been offering NC systems for some time that include design and planning systems on the same platform [Sharnoa-91, Yellowley-94]. From the point of view of system design, this is nothing more than packaging: the same interfaces are present between the layers as at off-line systems. Nonetheless, this an improvement from the users point of view, the inter-operation between the layers and modules are sorted out, and last but not least, the user only has to deal with one system provider.

The systems which provide real-time higher order curve generation, usually do it in a pre-processing fashion: the actual tool path still consists of line segments, and the approximation is done run-time. That means that the functionality of the interpolator has not improved in the controller, except that the task of interpreting the higher order curves got off-loaded to a preprocessor. The coupling between the preprocessor and the path generator can be tight, in which case the preprocessor is part of the controller [Hermann-84b, Euclid-86, Haapaniemi-86, Bedi-92, Suzuk-93], or it could be

loosely coupled, where the preprocessor is not part of the controller, and the controller is driven in the "behind tape reader" mode [Sata-81, Broomhead-86].

The above systems, which do run-time higher order curve generation, do it only for 2-axis and 3-axis control; 5-axis solutions are only implemented with off-line data processing.

The other problem with the higher order curve interpolation is that the curve still describes the trajectory of the tool end point, and not the contact point. This shortcoming is equally true for commercial controllers [Siemens-94] as well as for research papers and methods discussing higher order curve interpolators [Enlin-82, Bedi-92, Huang-92, Kiritsis-94, Shpitalni-94, Yang-94]. This already allows for the reduction of the data sent to the controller; the tool path described by spline segments are more compact than the same path described with line segments, but correction for changes in tool size and part placement can not be implemented with this method. The speed of the machining might also vary, as not the speed of the contact point, but the speed of the tool end point is controlled. None of the systems described addressed this question fully and satisfactorily.

To reap the full benefits of advanced path generation, not only the tool path, but the part geometry has to be known to the controller as well. The systems which had the part geometry available at the controller [Broomhead-86, Chen-93, Suzuk-93] were systems where the planning/path generation was moved to the controller, but the interpolator still generated line segments.

Reviewing the existing solutions, it can be concluded that most of the problems mentioned in Chapter 2 have been addressed, but not all of them

solved. There is still a need for a method in path generation that deals with *all* of the problems discussed and not only with some. In this thesis, in Section 2 of Chapter 4, in the System Description, the requirements for such an advanced path generator are outlined, and in the consecutive chapters, the problems answered in detail.

3 Foundations of Sculptured Surface Machining

In this chapter the background information that is being used during the discussion of the Advanced Path Generator is presented.

Section 1 offers a mathematical discussion on Geometric Modeling, on the different curve and surface description methods, and on related calculations, while Section 2 summarizes the different machining strategies that are being used in sculptured surface machining.

3.1 Geometric Modeling

Three kinds of computer aided geometric modeling systems have been developed for use by industry: one based on curves, another one based on surfaces, and the third one using solids. The objects are usually entered interactively at a graphics workstation and then converted into the internal representations by the design systems. The internal representation of the geometric objects progressed through these stages together with the ever increasing complexity and functionality of the evolving CAD/CAM systems [Goldman-87].

Wire-frame models represent an object's bounding edges with interconnected lines. Introduced on CAD systems in the late 60's, they were the predominant modeling method. They required little computational power to create and manipulate the objects, and the models could be constructed with ease. Wire-frame models lend themselves well to 2D applications, such as designing and drafting of flat parts. The wire-frame

representation has severe limitations. It is incomplete since surfaces, solid, and void spaces are not represented in the computer and can often be interpreted to represent more than one object. Also, representation can be ambiguous. Moreover, wire-frame models of complex 3D objects often become too crowded and confusing to the user.

Surface models overcome many of these limitations by completely defining an object's surface. The capacity to define contoured surfaces makes surface modelers extremely useful where complex 3D geometries must be defined. However, surface models do not convey information about the interior of the object. The model does not specify which side of the surface is solid and where it is void. The modeling does not guarantee that the surfaces bound completely a solid object. The user must keep track of the structure of the model when performing cross-sectioning, interference checking, or other engineering applications.

A solid model contains enough information to decide if a point lies inside, outside, or on the surface of an object. This is the feature that distinguishes the solid modeler from the surface modeler. From a solid model, one can readily compute mass properties, study internal details, and it can serve as a starting point for structural analysis. In other words, a solid model always represents a valid, realizable object. In contrast, wire-frame and surface models can represent physically impossible objects as well.

Many techniques have been developed for generating and storing computer models of solid objects. The most important and popular representations are the constructive solid geometry (CSG) and the boundary representations (B-rep) models [Wilson-87].

In constructive solid geometry, complex objects are built by performing Boolean operations on a fixed collection of simple primitives. The primitives usually include several solids with simple features like boxes, cylinders, spheres, tori, etc., but primitives with more complicated surfaces can also be incorporated into these systems. By performing the Boolean operations of union, difference, and intersection, an unlimited variety of parts can be constructed. The internal representation of the object in CSG is a binary tree where the nodes are the operations and the leaves are the primitives.

In the boundary representation the solid is described by each of its bounding entities and their relations to each other, the surfaces, edges, and vertices. The information stored in this case is much more complex and more expensive to compute and store, but it allows more flexibility to the designer. Commercial systems usually support both representations, keeping it transparent from the user and providing the added flexibility [Klein-84].

Due to the complexity of the software of solid modeling systems, the incorporation of sculptured surfaces has been slow. This is fortunately changing, and free-form surfaces are now making their way into solid modeling systems [Sarraga-83, Kimura-83, Chiyokura-88, Goldman-87].

3.1.1 Surface Representation

A surface in computer aided design is described by a two variable vector-scalar function.

$$\mathbf{r} = \mathbf{r}(u, v) \tag{3.1}$$

or in detail:

$$\mathbf{r} = x(u,v)\,\mathbf{i} + y(u,v)\,\mathbf{j} + z(u,v)\,\mathbf{k} \tag{3.2}$$

By using this parametric description, the representation is invariant to the coordinate system selected, and translation, rotation and other transformations can easily be described by matrix multiplications. This vector-scalar description can be considered as a one to one mapping between the u, v parameter space and a three dimensional surface patch.

As engineering surfaces are far too complicated to be described by a single surface patch, they are made up of a set of piecewise patches. The patches are connected to each other with the required degree of continuity.

In order to investigate the properties of the different surface description methods, it is best to start with the underlying curve scheme. The extension of the curves into surfaces is a generalization of the single parameter curve description into a two parameter vector-scalar function.

3.1.2 Space Curves

There are many ways to specify a curve in the space through a set of points. Curve generation can be classified into two main groups with respect to the points used to define the curves. The first group is interpolation, where the curve goes through the data points, and the points are actually part of the curve. In the other case, which is called approximation, the curve just follows the points to a given degree. Here, the points just guide the general shape of the curve, and are usually not part of the curve.

Both methods of curve definition have applications for which they are best suited. Commercial CAD systems usually support several methods of curve and surface generation, and it is up to the designer to use the most appropriate one.

3.1.2.1 Cubic Splines

In many industries, such as ship, automotive and aircraft building, the final, full shape drawings used to be done by lofting. This is the process where the shape is given by a narrow and long elastic strip, called a spline, fixed to the specified data points. The form of the mathematical spline is derived from its physical counterpart. For small deflections, the shape of the curve between two points, $\mathbf{p}(t_1)$ and $\mathbf{p}(t_2)$, can be described by a third order polynomial expression [Rogers-90]:

$$\mathbf{p}(t) = \sum_{i=1}^{4} \mathbf{B}_i \; t^{i-1} \qquad t_1 <= t <= t_2$$

(3.3)

where $\mathbf{p}(t)$ is a point on the curve at parameter value t and $\mathbf{B}_i$ are the coefficients in 3D.

Writing it out:

$$\mathbf{p}(t) = \mathbf{B}_1 + \mathbf{B}_2\, t + \mathbf{B}_3\, t^2 + \mathbf{B}_4\, t^3 \qquad t_1 <= t <= t_2$$

(3.4)

This equation describes the curve between two points. A full curve, going through several points, can be described by piecewise segments of such splines.

A spline with degree r can be made continuous of order r-1 at each joint. The coefficients of the spline can be calculated from the boundary conditions for each segment. For simplicity, the parameter value of a segment is limited between t_k and t_{k+1}:

$t_k <= t <= t_{k+1}$

The selection of the parameter value t_{k+1} has an effect on the smoothness of the curve, which is a concern for the design function.

The curve of the k-th segment can be written in a matrix form:

$$\mathbf{p}_k(t) = \begin{bmatrix} 1 & t-t_k & (t-t_k)^2 & (t-t_k)^3 \end{bmatrix} \begin{bmatrix} \mathbf{B}_{1k} \\ \mathbf{B}_{2k} \\ \mathbf{B}_{3k} \\ \mathbf{B}_{4k} \end{bmatrix} \qquad t_k <= t <= t_{k+1}$$

(3.5)

The coefficients for the cubic spline of the k-th segment are given by the following equations:

$$\mathbf{B}_{1k} = \mathbf{P}_k$$

(3.6)

$$\mathbf{B}_{2k} = \mathbf{P}_k'$$

(3.7)

$$\mathbf{B}_{3k} = \frac{3\ (\mathbf{P}_{k+1} - \mathbf{P}_k)}{(\Delta t_k)^2} - \frac{2\ \mathbf{P}_k'}{\Delta t_k} - \frac{\mathbf{P}_{k+1}'}{\Delta t_k}$$

(3.8)

$$\mathbf{B}_{4k} = \frac{2\ (\mathbf{P}_k - \mathbf{P}_{k+1})}{(\Delta t_k)^3} + \frac{\mathbf{P}_k'}{(\Delta t_k)^2} + \frac{\mathbf{P}_{k+1}'}{(\Delta t_k)^2}, \qquad \Delta t_k = t_{k+1} - t_k$$

(3.9)

Where $\mathbf{P}_k$, $\mathbf{P}_{k+1}$, and $\mathbf{P}_k'$, $\mathbf{P}_{k+1}'$ are the points and the tangent vectors at the joints. By substituting and rearranging the expressions:

$$\mathbf{p}_k(\tau) = \begin{bmatrix} F_1(\tau) & F_2(\tau) & F_3(\tau) & F_4(\tau) \end{bmatrix} \begin{bmatrix} \mathbf{p}_k \\ \mathbf{p}_{k+1} \\ \mathbf{p}'_k \\ \mathbf{p}'_{k+1} \end{bmatrix} \qquad 0 <= \tau <= 1$$

(3.10)

where

$$\tau = (t - t_k) / \Delta t_k \tag{3.11}$$

$$F_1(\tau) = 2\tau^3 - 3\tau^2 + 1 \tag{3.12}$$

$$F_2(\tau) = -2\tau^3 + 3\tau^2 \tag{3.13}$$

$$F_3(\tau) = \tau (\tau^2 - 2\tau + 1)\ \Delta t_k \tag{3.14}$$

$$F_4(\tau) = \tau (\tau^2 - \tau)\ \Delta t_k \tag{3.15}$$

The $F_i(\tau)$ functions are also called the blending or weighting functions. The F_i functions, which are based on the end points and the tangents at the end points, are also known as the Hermite polynomials.

They can be written again in a matrix form:

$$\mathbf{p}_k(\tau) = \mathbf{F}\,\mathbf{G} \tag{3.16}$$

where

$$\mathbf{F} = [F_1(\tau)\ F_2(\tau)\ F_3(\tau)\ F_4(\tau)] \tag{3.17}$$

$$G^T = [P_k \; P_{k+1} \; Pk' \; P_{k+1}']$$

(3.18)

An alternate method for the t_k spline segment parameter values is to normalize the parameter interval for each segment:

$0 <= t <= 1$

This simplifies the expression for the blending functions, and the **F** blending matrix can be further decomposed:

$$\mathbf{F} = \mathbf{T}\,\mathbf{N} = [t^3 \; t^2 \; t \; 1] \begin{bmatrix} 2 & -2 & 1 & 1 \\ -3 & 3 & -2 & -1 \\ 0 & 0 & 1 & 0 \\ 1 & 0 & 0 & 0 \end{bmatrix}$$

(3.19)

The matrix equation for the cubic spline can now be written in the following form:

$$\mathbf{p}(t) = \mathbf{T}\,\mathbf{N}\,\mathbf{G}$$

(3.20)

where **G** contains the geometric information about the curve.

3.1.2.2 Bézier Curves

A Bézier curve is determined by a defining polygon, called the control polygon. Mathematically a parametric Bézier curve in polynomial form is given by:

$$\mathbf{b}_n(t) = \sum_{i=0}^{n} C_i^n \, t^i (1-t)^{n-i} \, \mathbf{b}_i \tag{3.21}$$

where

$$C_i^n = \frac{n!}{i!\,(n-i)!} = \binom{n}{i}$$ are the binomial coefficients, (3.22)

$\mathbf{b}_i$, i = 0, ..., n is the control polygon, and

$0 \le t \le 1$ is the parameter.

A geometric interpretation of the Bézier curve can be given by the de Casteljau algorithm [Farin-93] which is basically a repeated linear interpolation. Using the algorithm, the Bézier curve of degree n can be expressed in a recursive way:

$$\mathbf{b}_{i,r}(t) = (1-t)\,\mathbf{b}_{i,r-1}(t) + t\,\mathbf{b}_{i+1,r-1}(t); \qquad \begin{matrix} r = 1,..n \\ i = 0,..n-r \end{matrix} \tag{3.23}$$

where

$\mathbf{b}_{i,0}(t) = \mathbf{b}_i$ is the control polygon

$\mathbf{b}_{0,n}(t) = \mathbf{b}_n(t)$ is the point with parameter value t

$\mathbf{b}_{i,t}(t)$ are the intermediate coefficients

The terms from equation (3.21)

$$B_i^n(t) = C_i^n \, t^i (1 - t)^{n - i} \tag{3.24}$$

are also known as the Bernstein polynomials. The Bézier curve with the Bernstein polynomials is expressed as:

$$\mathbf{b}_n(t) = \sum_{i=0}^{n} B_i^n(t) \; \mathbf{b}_i \tag{3.25}$$

The monomial form can be written in a concise matrix form:

$$\mathbf{b}(t) = \mathbf{T}\,\mathbf{M}\,\mathbf{B}, \tag{3.26}$$

where

$$\mathbf{T} = [1, t, t^2, .. t^n], \tag{3.27}$$

$$\mathbf{B}^T = [\mathbf{b}_0, \mathbf{b}_1, .. \mathbf{b}_n], \tag{3.28}$$

and **M** is the Bézier matrix whose elements can be calculated as below:

$$\mathbf{M}_{i,j} = (-1)^{j-i} \binom{n}{j} \binom{j}{i} \tag{3.29}$$

The derivative of a Bézier curve is needed for many calculations. To get the derivative, it is convenient to use the polynomial representation:

$$\frac{d}{dt}\,\mathbf{b}_n(t) \;=\; \frac{d}{dt}\left(\sum_{i=0}^{n} B_i^n(t)\;\mathbf{b}_i\right) \;=\; \sum_{i=0}^{n} \mathbf{b}_i\;\frac{d}{dt}\,B_i^n(t)$$

(3.30)

Using the chain rule with the Bernstein polynomials the derivative is:

$$\frac{d}{dt}\,\mathbf{b}_n(t) \;=\; n\sum_{i=0}^{n-1}(\mathbf{b}_{i+1} - \mathbf{b}_i)\;B_i^{n-1}(t)$$

(3.31)

The derivative is another Bézier curve of degree n-1, where the control points are the difference vectors of the original control points in the 3D space [Pavlidis-82]. This curve is often called the hodograph of the original curve [Bézier-86].

3.1.2.3 B-splines

The Bézier curves are in essence vector-valued approximations with the given points as coefficients and the family of functions of the Bernstein polynomials as basis.

Two features of the Bernstein basis functions limit the flexibility of the resulting curves. First, the number of vertices in the control polygon fixes the degree of the resulting polynomial, and, hence, the degree of the curve. For example, a cubic curve needs four vertices. Complex curves might need a huge number of vertices to define them, and, consequently, the degree of the curve will also be high.

The other disadvantage is that Bézier curves are global in nature. Modifying a single vertex influences the whole shape of the curve.

By using B-spline basis functions the disadvantages of the Bézier curves can be overcome. This was first investigated by Gordon and Riesenfeld [Böhm-84]. The B-spline basis functions are a generalization of the Bernstein polynomials, the Bernstein polynomials being a special case of them. The basis functions are non global, they are non zero only on a range of parameter values, associated with a vertex. The degree of the equation describing the curve is also independent of the number of the vertices. The B-spline curve of order[1] k is given by:

$$\mathbf{b}(t) = \sum_{i=1}^{n+1} \mathbf{b}_i \; N_{i,k}(t) \qquad k <= n+1 \tag{3.32}$$

where

$\mathbf{b}_i$ are points of the control polygon,

$N_{i,k}$ is the i-th normalized B-spline basis function of order k

[1]Usually, for B-splines, order = degree + 1

The basis function can be defined in a recursive way, suggested by de Boor [Boor-78]:

$$N_{i,k}(t) = \frac{(t - x_i)\ N_{i,k-1}(t)}{x_{i+k-1} - x_i} + \frac{(x_{i+k} - t)\ N_{i+1,k-1}(t)}{x_{i+k} - x_{i+1}}$$

$$N_{i,1}(t) = \begin{cases} 1 \text{ if } x_i <= t < x_{i+1} \\ 0 \text{ otherwise} \end{cases}$$

(3.33)

The values of x_i are elements of a knot vector in the t parameter space, satisfying the relation $x_i <= x_{i+1}$.

The $\mathbf{b}(t)$ B-spline curve of order k and its derivatives of order 1, 2,.. k-2 are all continuous over the entire curve. The derivative of a B-spline curve at any point on the curve are obtained by formal differentiation:

$$\frac{d}{dt}\mathbf{b}(t) = \sum_{i=1}^{n+1} \mathbf{b}_i \frac{d}{dt} N_{i,k}(t)$$

(3.34)

The differentiation of the basis function yields:

$$\frac{d}{dt} N_{i,k}(t) = (k - 1)\left(\frac{N_{i,k-1}(t)}{x_{i+k-1} - x_i} - \frac{N_{i+1,k-1}(t)}{x_{i+k} - x_{i+1}}\right)$$

(3.35)

As can be seen from the above expression, the derivatives of the B-spline curves are in terms of lower order B-splines.

The B-spline curves can also be represented in a matrix form:

$$\mathbf{b}(t) = \mathbf{T}\,\mathbf{M}\,\mathbf{B}, \tag{3.36}$$

where

$$\mathbf{T} = [1, t, t^2, ..t^n], \tag{3.37}$$

$$\mathbf{B}^T = [b_0, b_1, ..b_n], \text{ and} \tag{3.38}$$

M is the B-spline matrix

The **M** B-spline matrix can easily be evaluated for uniform knot sequences, where $x_i - x_{i-1} = 1$.

3.1.2.4 Rational B-spline curves

Rational curve and surface descriptions were introduced into computer graphics and computer aided design in the late sixties and evolved through the seventies [Piegl-91]. Rational B-splines provide a single precise mathematical form capable of representing the common analytical shapes: lines, planes, conic curves including circles, free-form curves, and sculptured surfaces. The nonuniform rational B-spline representation is a versatile model, and, as a result, it is gaining popularity [Briere-92]. Nonuniform

rational B-splines (NURBS) have been included in the Initial Graphics Exchange Specification standard since 1983 [IGES-86].

A rational B-spline curve is the projection of a nonrational (polynomial) B-spline curve, defined in four dimensional (4D) homogeneous coordinate space, back into three dimensional (3D) physical space. The curve in the 4D space is:

$$\mathbf{b}^w(t) = \sum_{i=1}^{n+1} \mathbf{b}_i^w \, N_{i,k}(t) \tag{3.39}$$

where

$\mathbf{b}^w(t) = [wx(t), wy(t), wz(t), w]^T$ is the curve in the 4D space,

$\mathbf{b}_i^w$ are the points of the control polygon in the 4D space,

$N_{i,k}(t)$ are the B-spline basis functions of order k.

To get the 3D curve, the 4D curve has to be projected onto the plane w = 1 in the 4D space. The mapping is done formally by dividing the wx(t), wy(t), wz(t) coordinates by the w coordinate value [Rogers-90]. The rational B-spline curve in the 3D space is given as follows:

$$\mathbf{b}(t) = \frac{\sum_{i=1}^{n+1} w_i \, \mathbf{b}_i \, N_{i,k}(t)}{\sum_{i=1}^{n+1} w_i \, N_{i,k}(t)} = \sum_{i=1}^{n+1} \mathbf{b}_i \, R_{i,k}(t) \tag{3.40}$$

here the $\mathbf{b}_i$'s are the 3D control vertices, w_i's are the weights associated with the vertices and also fulfilling the condition $w_i >= 0$ for all i. The terms

$$R_{i,k}(t) = \frac{w_i \; N_{i,k}(t)}{\sum_{j=1}^{n+1} w_j \; N_{j,k}(t)} \tag{3.41}$$

are the rational B-spline basis functions.

As can be seen, the rational B-splines are a generalization of nonrational B-spline curves. The nonrational B-spline curves are a special case of the rational ones, by having all weights $w_i = 1$.

The derivative of the rational B-spline curve can be obtained by formally differentiating it:

$$\frac{d}{dt}\,\mathbf{b}(t) = \frac{d}{dt}\left(\sum_{i=1}^{n+1} \mathbf{b}_i \; R_{i,k}(t)\right) = \sum_{i=1}^{n+1} \mathbf{b}_i \; \frac{d}{dt} \; R_{i,k}(t) \tag{3.42}$$

Differentiating the basis functions (3.41) with the chain rule yields:

$$\frac{d}{dt}R_{i,k}(t) = w_i \; \frac{\frac{d}{dt}N_{i,k}(t) \sum_{j=1}^{n+1} \left(w_j \; N_{j,k}(t)\right) - N_{i,k}(t) \sum_{j=1}^{n+1} w_j \; \frac{d}{dt}N_{j,k}(t)}{\left(\sum_{j=1}^{n+1} w_j \; N_{j,k}(t)\right)^2} \tag{3.43}$$

3.1.3 Surfaces

There are two main methods used by CAD systems to construct surfaces from curves. One of them is bivariate blending, also called the transfinite surface generation, producing Boolean sum patches. The other method is the tensor-product surface generation [Böhm-84].

3.13.1 Transfinite Surfaces

In the transfinite surface generation the surface is bivariately blended between four boundary curves. This method was first suggested by Coons [Coons-64].

Coons first used linear blending between the curves. This only gave C^0 continuity between the patches despite the fact that the curves are C^1 continuous. By using the Hermite cubic blending functions for creating the surface, the adjacent patches will be C^1 continuous. This surface is called the Coons bicubic patch or the Hermite patch.

Using normalized cubic splines, the four boundary curves $\mathbf{p}(u,0)$, $\mathbf{p}(u,1)$, $\mathbf{p}(0,v)$, $\mathbf{p}(1,v)$ are given in the form:[2]

$$\mathbf{p}(t) = \mathbf{T}\,\mathbf{N}\,\mathbf{G} \tag{3.44}$$

[2] The following material on Coons patches is taken from Rogers and Adam [Roger-90].

where t becomes u or v, according to the boundary curves, **N** is the blending matrix, as discussed earlier with respect to cubic splines, and **G** contains the geometric information on the end points of the boundary curves. Writing out the blending functions:

$$\mathbf{F} = \mathbf{T}\,\mathbf{N} \tag{3.45}$$

$$F_1(t) = 2t^3 - 3t^2 + 1 \tag{3.46}$$

$$F_2(t) = -2t^3 + 3t^2 \tag{3.47}$$

$$F_3(t) = t^3 - 2t^2 + t \tag{3.48}$$

$$F_4(t) = t^3 - t^2 \tag{3.49}$$

The definition of the Coons bicubic patch is:

$$\mathbf{r}(u,v) = \begin{bmatrix} F_1(u) & F_2(u) & F_3(u) & F_4(u) \end{bmatrix} \times \begin{bmatrix} \mathbf{P}(0,0) & \mathbf{P}(0,1) & \mathbf{P}_v(0,0) & \mathbf{P}_v(0,1) \\ \mathbf{P}(1,0) & \mathbf{P}(1,1) & \mathbf{P}_v(1,0) & \mathbf{P}_v(1,1) \\ \mathbf{P}_u(0,0) & \mathbf{P}_u(0,1) & \mathbf{P}_{uv}(0,0) & \mathbf{P}_{uv}(0,1) \\ \mathbf{P}_u(1,0) & \mathbf{P}_u(1,1) & \mathbf{P}_{uv}(1,0) & \mathbf{P}_{uv}(1,1) \end{bmatrix} \begin{bmatrix} F_1(v) \\ F_2(v) \\ F_3(v) \\ F_4(v) \end{bmatrix} \tag{3.50}$$

for 0 <= u <= 1 and 0 <= v <= 1. This expression can also be written in more concise, matrix form:

$$\mathbf{r}(u,v) = \mathbf{U}\,\mathbf{N}\,\mathbf{P}\,\mathbf{N}^T\,\mathbf{V} \tag{3.51}$$

where

$$\mathbf{U} = [u^3\ u^2\ u\ 1], \tag{3.52}$$

$$\mathbf{V}^T = [v^3\ v^2\ v\ 1] \tag{3.53}$$

and **P** contains the geometric information on the surface patch. **P** is often called the hyper matrix, and it can be constructed from four 2 x 2 submatrices in the corner of **P**:

$$\mathbf{P} = \begin{bmatrix} \begin{matrix}\text{corner}\\ \text{position}\\ \text{vectors}\end{matrix} & \begin{matrix}\text{v}\\ \text{tangent}\\ \text{vectors}\end{matrix} \\ \begin{matrix}\text{u}\\ \text{tangent}\\ \text{vectors}\end{matrix} & \begin{matrix}\text{twist}\\ \text{vectors}\end{matrix} \end{bmatrix} \tag{3.54}$$

The parametric derivatives at any point on the surface can be obtained by formally differentiating the matrix equation of the surface:

$$\mathbf{r}_u(u,v) = \mathbf{U}'\ \mathbf{N}\ \mathbf{P}\ \mathbf{N}^T\ \mathbf{V} \tag{3.55}$$

$$\mathbf{r}_v(u,v) = \mathbf{U}\ \mathbf{N}\ \mathbf{P}\ \mathbf{N}^T\ \mathbf{V}' \tag{3.56}$$

$$\mathbf{r}_{uv}(u,v) = \mathbf{U}'\ \mathbf{N}\ \mathbf{P}\ \mathbf{N}^T\ \mathbf{V}' \tag{3.57}$$

$$\mathbf{r}_{vv}(u,v) = \mathbf{U}\ \mathbf{N}\ \mathbf{P}\ \mathbf{N}^T\ \mathbf{V}'' \tag{3.58}$$

3.1.3.2 Tensor Product Polynomial Surfaces

The properties of tensor product surfaces can easily be deduced from the properties of the underlying curve scheme. The most intuitive derivation of tensor product surfaces is given by Böhm [Böhm-84]. Let

$$\mathbf{r}(u) = \sum_{i=0}^{n} \mathbf{c}_i \; F_i(u) \tag{3.59}$$

be a 3D curve expressed in terms of basis functions F_i. Let this curve sweep out a surface by moving it through space and also changing it along the way. Such a sweep can be described by letting each $\mathbf{c}_i$ trace out a curve $\mathbf{c}_i(v)$. Again, $\mathbf{c}_i(v)$ can be described in terms of $G_j(v)$ basis functions:

$$\mathbf{c}_i(v) = \sum_{j=0}^{m} \mathbf{a}_{i,j} \; G_j(v) \tag{3.60}$$

By substituting this into the expression of $\mathbf{p}(u)$ we get the tensor product surface:

$$\mathbf{r}(u,v) = \sum_{i=0}^{n} \mathbf{c}_i(v) \; F_i(u) = \sum_{i=0}^{n} \sum_{j=0}^{m} \mathbf{a}_{i,j} \; F_i(u) \; G_j(v) \tag{3.61}$$

Here the surface patch is described in terms of F(u) and G(v) basis functions. These basis functions are independent of each other, and any of the known functions can be used for the surface definition. The $\mathbf{a}_{i,j}$ coefficients are the control points of the surface patch. These points should form an orthogonal network of points.

Finding the tangent vectors of the surface patch in the u and v direction is necessary to calculate the surface normal. It is done by forming the partial derivatives with respect to u and v:

$$\frac{\partial \mathbf{r}(u,v)}{\partial u} = \frac{\partial}{\partial u}\left(\sum_{i=0}^{n}\sum_{j=0}^{m} \mathbf{a}_{i,j}\ F_i(u)\ G_j(v)\right) = \sum_{i=0}^{n}\sum_{j=0}^{m} \mathbf{a}_{i,j}\ \frac{\partial F_i(u)}{\partial u}\ G_j(v) \tag{3.62}$$

$$\frac{\partial \mathbf{r}(u,v)}{\partial v} = \frac{\partial}{\partial v}\left(\sum_{i=0}^{n}\sum_{j=0}^{m} \mathbf{a}_{i,j}\ F_i(u)\ G_j(v)\right) = \sum_{i=0}^{n}\sum_{j=0}^{m} \mathbf{a}_{i,j}\ F_i(u)\ \frac{\partial G_j(v)}{\partial v} \tag{3.63}$$

The normal vector can be formulated as the cross product of the two tangent vectors. The normal vector is needed for the various geometrical calculations for further manipulation and processing of the surfaces including computations of points on offset surfaces.

3.2 Machining Strategies

So far, in Section 3.1, on Geometric Modeling, the methods of shape descriptions of a part were discussed. In this Section, different strategies will be looked at to see how the tool can be moved on the surface of the part to be machined.

Tool path generation is the process of producing motion commands to move the tool for metal removal from the part. As mentioned previously, during the review of the sculptured surface part production, the metal removal consists of two stages: the roughing process and the finishing cut. The roughing process is relatively simple from the tool motion point of view: the tool moves along straight lines to remove as much material as efficiently as possible. At the final contouring, or finishing cut, the tool has to follow the surface of the free-form shape with the required tolerance to produce the final shape. Here, in this thesis, the tool path generation for the final, or the contouring cut of the machining is addressed.

There are several methods to cut a free-form shape on a machine tool [Giessen-86a, Giessen-86b, Renner-78]. The simplest is 2.5-axis machining. Here the tool follows isoheight contour lines in 2D, the third dimension is used to set the height values. The orientation of the tool axis does not change during machining. The shape of the tool end, which does the machining is a sphere. The tool center point is moved on an offset surface. The contact point between the tool and the part, where the cutting is taking place, does move around the sphere as the normal of the part surface changes. As the contact point varies along the tool path during machining, the machining efficiency,

accuracy, tolerance and machining time are all effected. The main advantage of this technology is that it requires a simple machine tool with only two axis necessitating continuous positional control. These days the significance of this technique is diminishing as multiple axis motion control systems are getting more affordable.

3-axis contouring is more widespread. This is very much like 2.5-axis machining, except in this case, the tool follows a general path in three dimension around the part. The contact point between the tool and the part still changes continuously, as the surface normal varies along the tool path. This technique also has the same disadvantages as the 2.5D machining because of the similarly fixed tool axis orientation, although to a lesser degree, as a more general tool path can be defined in 3D, minimizing the contact point variation [Renner-78]. Another drawback of 3D machining is that usually several different part set-ups are required to machine the part fully, because of the limited access of the tool to the part.

5-axis machining eliminates most of the problems associated with 2.5- and 3-axis machining: the tool orientation changes, and it is kept usually in a constant relation to the surface normal of the part during machining. The contact point between the tool and the part does not change along the tool path, the tool is always cutting with high efficiency. Also, the number of set-ups is reduced due to the extra degrees of freedom. Despite the requirements for more complex machinery, the popularity of 5-axis machining is increasing due to its advantages: higher accuracy, better surface finish, reduced setup time, reduced fixturing and tooling costs, reduced machining time and, in

general, a better quality product [Giessen-86c, Wildish-86, Khalil-87, Rolls-Royce-87, Schultz-93].

4-axis contouring is also used. This is basically 3-axis machining from a computational point of view, with an extra degree of freedom to keep the contact point on the tool close to the optimal value and to reduce the number of required part set-ups. The main area of 4D machining is cutting axially symmetrical parts.

4 Advanced Tool Path Generation

In this part of the dissertation, the results of the research are presented. Section 1 develops the mathematics for the various tool path generation methods which is fundamental to the design of the advanced path generator. In Section 2, the detailed specification for the advanced path generator is given. It also includes a discussion about the specification, while Section 3 provides the details of the real-time advanced tool path generation.

4.1 The Mathematics of Tool Path Generation

The surfaces, as seen in the previous chapters, are described by two-parameter vector-scalar functions:

$$\mathbf{r} = \mathbf{r}(u,v) \tag{4.1}$$

The tool path on the surface is the specification of the surface traversal. The tool path is first defined in the u, v parameter space as a function of a general t parameter (4.2), then it is mapped into the 3D space (4.3). Mathematically expressed:

$$u = u(t),\ v = v(t),\ \text{and} \tag{4.2}$$

$$\mathbf{r} = \mathbf{r}(u(t),v(t)) = \mathbf{r}(t) \tag{4.3}$$

From these tool path coordinates on the surface, together with the knowledge of the geometry of the tool and the kinematics of the machine tool, the coordinates to control the machine axes has to be devised. In the following sections the mathematics and calculations for 3- and 5-axis machining are developed, that are fundamental to tool path generation.

4.1.1 3-axis Tool Path Generation

3D machining employs a ball nose cutter. The tool center point, which is the feature that can be controlled by the NC machine, moves on an offset surface. Figure. 4.1.

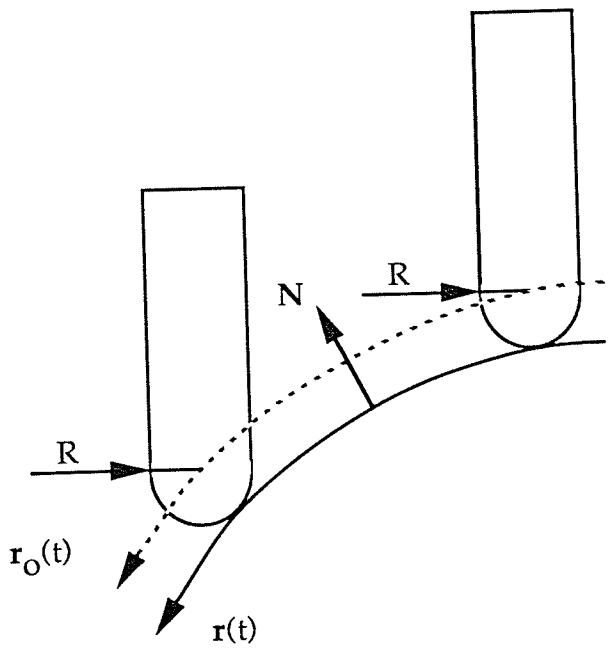

Figure 4.1. 3-axis tool path.

The movement of the tool center point can be described as follows:

$$\mathbf{r}_o(t) = \mathbf{r}(t) + \mathbf{N}(t)\, R; \tag{4.4}$$

Where $\mathbf{r}(t)$ is the tool path on the 3D surface, $\mathbf{N}(t)$ is the surface normal unit vector and R is the tool radius. The surface normal can be expressed as follows:

$$\mathbf{N}(t) = \frac{\mathbf{r}_u \times \mathbf{r}_v}{H}, \quad H = \left|\mathbf{r}_u \times \mathbf{r}_v\right| \neq 0, \quad u = u(t), \quad v = v(t) \tag{4.5}$$

where $\mathbf{r}_u$, $\mathbf{r}_v$ are the partial derivatives of $\mathbf{r}$ with respect to u and v:

$$\mathbf{r}_u = \frac{\partial \mathbf{r}}{\partial u}, \quad \mathbf{r}_v = \frac{\partial \mathbf{r}}{\partial v}, \quad u = u(t), \quad v = v(t) \tag{4.6}$$

Offset curves, which have the same principal normals as the original ones, are also known in differential geometry as Bertrand curves [Eisenhart-09, Willmore-59]. Such curves also have common centers of curvatures. These features imply that if the progenitor curves are composed of several segments with a given degree of continuity, the offset curves will preserve the same degree of continuity piecewise [Papaioannou-85, Qiulin-87].

Another way to look at the 3D tool path generation is to construct first an offset surface with the tool radius R to the original surface, and then to specify the tool path on the offset surface.:

$$\mathbf{r}_o(u,v) = \mathbf{r}(u,v) + \mathbf{N}(u,v)\ R \tag{4.7}$$

$$\mathbf{N}(u,v) = \frac{\mathbf{r}_u \times \mathbf{r}_v}{H}, \qquad H = \left|\mathbf{r}_u \times \mathbf{r}_v\right| \neq 0 \tag{4.8}$$

$$\mathbf{r}_u = \frac{\partial \mathbf{r}}{\partial u}, \qquad \mathbf{r}_v = \frac{\partial \mathbf{r}}{\partial v} \tag{4.9}$$

$$u = u(t),\ v = v(t), \ \rightarrow \ \mathbf{r}_o(u,v) = \mathbf{r}_o(u(t),v(t)) = \mathbf{r}_o(t) \tag{4.10}$$

The mathematical expression of the offset surface to a polynomial surface is no longer polynomial in nature, as the denominator of the surface normal involves the square root of a polynomial.

Several authors have expanded the theory of Bertrand curves to surfaces [Papaioannou-85, Farouki-86, Ravani-91]. They have showed that offset surfaces retain the same geometric features - the surface normals and centers of curvatures - as the original surfaces, similarly to the Bertrand curves. Offset surfaces also retain the same degree of continuity piecewise as the original surfaces. The significance of this is that offset surfaces themselves

can easily be approximated by polynomial surfaces. The accuracy of the approximation depends on the differential features of the original surface. Farouki suggests a post approximation accuracy check and subdivision of the surface patch if the tolerance is more than the allowed value [Farouki-86].

Offset surfaces can have anomalies depending on the original surfaces. The offset surface will have holes where the original surface has a vertex or an edge, or self intersecting loops where the offset distance is more than the principal radius of the surface in a concave section. In order to find the areas of difficulties on the surface, an analysis of the surface is required in the tool path planning stage [Farouki-86, Chen-87, Su-91].

4.1.2 5-axis Tool Path Generation with an End Cutter

In 5-axis machining the tool is kept at a constant relation to the part surface along the tool path. Consequently, the contact point on the tool between the tool and the part does not change during the machining process. The tool center point **TCP** is always offset with a vector, with the length of the tool radius R as shown in Figure 4.2. The vector is always in a constant relation to the plane specified by the surface normal **N** and by the tangent vector **T** to the tool path.

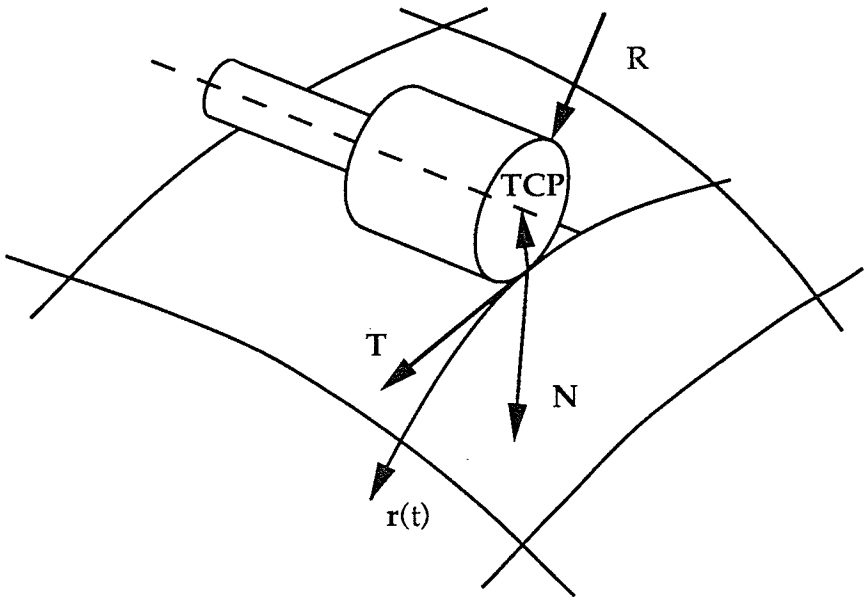

Figure 4.2. 5-axis tool path.

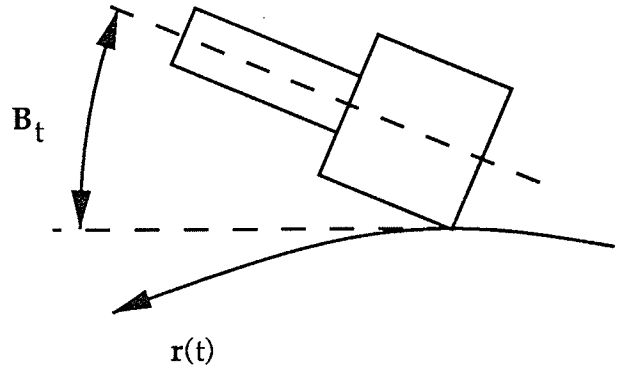

Figure 4.3. Tool tilt angle.

The relation of the tool to the part at the contact point is described by two angles, the lead angle A_t, and the tilt angle B_t as shown in Figure 4.4 and Figure 4.3.

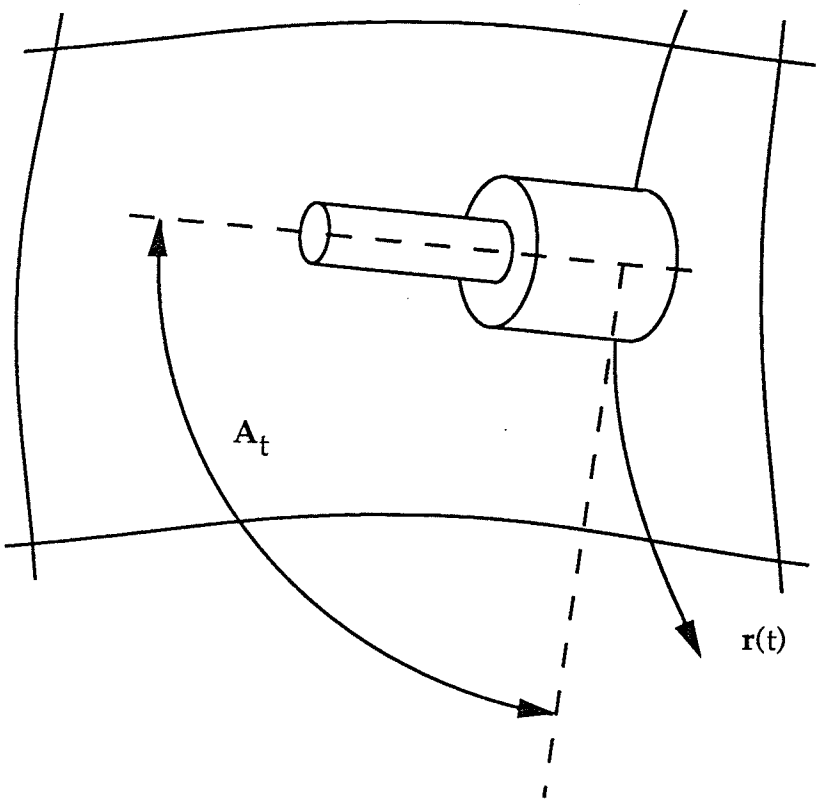

Figure 4.4. Tool lead angle.

A five axis machine tool has two rotary axes to maintain the constant relation between the tool and the part. Figure 4.5 shows the coordinate system layout of a 5-axis machine tool according to the EIA standard RS-267 [Pressman-77].

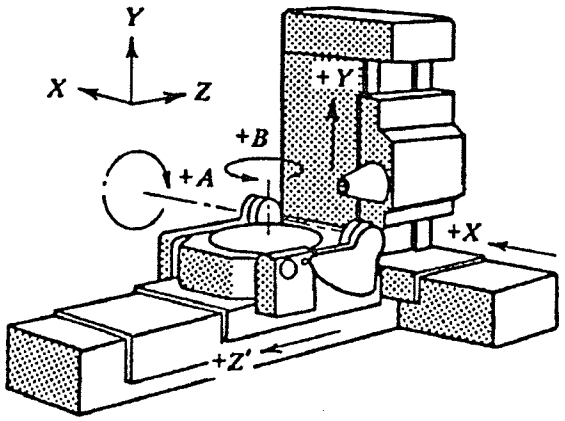

Figure 4.5. 5-axis machine tool.

Coordinates for machining are given in a coordinate system attached to the part. These coordinates have to be transformed into the coordinate system of the machine tool, which can be controlled by the Numerical Controller. The part is attached to the rotary table, and it has a part offset, the offset between the origin of the part coordinate system and the intersection of the rotary axes. If the A and B rotary axes are turned by angles of α and β about the x and y axis, and the linear axis displacements are x, y, and z, the transformation from the part coordinate system to the machine coordinate system can be calculated by using the methodology developed by Paul [Paul-81, Snyder-85] for robot kinematics calculations:

$$\mathbf{p}_m = \mathbf{T}(x,y,z)\, \mathbf{R}_x(\alpha)\, \mathbf{R}_y(\beta)\, (\mathbf{p}_o + \mathbf{p}_p) \tag{4.11}$$

$\mathbf{p}_p$ is a point on the part given in the part coordinate system, $\mathbf{p}_m$ is the same point in the machine tool coordinate system, and $\mathbf{p}_o$ is the part offset. The representation of $\mathbf{p}_i$ are in homogeneous coordinates, the definition of a vector augmented by an additional component with a value of 1, allowing for a concise matrix representation for both the translation and rotation transformations:

$$\mathbf{p}_p = [x_p, y_p, z_p, 1]^T \tag{4.12}$$

$$\mathbf{p}_m = [x_m, y_m, z_m, 1]^T \tag{4.13}$$

$$\mathbf{p}_o = [x_o, y_o, z_o, 1]^T \tag{4.14}$$

The transformation matrixes are given as below:

$$\mathbf{T}(x,y,z) = \begin{bmatrix} 1 & 0 & 0 & x \\ 0 & 1 & 0 & y \\ 0 & 0 & 1 & z \\ 0 & 0 & 0 & 1 \end{bmatrix}, \tag{4.15}$$

$$\mathbf{R}_x(\alpha) = \begin{bmatrix} 1 & 0 & 0 & 0 \\ 0 & \cos\alpha & -\sin\alpha & 0 \\ 0 & \sin\alpha & \cos\alpha & 0 \\ 0 & 0 & 0 & 1 \end{bmatrix}, \tag{4.16}$$

$$\mathbf{R}_y(\beta) = \begin{bmatrix} \cos\beta & 0 & \sin\beta & 0 \\ 0 & 1 & 0 & 0 \\ -\sin\beta & 0 & \cos\beta & 0 \\ 0 & 0 & 0 & 1 \end{bmatrix} \tag{4.17}$$

Note that different 5-axis machine tools can have different morphologies, i.e. different kinematic chains with different transformation matrices associated with them. Examples are machine tools which have a tilting head and a rotary table and machine tools with rotary tables whose rotational axes do not intersect. Sakamoto and Inasaki made an exhaustive theoretical analysis of all the possible 5-axis machine tool configurations and the mathematical descriptions of their kinematics [Sakamoto-93].

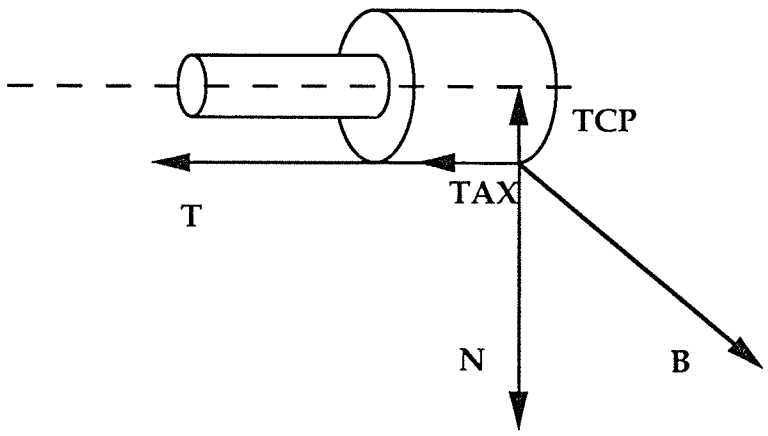

Figure 4.6. 5-axis tool center point vector.

Figure 4.6 introduces the **TCP** and **TAX** vectors which are attached to the tool and their relation to the **TNB** coordinate system when the $\mathbf{A_t}$ and $\mathbf{B_t}$ tool lead and tilt angles are both zero.

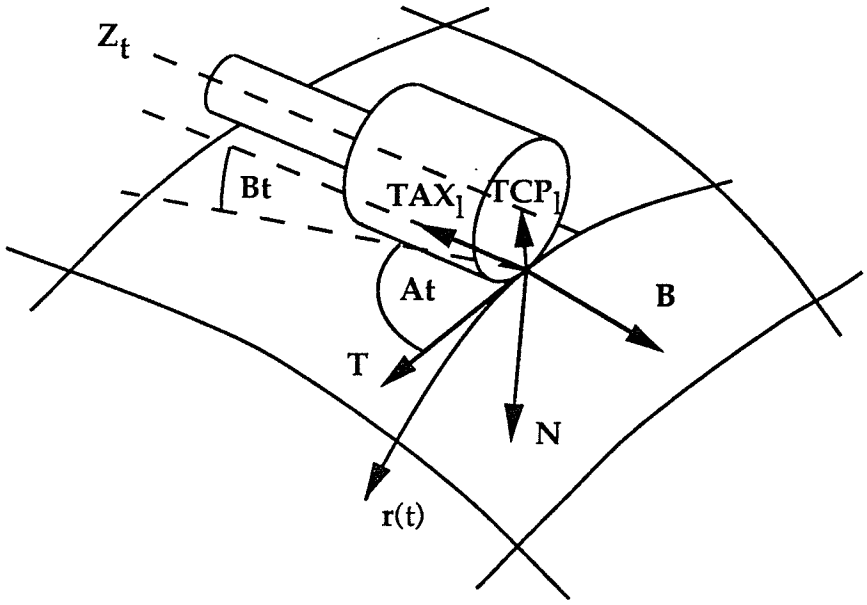

Figure 4.7. 5-axis tool center point vector.

The α and β rotational angles can be defined from the local **TNB** coordinate system and from the required $\mathbf{A_t}$ and $\mathbf{B_t}$ tool lead and tilt angles. (See Figure 4.7.) The diagram shows the angles to the **TAX** vector for clarity, which is parallel to the $\mathbf{Z_t}$ tool axis.

The α and β angles of the **A** and **B** rotational axis should be set in a way such that the $\mathbf{Z_t}$ tool axis would line up parallel with the machine tool **Z** axis.

The **TNB** local coordinate system moves along the tool path with the contact point on the surface and is constructed from the tool path tangent

unit vector **T**, the surface normal **N** unit vector, and the binormal vector **B** at the contact point.

The **T** vector can be calculated in the following way:

$$\mathbf{T} = \frac{\mathbf{r}'}{|\mathbf{r}'|} \tag{4.18}$$

where $\mathbf{r}'$ can be calculated with the chain rule:

$$\mathbf{r}' = \frac{d\ \mathbf{r}(t)}{dt} = \frac{\partial \mathbf{r}}{\partial u}\frac{\partial u}{\partial t} + \frac{\partial \mathbf{r}}{\partial v}\frac{\partial v}{\partial t} = \mathbf{r}_u\ u' + \mathbf{r}_v\ v' \tag{4.19}$$

The **N** normal vector:

$$\mathbf{N} = \frac{\mathbf{r}_u \times \mathbf{r}_v}{H}, \quad H = |\mathbf{r}_u \times \mathbf{r}_v| \neq 0 \tag{4.20}$$

B is the cross product of **T** and **N**. **B** is a unit vector itself, as **T** and **N** are unit vectors, and **T** and **N** are also at right angles to each other:

$$\mathbf{B} = \mathbf{T} \times \mathbf{N} \tag{4.21}$$

The **TNB** coordinate system is also known as the Frenet Frame [Faux-79, Farin-93].

The **TCP** tool center point in the local **TNB** coordinate system can be defined as two successive rotations of the -**RN** vector, first about the **B**, then about the **N** axis by $\mathbf{B_t}$ and $\mathbf{A_t}$ angles:

$$\mathbf{TCP} = [0\ -R\ 0\ 1]^T \tag{4.22}$$

$$\mathbf{TCP_1} = \mathbf{R_N}(A_t)\ \mathbf{R_B}(B_t)\ \mathbf{TCP} \tag{4.23}$$

The **TAX** tool axis vector in the local **TNB** coordinate system can be similarly calculated, as two successive rotations of the **T** vector:

$$\mathbf{TAX} = [1\ 0\ 0\ 1]^T \tag{4.24}$$

$$\mathbf{TAX_1} = \mathbf{R_N}(A_t)\ \mathbf{R_B}(B_t)\ \mathbf{TAX} \tag{4.25}$$

And the rotational matrixes are:

$$\mathbf{R_N}(A_t) = \begin{bmatrix} \cos A_t & 0 & \sin A_t & 0 \\ 0 & 1 & 0 & 0 \\ -\sin A_t & 0 & \cos A_t & 0 \\ 0 & 0 & 0 & 1 \end{bmatrix}, \tag{4.26}$$

$$\mathbf{R}_B(B_t) = \begin{bmatrix} \cos B_t & -\sin B_t & 0 & 0 \\ \sin B_t & \cos B_t & 0 & 0 \\ 0 & 0 & 1 & 0 \\ 0 & 0 & 0 & 1 \end{bmatrix} \tag{4.27}$$

The tool center point and the tool axis vector in the part coordinate system can be obtained with the following transformations:

$$\mathbf{TCP}_p = \mathbf{T}_{TNB}\,\mathbf{TCP}_l \tag{4.28}$$

$$\mathbf{TAX}_p = \mathbf{T}_{TNB}\,\mathbf{TAX}_l \tag{4.29}$$

The $\mathbf{T}_{TNB}$ transformation matrix is formed in the following way:

$$\mathbf{T}_{TNB} = \begin{bmatrix} T_x & N_x & B_x & x_p \\ T_y & N_y & B_y & y_p \\ T_z & N_z & B_z & z_p \\ 0 & 0 & 0 & 1 \end{bmatrix} \tag{4.30}$$

where **T**, **N** and **B** are the axis of the **TNB** local coordinate system and x_p, y_p, z_p are the origin of the **TNB** coordinate system.

The tool center point coordinates now can be calculated in the machine coordinate system with the following general transformation:

$$TCP_m = T(x,y,z)\, R_x(\alpha)\, R_y(\beta)\, (p_o + T_{TNB}\, TCP_l) \tag{4.31}$$

Note that this treatment of the coordinate transformation differs from the one generally used for robot kinematics calculations, though it uses the same tools, originally introduced by Paul [Paul-81] to solve robotic problems. Robot kinematics is usually described from the robot's point of view: the position and orientation of the endeffector is described in the world coordinate system, the coordinate system of the robot's base. This is well suited to problems usually faced by robots: manipulating objects, given in the world coordinate system. This contrasts with the problems in 5-axis machining, i.e. moving the tool along a tool path which is described in the part's local coordinate system. Both approaches are equivalent, resulting in the same solution. Rüegg and Gygax used the inverse kinematics approach, for moving the machine tool axes and executing the inversion in real-time [Rüegg-92].

4.1.3 5-axis Tool Path Generation with a Ball Nose Cutter

Doing 5-axis machining with a ball nose cutter is a variation of 5-axis machining. When machining with a ball nose cutter, the orientation of the tool to the part surface along the tool path is allowed to change, actually, it is programmed to change. The reason is that the access of the tool to some parts of the surface could be limited due to the fixturing and due to the complex geometry of a part. For reducing the number of set-ups necessary to machine

the part, the orientation of the tool to the part surface is changed during the tool path to allow for better access to the part. The consequence of this is that the contact point on the tool between the tool and the part surface does change during the machining process. As the contact point moves around the tool tip, the effective length T_l and radius of the tool T_r changes. In other words, the tool center point transformation is changing continuously. Figure 4.8.

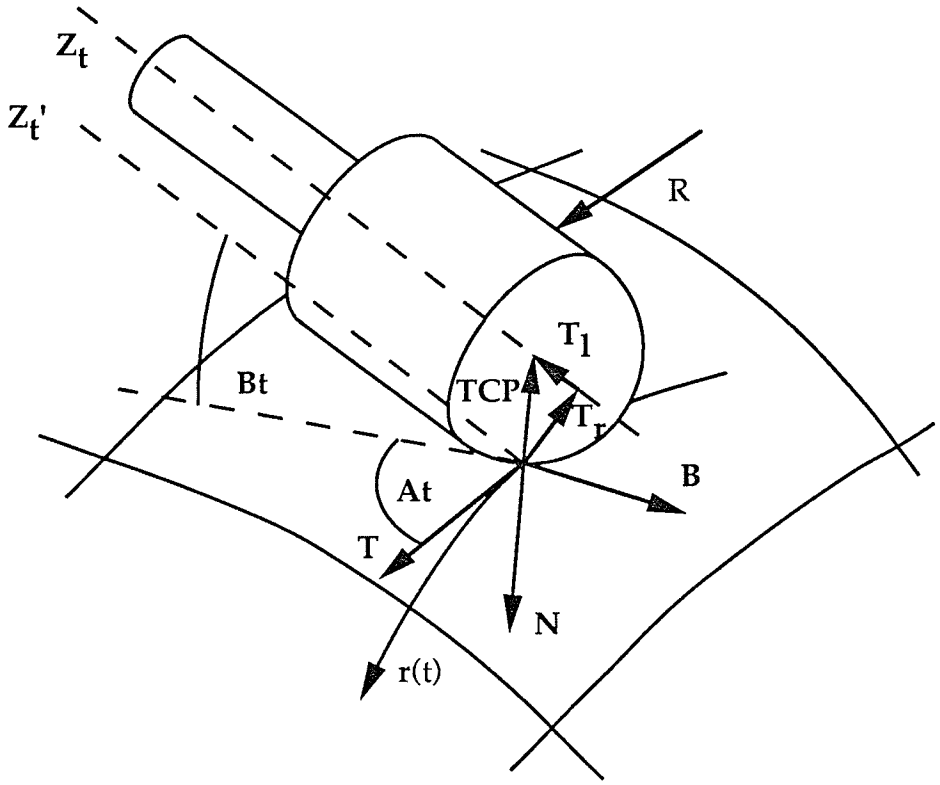

Figure 4.8. 5-axis tool center point vector with ball nose cutter.

Because the tool end is a sphere, the tool center point can be calculated very easily, as it is along the surface normal at a distance R from the surface.

This means that the tool center point transformation does not need to be evaluated for finding the tool center point, as is the case for the regular 5-axis machining. Figure 4.9 shows a side view of the tool center point.

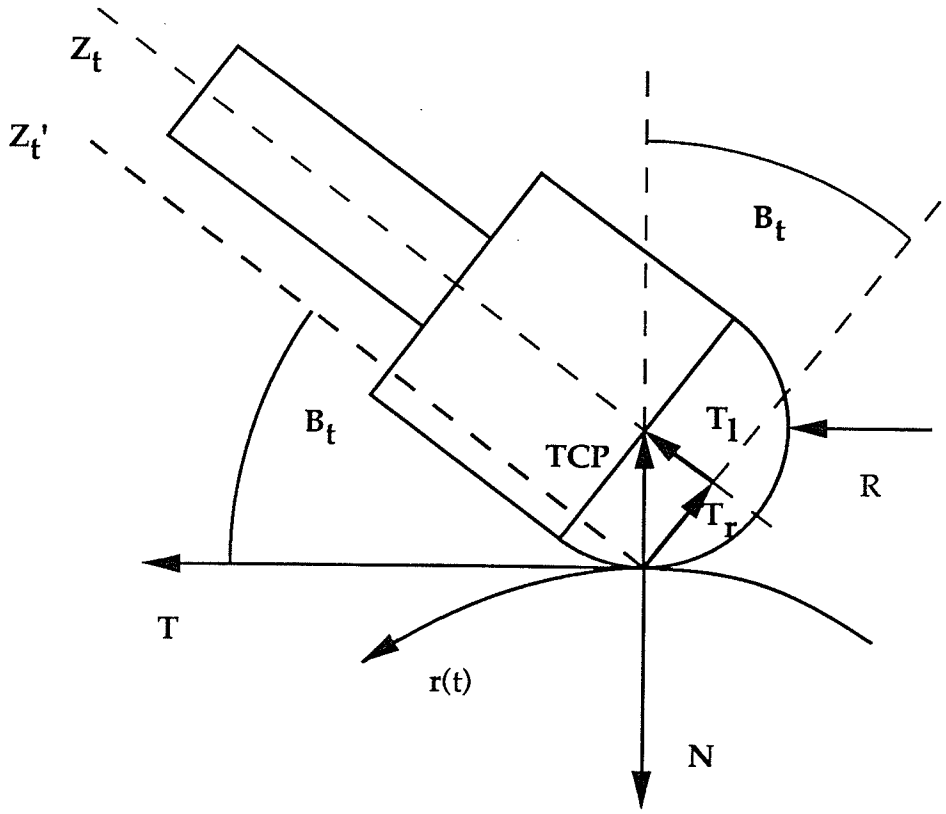

Figure 4.9. 5-axis tool center point angles with ball nose cutter.

Mathematically speaking, the **TCP** tool center point in the local **TNB** coordinate system can be defined as the -**RN** vector:

$$\mathbf{TCP}_l = [0\ -R\ 0\ 1]^T, \tag{4.32}$$

From this step on, mathematically, the tool path calculation is the same as for the 5-axis machining with an end cutter.

4.2 Advanced Path Generator System Description

As discussed in Section 1 of Chapter 2, the optimal system design for the part production consists of three layers: design, planning and production. This layering also determines the partitioning and task distribution of the implementation. In other words, the layering is what establishes the specifications for the individual modules and, consequently, for the path generator in the controller. The detailed specification for the path generator module is now given.

4.2.1 Advanced Path Generator Specification

The key elements of the specifications for the advanced path generator of the NC controller are:

(1) The tool path is given either as a 3-axis or a 5-axis machining command. This states that the path generator should be able to control the machine tool according to the popular sculptured surface machining techniques.

(2) The surfaces to be machined are described by NURBS patches. The path generator has to have access to the description of the surfaces. As machining across surface boundaries is a requirement, all or several of the patches has to be available in the controller before the machining takes place.

(3) The tool path is given as consecutive blocks of motions. A particular block of tool path motion is given as a linear function in the parameter space of a single surface patch. The tool path should also include the surface identifier.

(2) and (3) address the data abstraction problem. Instead of passing low level information to the controller, the commands are given in a concise, high level format. The geometry of the surface is passed to the controller in the form of NURBS data description. The tool path is given in the NURBS variable space, in the u, v parameters. Limiting the tool path in the parameter space to a linear function restrains the degree of calculations necessary to evaluate the surface in the controller. If a single linear tool path representation in the u, v space does not give enough control over the desired trajectory of the tool path on the surface patch, then that tool path should be composed of several linear segments. That segmentation has to be implemented in the planning stage. The amount of information passed to the controller is decreased, instead of the huge amount of line segments, only the data to calculate the tool path is passed. The expansion of the motion segments into axis motion is done in the controller, resulting in a much finer representation of the surface than the conventional line segment approximation. This results in better part surface, requiring less hand finishing. Also, as the machine tool motion commands are not

discontinuous (in acceleration) line segments, the movement of the machine tool is smoother, absent of sudden directional changes.

(4) For 5-axis machining, the tool path should also include the tool orientation to the surface, the tool tilt angle, and the tool lead angle. 5-axis machining with a ball nose cutter permits the changing of the tool tilt and lead angles during a motion block. The tilt and lead angles are kept constant during a motion block for machining with an end cutter. This constraint has implications only in terms of computational load. Limiting the tool orientation angles for end cutters to constants during a tool path segment does not have any theoretical significance, it only means that the tool transformation matrix needs to be calculated only once before a tool path segment and not at every sampling period. 5-axis machining with an end cutter usually keeps the tool orientation angle constant. Strictly speaking, this is only an implementation issue.

(5) The machining speed is given as the surface speed of the contact point between the tool and the part, and it is kept constant during a motion block. Because of this, even if the contact point moves around, as is the case with 3-axis machining, the machining speed does not change. This is in contrast with the conventional machining, where the motion of the tool end point is programmed resulting in wide variations in the machining speed when cutting areas with high curvature. Keeping the speed under control results in better finish and accuracy.

(6) The path generator should compensate for part placement and tool geometry, based on the actual part and tool set-up data and the type of machining. The part and tool set-up can be defined at the planning stage of the production process. Values need to be known only nominally while

planning, and the actual values can be applied at the time of machining. The part and tools need not be set up accurately on the machine, only the result of the set-up needs to be known. It is simpler and faster to measure them than to set them to predefined numbers. Only one set of NC programs needs to be prepared with the nominal tool and part set-up and individual tapes corresponding to actual tools and part placements are not needed.

In summary, an NC controller equipped with the above specified path generator addresses the problems described in Chapter 2.2. The disadvantages mentioned there are the consequence of doing the sculptured surface machining with line segment approximation. Generating the tool path on the NURBS surfaces in the controller results in better part finish, less intermediate data, and manufacturing decisions made at the right place and right time. This makes the sculptured surface part production less prone to human error, faster and more efficient, and ultimately resulting in lower production costs.

4.3 Real Time Tool Path Generation

Tool path generation in the machine tool controller means the real-time generation of the components of the trajectory for each of the machine tool axes. The combination of the motion components through the kinematics of the machine tool results in the desired relative motion of the tool and the part to be machined. The tool path given to the advanced path generator describes the motion of the contact point between the tool and the

part, and the components of this motion have to be calculated in real-time. Existing methods, using conventional NC machines, program the components of the motion, and the NC controller simply executes those commands, it does not do any geometric calculation to control the axes.

The path generator is the core part of any NC controller. The output from the path generator feeds the servo modules directly. Servo modules are digitally realized in state of the art controllers, implementing the control loops with sampled data control systems. The implication of this is that the path generator should work synchronously with the servo control loop, providing the servo loop with new data in each sample period. In other words, the cycle time of the tool path calculation is the same as that of the servo control loop. This statement assumes that the path generation is implemented in one level. The calculations for two level path generation theoretically do not differ from the single level one. In this case the top level calculation provides data points to the low level interpolator only at every n-th point - n being an installation value - and the low level interpolator does the fine interpolation. It has to be assured that the loss of accuracy resulting from the two level interpolation is below a given tolerance for all trajectories.

In the following chapters, the details of the advanced path generator will be given with simulation results and test data.

4.3.1 Steps of Real Time Tool Path Generation

Without over simplifying the real-time tool path generation, it consists of two main steps that has to be accomplished at each sampling period:

First, calculation of the contact position on the surface based on the surface description and the tool path given in the parameter space has to be carried out.

Secondly, the tool transformation has to be evaluated based on the type of machining and on the part and tool set-up data to position the individual axes of the machine tool accordingly.

The machining speed control is done at the contact position calculation stage. The speed given in an NC block is the surface traversal speed, the speed of the tool contact point with the part, in relation to the part surface.

4.3.1.1 Contact Position Calculation

Contact position calculation means finding the contact point on the surface patch. According to the specification, the tool path is given as a line in the u, v parameter space with t being the independent parameter (4.33). The speed of incrementing t controls the speed of the trajectory traversal, hence it controls the speed of machining:

$$u = a_u + b_u * t$$
$$v = a_v + b_v * t \qquad (4.33)$$

The parameters a_u, b_u, a_v, b_v can be calculated from the start and end points of the u, v line, assuming that the t parameter runs from 0 to 1:

$$a_u = u_s$$

$$b_u = u_e - u_s$$

$$a_v = v_s$$

$$b_v = v_e - v_s$$

(4.34)

where

u_s, v_s are the start points of the u, v parameters,

u_e, v_e are the end points of the u, v parameters

When u and v are evaluated - these are the u and v parameter values at the sampling period - the surface point can be calculated. The calculation means the evaluation of equation 3.61, as the NURBS surfaces are tensor product polynomial surfaces. The $F_i(u)$ and $G_j(v)$ basis functions are rational B-spline basis functions as used in equation (3.41):

$$\mathbf{r}(u,v) = \sum_{i=1}^{n+1} \sum_{j=1}^{m+1} \mathbf{a}_{i,j} \; R_{i,k}(u) \; R_{j,l}(v) = \sum_{i=1}^{n+1} \sum_{j=1}^{m+1} \mathbf{a}_{i,j} \; S_{i,j}(u,v)$$

(4.35)

where

$R_{i,k}(u)$, $R_{j,l}(v)$ are the rational B-spline basis functions,

$\mathbf{a}_{i,j}$ are the 3D control points, and

$S_{i,j}(u,v)$ are the bivariate non-uniform rational B-spline surface basis functions:

$$S_{i,j}(u,v) = \frac{w_{i,j}\ N_{i,k}(u)\ N_{j,l}(v)}{\sum_{i=1}^{n+1}\sum_{j=1}^{m+1} w_{i,j}\ N_{i,k}(u)\ N_{j,l}(v)} \tag{4.36}$$

where

$w_{i,j}$ is the weight associated with the i, j control point, and

$N_{i,k}(u)$ and $N_{j,l}(v)$ are the B-spline basis functions.

By substituting the bivariate surface basis function into equation (4.36):

$$\mathbf{r}(u,v) = \frac{\sum_{i=1}^{n+1}\sum_{j=1}^{m+1} \mathbf{a}_{i,j}\ w_{i,j}\ N_{i,k}(u)\ N_{j,l}(v)}{\sum_{i=1}^{n+1}\sum_{j=1}^{m+1} w_{i,j}\ N_{i,k}(u)\ N_{j,l}(v)} \tag{4.37}$$

The $N_{i,k}(u)$ and $N_{j,l}(v)$ basis functions can be defined in a recursive way as given in equation (3.33).

Faster evaluation of the B-spline basis function can be accomplished by observing the features of the B-splines and calculating the values in a forward fashion as opposed to the recursive way. Pavlidis [Pavlidis-82] and Bartels *et. al.* [Bartels-87] describe the algorithm in detail.

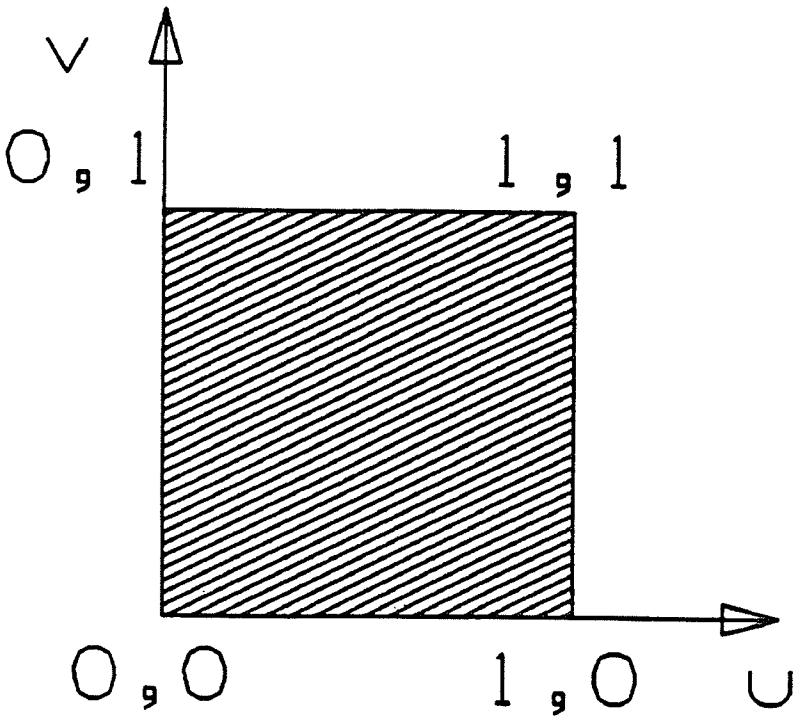

Figure 4.10. UV values for contact position calculation.

By substituting (4.33), the u = u(t) and v = v(t) dependencies into (4.36), the tool path is expressed as a function of the t parameter:

$$\mathbf{r}(t) = \mathbf{r}(u(t), v(t));$$

$$\mathbf{r}(t) = \frac{\sum_{i=1}^{n+1} \sum_{j=1}^{m+1} \mathbf{a}_{i,j}\ w_{i,j}\ N_{i,k}(u(t))\ N_{j,l}(v(t))}{\sum_{i=1}^{n+1} \sum_{j=1}^{m+1} w_{i,j}\ N_{i,k}(u(t))\ N_{j,l}(v(t))} \tag{4.38}$$

The results of the calculations were simulated and verified with a CAD/CAM system. The programming environment was running on a VAX/VMS system, and for graphics rendering and verification the services of the UNIGRAPHICS CAD/CAM[3] system were used. The various steps of the tool path generation were written in the FORTRAN programming language, and linked to the UNIGRAPHICS system.

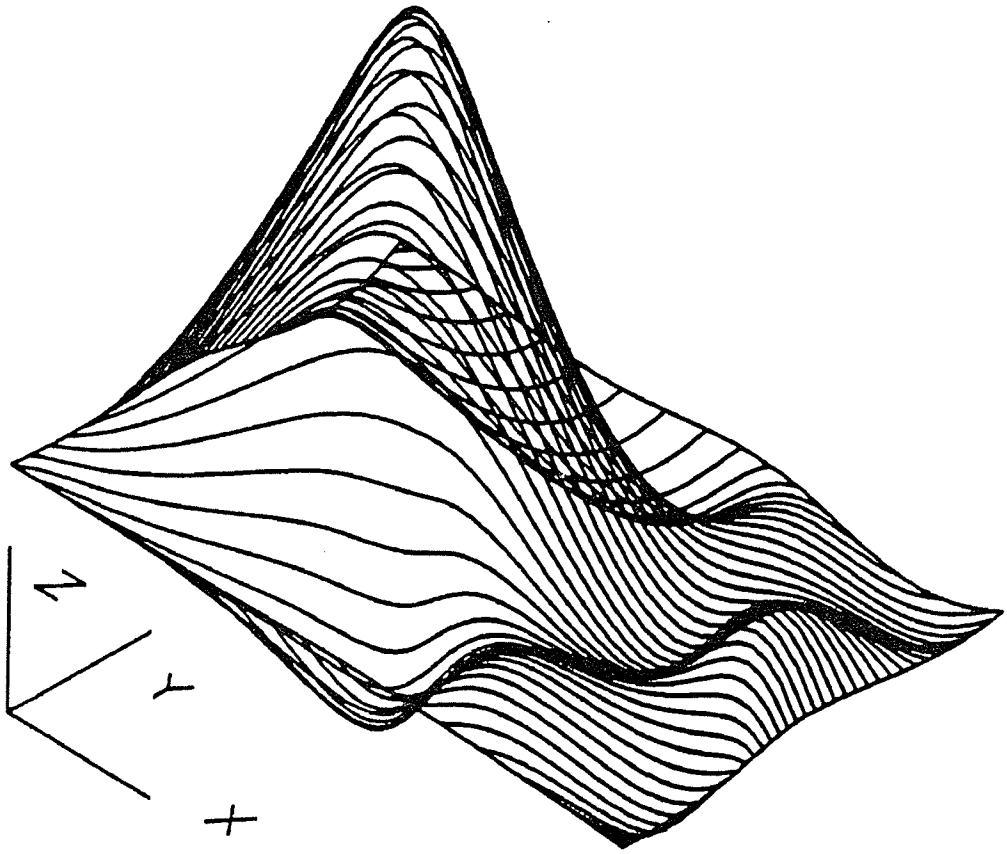

Figure 4.11. 3D test surface.

[3] The UNIGRAPHICS CAD/CAM system is a high-end geometric design and machining system developed by EDS Corporation.

Several test surfaces were used for the simulation. Figure 4.10 shows the uv lines for the contact position calculation.

The figure represents 40 lines, or "tool path" on the surface patch. On the following test surfaces, which are rendered by the above uv lines, the contact points were evaluated 50 times along a single tool path, and connected with line segments to each other. Figure 4.11 shows the tool path on an arbitrary 3D surface.

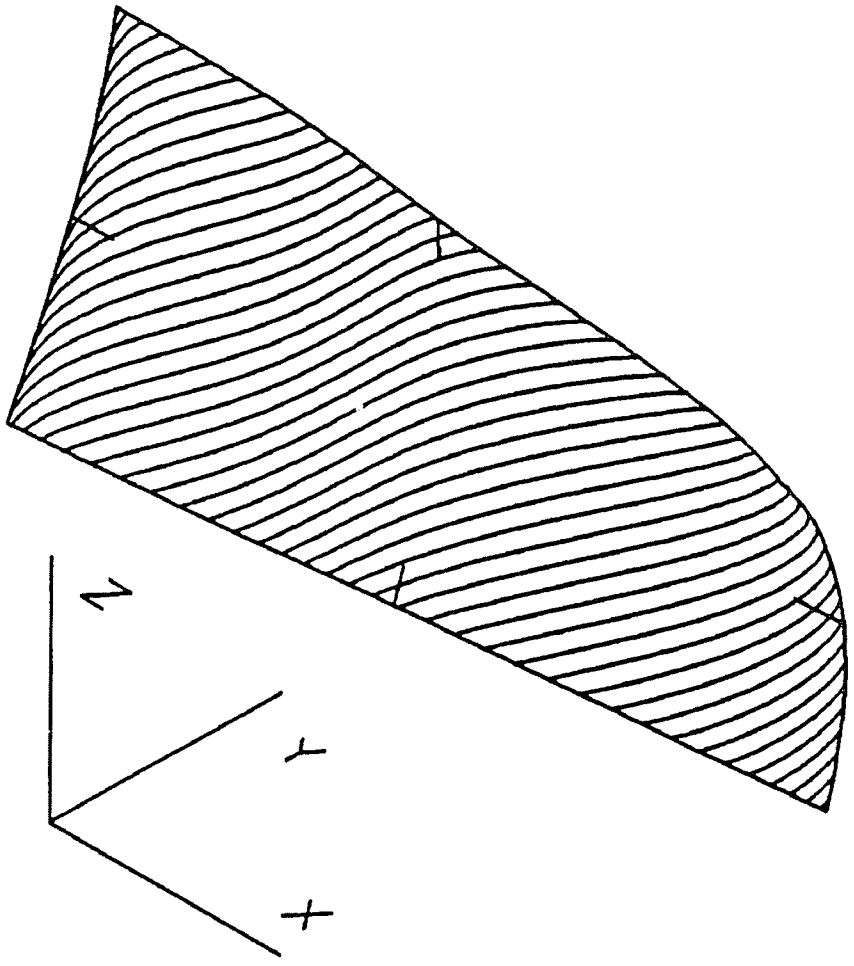

Figure 4.12. Turbine blade test surface.

Figure 4.12 shows the tool path on a turbine blade, where the surface description was taken from a production item.

Figure 4.13 shows the evaluated contact positions on sphere, described by NURBS terms.

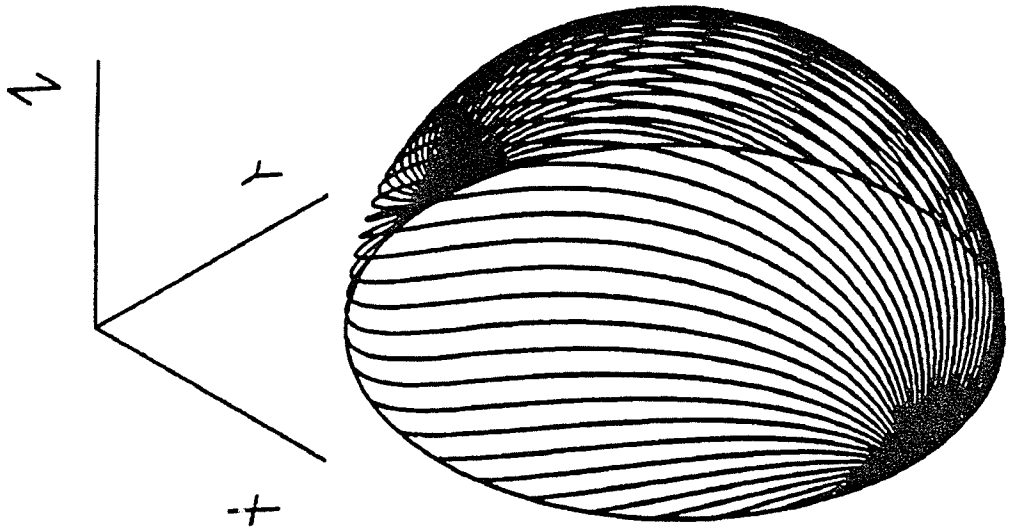

Figure 4.13. Sphere test surface.

The IGES format description of the test surfaces can be found in the Appendix.

4.3.1.2 Speed Control

Controlling the speed of the machining is done by controlling the increments of the t parameter. The t parameter is a general parameterization of the tool path on the surface, and not a curve length parameterization (not even isoparameter curves on the NURBS surfaces are curve length parameterized). The consequence of this is that for controlling the speed, the differential features of the tool path curve have to be evaluated to derive the proper t increment.

By knowing the sampling time T_s and the feedrate, or surface speed F, the tool path increment ΔS is:

$$\Delta S = F * T_s \tag{4.39}$$

Expressing the speed of the tool path as a function of the t parameter[4] is given by the absolute length of the tangent vector of the tool path:

$$v = |\mathbf{T}_t| = \left|\frac{d\mathbf{r}(t)}{dt}\right| \tag{4.40}$$

where v is the speed and

$\mathbf{T}_t$ is the tangent vector

The tool path increment, assuming constant speed during the sampling period, can be calculated from the speed vector:

[4] Note that t is not time.

$$\Delta S = v * \Delta t \tag{4.41}$$

From here the required Δt parameter increment can be derived:

$$\Delta t = \frac{\Delta S}{v} \tag{4.42}$$

And by substituting ΔS from (4.39):

$$\Delta t = \frac{F * T_s}{v} \tag{4.43}$$

The tangent vector of the tool path can be obtained with the aid of the chain rule for partial derivatives of expression (4.38), as in (4.19):

$$\mathbf{T}_t = \frac{\partial \mathbf{r}}{\partial t} = \frac{\partial \mathbf{r}}{\partial u}\frac{\partial u}{\partial t} + \frac{\partial \mathbf{r}}{\partial v}\frac{\partial v}{\partial t} \tag{4.44}$$

The partial derivatives $\partial \mathbf{r}/\partial u$, $\partial \mathbf{r}/\partial v$ can be calculated based on equation (3.43) for the NURBS curves, while $\partial u/\partial t$, $\partial v/\partial t$ can be derived by formally differentiating equation (4.33):

$$\frac{\partial u}{\partial t} = b_u$$

$$\frac{\partial v}{\partial t} = b_v$$

(4.45)

The speed v can be calculated from the components of the $\mathbf{T}_t$ vector:

$$v = |\mathbf{T}_t| = \sqrt{T_x^2 + T_y^2 + T_z^2}$$

(4.46)

where T_x, T_y, T_z are the components of the $\mathbf{T}_t$ vector.

Simulations were carried out to check the accuracy of the speed control. Due to the sampled data nature of the interpolator, calculations are carried out only at the sampling points and not continuously along the path. This discretization of the calculations results in speed variation along the tool path. One of the factors is that the derivative of the $\mathbf{T}_t$ vector is calculated at the beginning of the increment and is thought to be constant during that increment, which it obviously is not. The other element is how the actual traveled distance, ΔS, is calculated. If the steps are small enough, the distance can be approximated by the linear distance, or cord length between the points. More accurate calculations can be carried out based on the length of arc with the radius of curvature of the tool path. Figure 4.14 shows the graphical depiction for this approach, exaggerated in scale for easier understanding.

$\mathbf{r}(t)$ is the tool path, $\mathbf{T}_{t,i}$, $\mathbf{T}_{t,i+1}$ are the tangent vectors, **Al** and **Cl** are the arc length and cord length respectively.

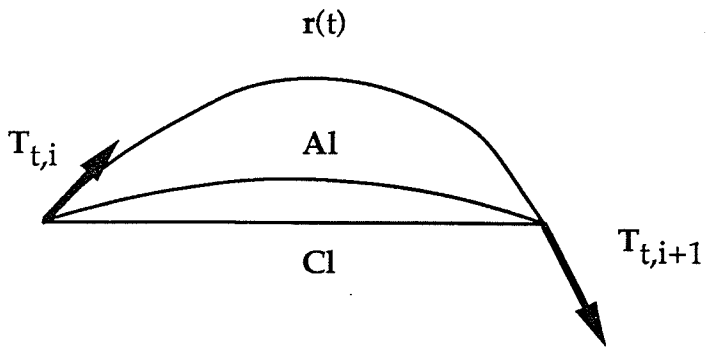

Figure 4.14. Speed calculation.

All the test surfaces were used for the evaluation. The tool path tested in all cases moved in the uv plane from 0, 0 to 1, 1 coordinates. Table 4.1 shows the results for the 3D test surface, Table 4.2 for the turbine blade test surface, and Table 4.3 shows the results for the sphere test surface.

The columns in the tables are as follows:

Step Size - the distance in inches that the tool should move between the sampling periods. This value comes from the given feed rate F and the sampling time period.

Cord Length Tolerance - the maximum variation in percentage of the incremental distances from each other, based on cord length calculation. This translates into the observed speed variation of the contact point.

Arc Length Tolerance - percentage of the maximum variation in the incremental distances from each other, based on arc length calculation. This again shows the actual speed variation of the contact point.

Derivative Tolerance - this is the maximum variation (in percentage) of the speed v, the variation of the absolute value of the $\mathbf{T}_{t,i}$, $\mathbf{T}_{t,i+1}$ vector at both ends of a segment.

Cycle - the number of steps required to cover the whole tool path.

Total Cord Length - the sum of the tool path increments based on cord length calculation.

Total Arc Length - the total tool path based on cord length calculation.

Table 4.1. Speed control accuracy on 3D test surface, with tool path from 0, 0 to 1, 1 in the uv plane.

Step size	Cord Length Tol.	Arc Length Tol.	Deriv. Tol.	Cycle	Total Cord Length	Total Arc Length
0.3	71	54	82.7	39	11.11	11.16
0.1	47	44	36.7	114	11.21	11.22
0.03	12.4	12.2	12.4	377	11.25	11.25
0.01	3.96	3.96	4.22	1129	11.27	11.27
0.003	1.17	1.17	1.26	3761	11.28	11.28

As it can be seen from the tables, there is a good correlation between the step size and the speed variation. As the steps decrease, the speed variation decreases as well. Using arc length calculations, as opposed to cord length calculation, did not make much difference when the steps were

reasonably small. This is also shown by the fact that the total distance traveled is the same obtained by both calculations. There is also a good correlation between the speed variation and the variation of the derivative. It can be concluded that the speed variation depends primarily on the differential features of the surface and the tool path taken. For example, looking at the sphere test surface, which has uniform differential features, the variation data is about a magnitude smaller than on the other surfaces, but the linear tool path in the uv plane translates into an S curve on the surface. (See Figure 4.13.) The effect of the curved traversal of the surface also shows up in the relatively high figures for the derivative tolerance of the tool path.

Table 4.2. Speed control accuracy on turbine blade test surface, with tool path from 0, 0 to 1, 1 in the uv plane.

Step size	Cord Length Tol.	Arc Length Tol.	Deriv. Tol.	Cycle	Total Cord Length	Total Arc Length
0.3	29.8	28.2	50.5	27	7.51	7.52
0.1	17.9	17.0	31.8	78	7.59	7.58
0.03	6.74	6.57	11.6	257	7.64	7.64
0.01	2.25	2.24	3.91	768	7.66	7.57
0.003	0.677	0.675	1.17	2555	7.66	7.66

Table 4.3. Speed control accuracy on sphere test surface, with tool path from 0, 0 to 1, 1 in the uv plane.

Step size	Cord Length Tol.	Arc Length Tol.	Deriv. Tol.	Cycle	Total Cord Length	Total Arc Length
0.3	15.0	14.5	14.3	14	3.59	3.62
0.1	4.97	4.95	4.85	40	3.79	3.80
0.03	1.47	1.47	1.46	129	3.81	3.81
0.01	0.488	0.488	0.487	384	3.82	3.82
0.003	0.146	0.146	0.146	1275	3.82	3.82

Limiting the tool path in the uv plane from 0.1, 0.1 to 0.9, 0.9, effectively leaving out the edges of the test surfaces, assuming that more uniform differential features exist inside the patch, the simulations were repeated. The results are in tables 4.4, 4.5, and 4.6 respectively.

Table 4.4. Speed control accuracy on 3D test surface, with tool path from 0.1, 0.1 to 0.9, 0.9 in the uv plane.

Step size	Cord Length Tol.	Arc Length Tol.	Deriv. Tol.	Cycle	Total Cord Length	Total Arc Length
0.3	141.7	103.5	85.46	34	9.73	9.82
0.1	46.39	43.6	35.21	100	10.11	10.12
0.03	12.31	12.19	12.34	329	9.91	9.91
0.01	3.96	3.96	4.22	985	9.86	9.86
0.003	1.17	1.17	1.26	3279	9.84	9.84

Table 4.5. Speed control accuracy on turbine blade test surface, with tool path from 0.1, 0.1 to 0.9, 0.9 in the uv plane.

Step size	Cord Length Tol.	Arc Length Tol.	Deriv. Tol.	Cycle	Total Cord Length	Total Arc Length
0.3	11.53	11.55	11.50	23	6.35	6.35
0.1	4.61	4.61	4.95	67	6.80	6.80
0.03	1.69	1.69	2.07	222	6.70	6.70
0.01	0.574	0.574	0.707	662	6.63	6.63
0.003	0.174	0.174	0.216	2203	6.61	6.61

Table 4.6. Speed control accuracy on sphere test surface, with tool path from 0.1, 0.1 to 0.9, 0.9 in the uv plane.

Step size	Cord Length Tol.	Arc Length Tol.	Deriv. Tol.	Cycle	Total Cord Length	Total Arc Length
0.3	12.84	12.9	13.57	12	3.00	3.02
0.1	4.91	4.91	4.82	34	3.48	3.49
0.03	1.47	1.47	1.47	109	3.31	3.31
0.01	0.487	0.487	0.486	323	3.24	3.24
0.003	0.146	0.146	0.146	1073	3.22	3.22

The speed variation is smaller when limiting the tool path within the patch. This reflects the fact that when designing the surface for the boundary regions, the CAD systems usually work with assumption about the differential features of the surfaces (tangents, curvatures, twist vectors).

Theoretically, controlling the machining speed accurately does not have any relevance to the accuracy of the resulting part geometry. In practice, there is a strong correlation between the proper machining technology (including the speed) for the part and the accuracy of the machined part.

The maximum allowable step size translates into maximum allowable machining speed, after by taking into consideration the sampling time T_s of the tool path calculation. For a fixed step size, the smaller the sampling time T_s, the faster the machine can be moved on the surface within the required speed tolerance.

4.3.1.3 5-axis Tool Transformation

In discussing the real-time tool transformations, the 5-axis case will be presented first. Then the 3-axis machining will be treated as a special case of the 5-axis machining.

Real-time five-axis tool transformation is based on equation (4.31), as presented in Section 1.2 of Chapter 4:

$$\mathbf{TCP}_m = T(x,y,z)\, R_x(\alpha)\, R_y(\beta)\, (\mathbf{p}_o + T_{TNB}\, \mathbf{TCP}_l) \tag{4.47}$$

The $\mathbf{TCP}_l$ and $\mathbf{TAX}_l$ vectors represent the tool center point and tool axis vector in the local **TNB** coordinate system (the one which is attached to the part at the contact point, Figures 4.6 and 4.7.) and describe the tool relation with respect to the surface. This is represented by the A_t and B_t tool lead and tilt angles. Mathematically speaking, the transformations are described by equations (4.22-23) and (4.24-25). If the tool orientation is kept constant to the part surface during machining, as specified in point (4) of Section 4.2.1, these vectors need to be evaluated only once before the actual tool path generation. When the A_t and B_t angles are allowed to vary during machining, the $\mathbf{TCP}_l$ and $\mathbf{TAX}_l$ vectors need to be calculated in real-time at each sampling period.

T_{TNB} represents the tool path on the part surface. It is described by the matrix given in (4.27), which in a concise form is:

$$T_{TNB} = [\, \mathbf{T}, \mathbf{N}, \mathbf{B}, \mathbf{r} \,]$$

where $\mathbf{r}$ gives the origin of the T_{TNB} frame. This is the contact point and its real-time calculation including speed control, as discussed in Section 4.3.1.2.

$\mathbf{T}$ is the unit tangent vector of the tool path and is given in equations (4.18) and (4.19).

$\mathbf{N}$ is the unit surface normal at the contact point, and can be calculated based on equations (4.19) and (4.20).

$\mathbf{B}$ is the binormal vector, and it is the cross product of the $\mathbf{T}$ and $\mathbf{N}$ unit vectors (4.21).

The T_{TNB} matrix must be calculated at every sampling point.

$\mathbf{p}_o$ is the part offset in equation (4.46). The usage of this term allows for the arbitrary translation of the part on the machine table. A more general approach is to use a general transformation T_p instead of $\mathbf{p}_o$ that also includes a general rotation of the part as well:

$$TCP_m = T(x,y,z)\, R_x(\alpha)\, R_y(\beta)\, T_p\, T_{TNB}\, TCP_l \qquad (4.48)$$

The T_p matrix takes the following general form:

$$T_p = [\, T_x, T_y, T_z, p_o \,] \tag{4.49}$$

where T_x, T_y, T_z are the **X**, **Y**, **Z** unit vectors of the coordinate system associated with the part and p_o is the offset vector of the origin. The T_p matrix has to be obtained and evaluated only once, from the part set-up on the machine tool, just before machining.

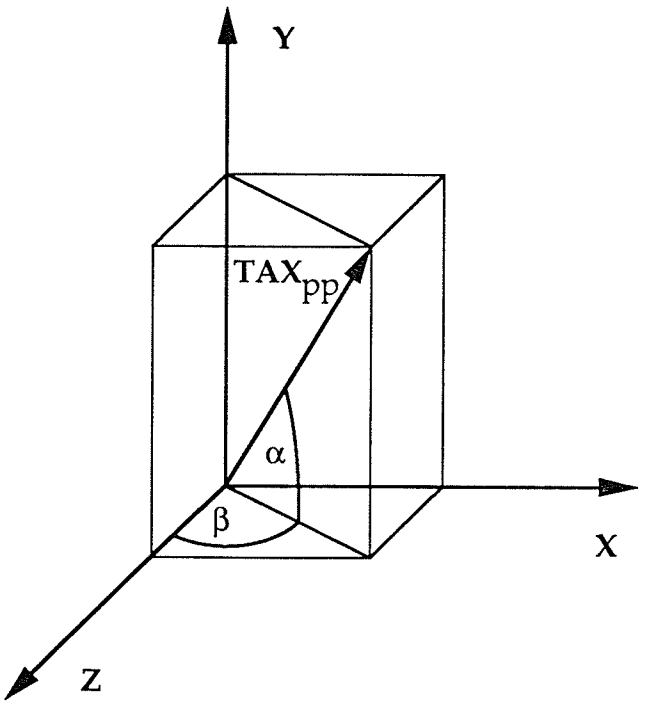

Figure 4.15. 5-axis rotational angles.

Figure 4.15 shows how the α and β angles of the **A** and **B** axis of the machine tool can be calculated to line up the tool axis, which is parallel with

the **TAX** vector, parallel with the machine tool **Z** axis. The α and β values can be derived from the $\mathbf{TAX}_{pp}$ coordinates. The $\mathbf{TAX}_{pp}$ vector is the **TAX** vector transformed by the tool orientation, tool path and part set up:

$$\mathbf{TAX}_{pp} = \mathbf{T}_p \, \mathbf{T}_{TNB} \, \mathbf{TAX}_I \tag{4.50}$$

$$\alpha = \text{atan} \frac{TAX_y}{\sqrt{TAX_x^2 + TAX_z^2}} \tag{4.51}$$

$$\beta = \text{atan} \frac{TAX_x}{TAX_z} \tag{4.52}$$

where TAX_x, TAX_y and TAX_z are components of the $\mathbf{TAX}_{pp}$ vector.

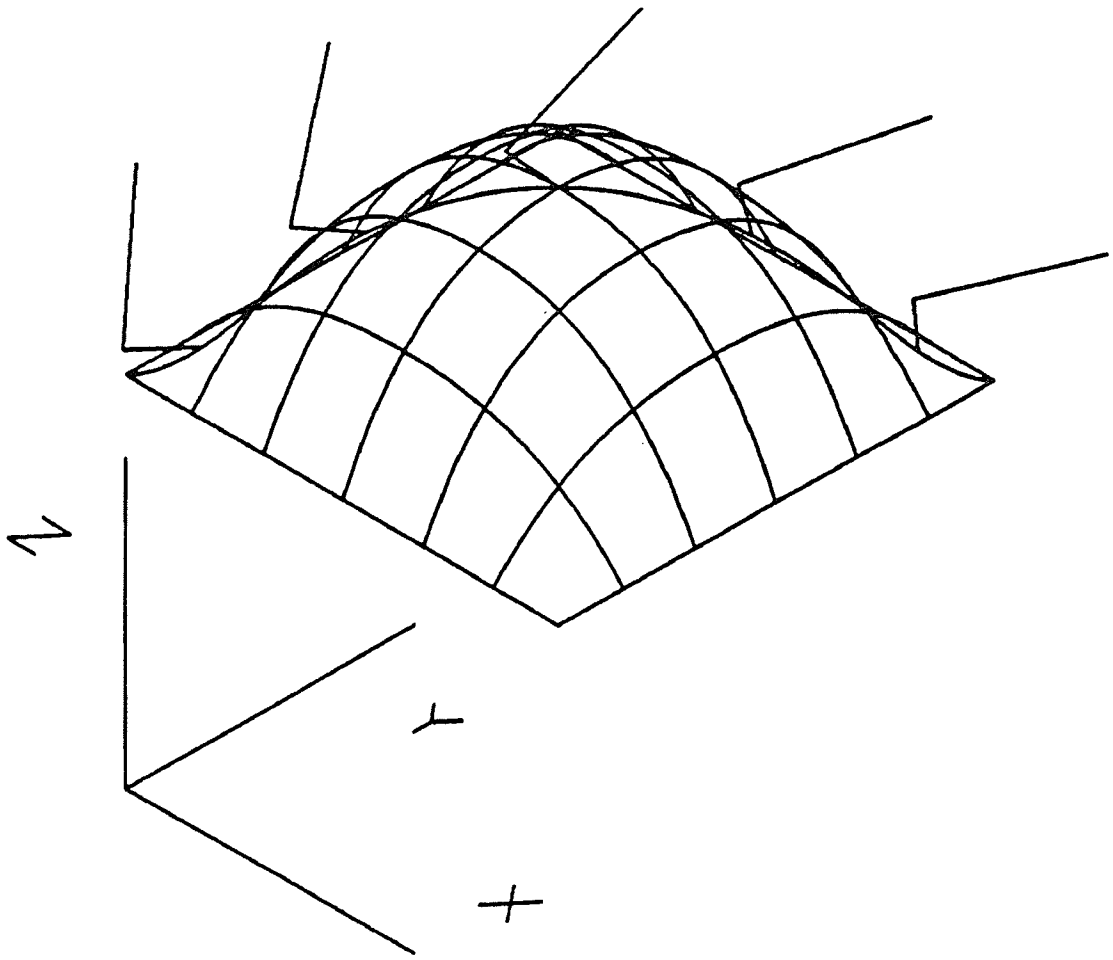

Figure 4.16. 5-axis tool path on a Hermite patch.

Similarly, this calculation has to be carried out at every sampling period. Again, the proper expressions for these angles do vary according to the kinematics of the machine tool.

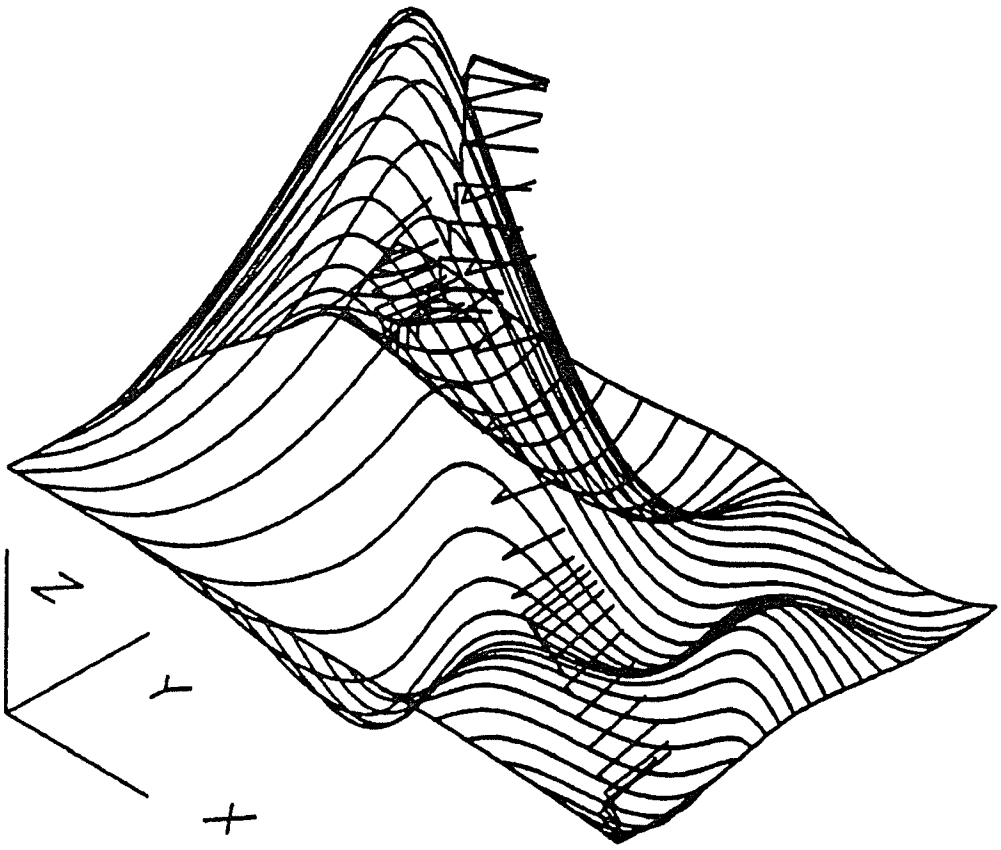

Figure 4.17. 5-axis tool path on 3D NURBS patch.

To obtain the machine coordinates, the final part of the **TCP** vector transformation has to be accomplished, the rotations by the α and β angles, and a general translation by x, y, and z, to move the origin of the machine coordinate system:

$$\mathbf{TCP}_m = \mathbf{T}(x,y,z)\, \mathbf{R}_x(\alpha)\, \mathbf{R}_y(\beta)\, \mathbf{TCP}_{pp} \tag{4.53}$$

This transformation has to be completed at each sampling period.

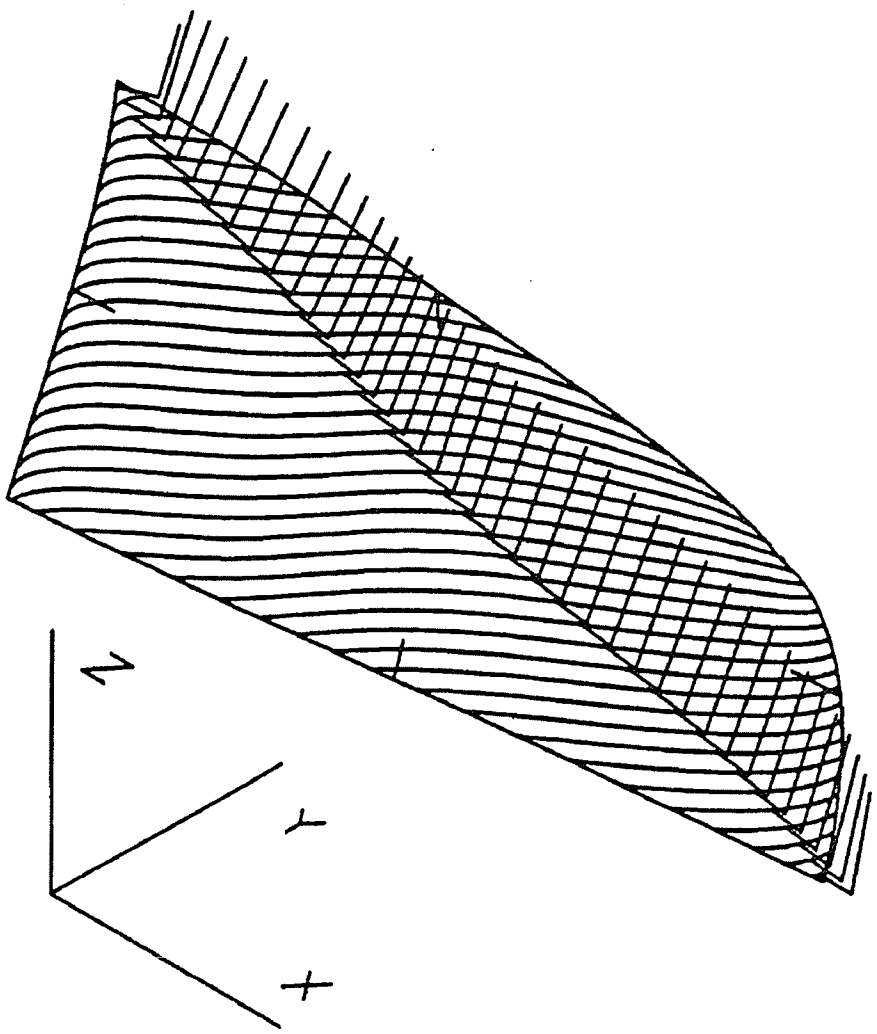

Figure 4.18. 5-axis tool path on turbine blade test surface.

The tool path generation simulations were carried with the test surfaces. Tool path generation on Hermite surfaces was implemented at an

earlier stage of the work, and was reported on in 1992 [Orban-92a, Orban-92b]. Figure 4.16 shows the tool path generated on a Hermite surface patch. The tool is represented by two lines representing the tool radius from the contact point and the tool axis. The tool path traversed from 0, 0 to 1, 1 in the uv plane. The tool symbol was displayed at five locations along the tool path.

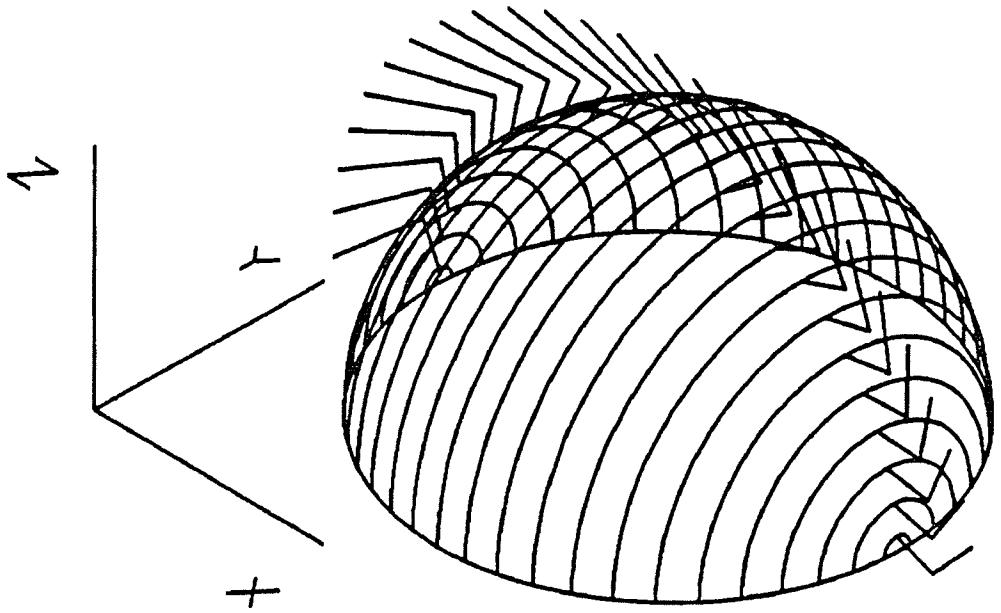

Figure 4.19. 5-axis tool path on sphere test surface.

Figures 4.17, 4.18 and 4.19 show the 5-axis tool path on the 3D test surface, turbine blade test surface, and sphere test surface respectively.

For the 3D test surface and the turbine blade the uv plane was traversed at a 45° angle, while for the sphere the tool paths are parallel with the v axis. The tool symbol is only displayed once along each tool path, in the middle, to

avoid crowding of the picture. For the simulation the tool lead angle was 70°, while for the tool tilt angle 45° was used.

4.3.1.4 5-axis Tool Transformation for Ball Nose Cutter

The 5-axis tool transformation for a ball nose cutter is similar to the general 5-axis calculation described in equation (4.31):

$$\mathbf{TCP}_m = \mathbf{T}(x,y,z)\, \mathbf{R}_x(\alpha)\, \mathbf{R}_y(\beta)\, (\mathbf{p}_o + \mathbf{T}_{TNB}\, \mathbf{TCP}_l) \tag{4.54}$$

As it is recalled, $\mathbf{TCP}_l$ represents the tool center point in the local (**TNB**) coordinate system. For the 5-axis transformation, this meant the transformation of the $\mathbf{TCP} = [0\ -R\ 0\ 1]^T$ (4.22) vector by the rotations for the tool tilt and lead angles. For the ball nose cutter, the tool center point is always along the surface normal, as the tool end is a sphere. That means that $\mathbf{TCP}_l$ will always be equivalent with **TCP**:

$$\mathbf{TCP}_l = \mathbf{TCP} \tag{4.55}$$

The $\mathbf{TAX}_l$ transformation still needs to be accomplished at every sampling point, as the component values of $\mathbf{TAX}_{pp}$ are needed for calculating

α and β angles for the machine tool rotary axes, as described in (4.51) and in (4.52).

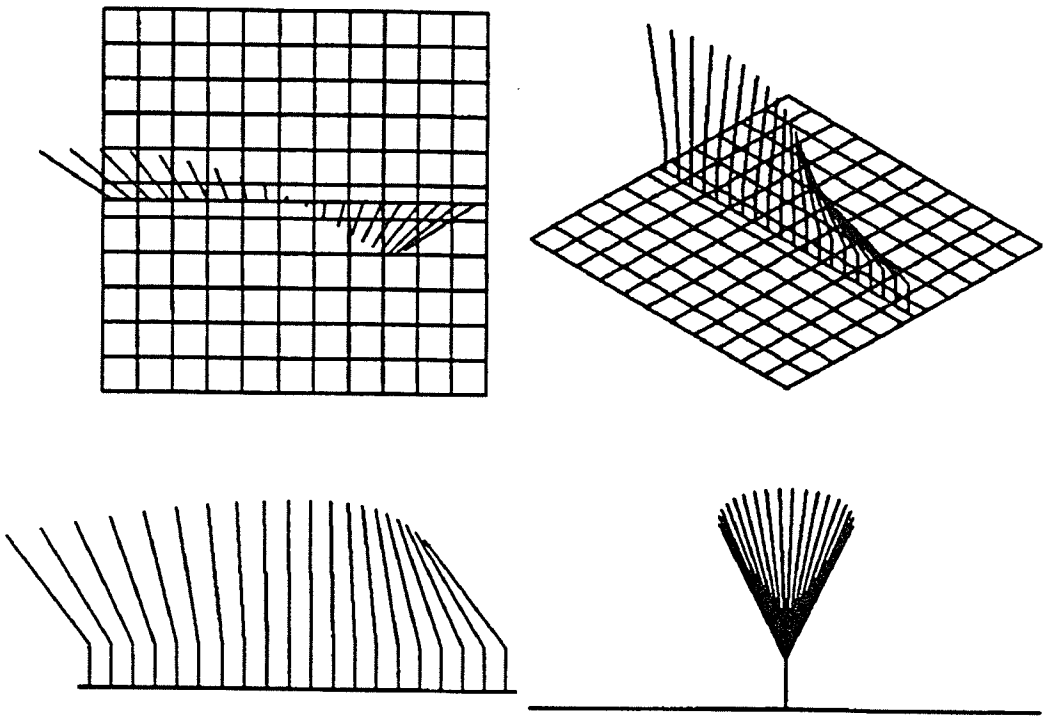

Figure 4.20. 5-axis tool path on plane test surface for ball nose cutter.

Simulations were carried out to verify the tool path generation for 5-axis machining with ball nose cutter. In the simulations, only a single tool path is displayed with the tool shown at several points along the path. The symbol for the tool shows the tool radius from the contact point and the tool axis from the tool center point. In the tests the tool lead angle varied linearly along the tool path from 30° to 150° while the tool tilt angle varied from 45°

to 135°. This can be seen on Figure 4.20, where the test surface was a flat plane, represented in NURBS form. Figures 4.21 and 4.22 show tool path on the blade test surface and on the sphere test surface.

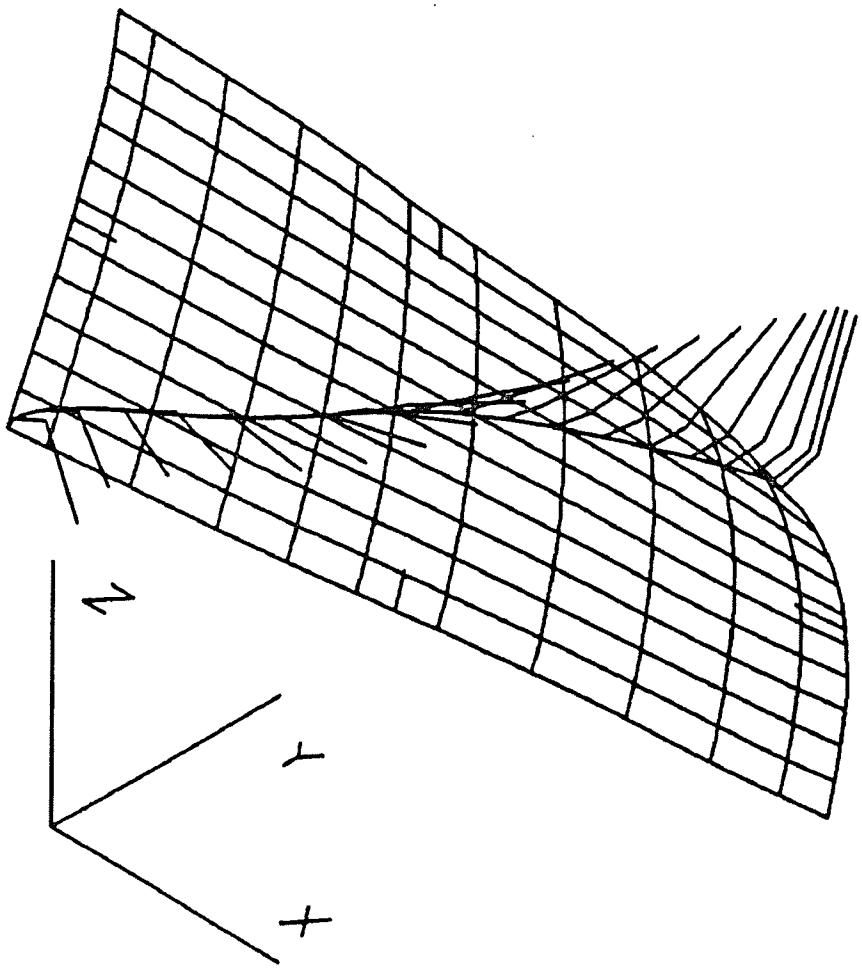

Figure 4.21. 5-axis tool path on blade test surface for ball nose cutter.

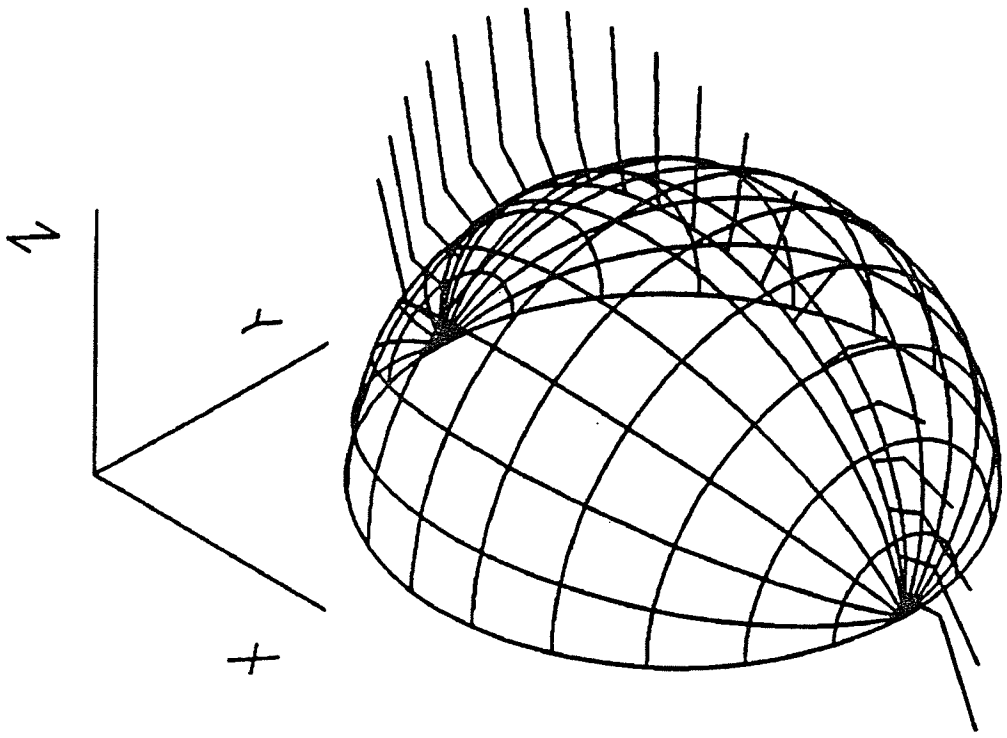

Figure 4.22. 5-axis tool path on sphere test surface for ball nose cutter.

4.3.1.5 3-axis Tool Transformation

The 3-axis tool transformation theoretically is based on equations (4.4), (4.5) and (4.6) as presented in Section 4.1.1. The method defines the tool path on the surface first then offsets the tool path as opposed to generating the tool path on an offset surface. The rationale for this is that the contact point calculation with the speed control is common with 5-axis tool path calculations. This also insures accurate machining speed control.

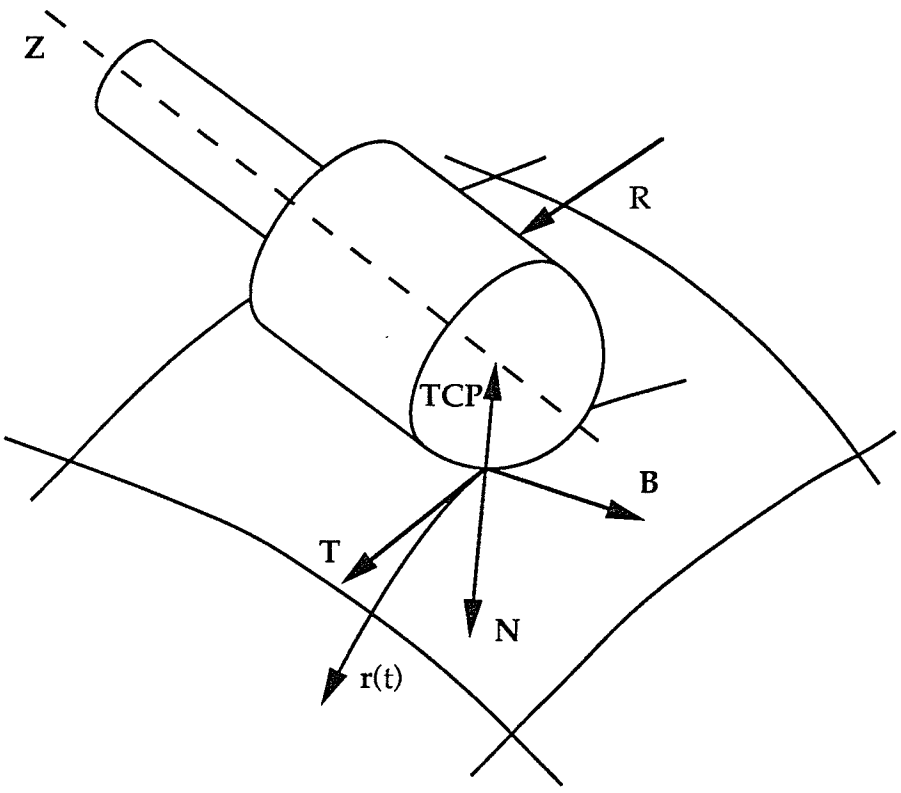

Figure 4.23. 3-axis tool transformation.

The equation for the real time 3-axis tool transformation can be obtained from equation (4.46) of the 5-axis case. The 3-axis machining does not use rotary axes, so the rotational transformations can be left out from the equation. As the tool center point is always on the surface normal, the calculation of the T_{TNB} tool transformation can be simplified. The translational p_o part offset can be lumped into the $T(x,y,z)$ general translational offset:

$$TCP_m = T(x,y,z)\ TCP_l \tag{4.56}$$

The TCP_l expression can be calculated by equations (4.4), (4.5) and (4.6). This has to be accomplished at every sampling period. Figure 4.23 shows the different vectors for 3-axis machining.

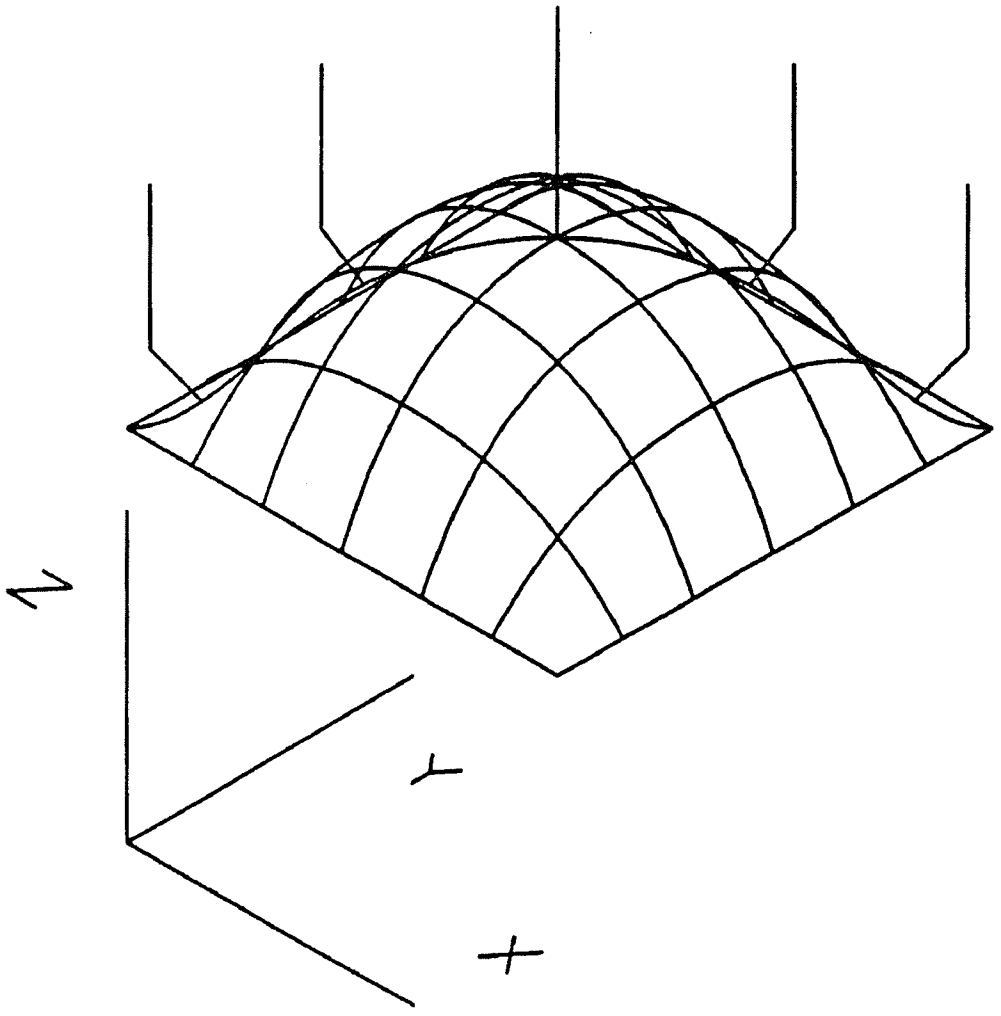

Figure 4.24. 3-axis tool path on Hermite surface patch.

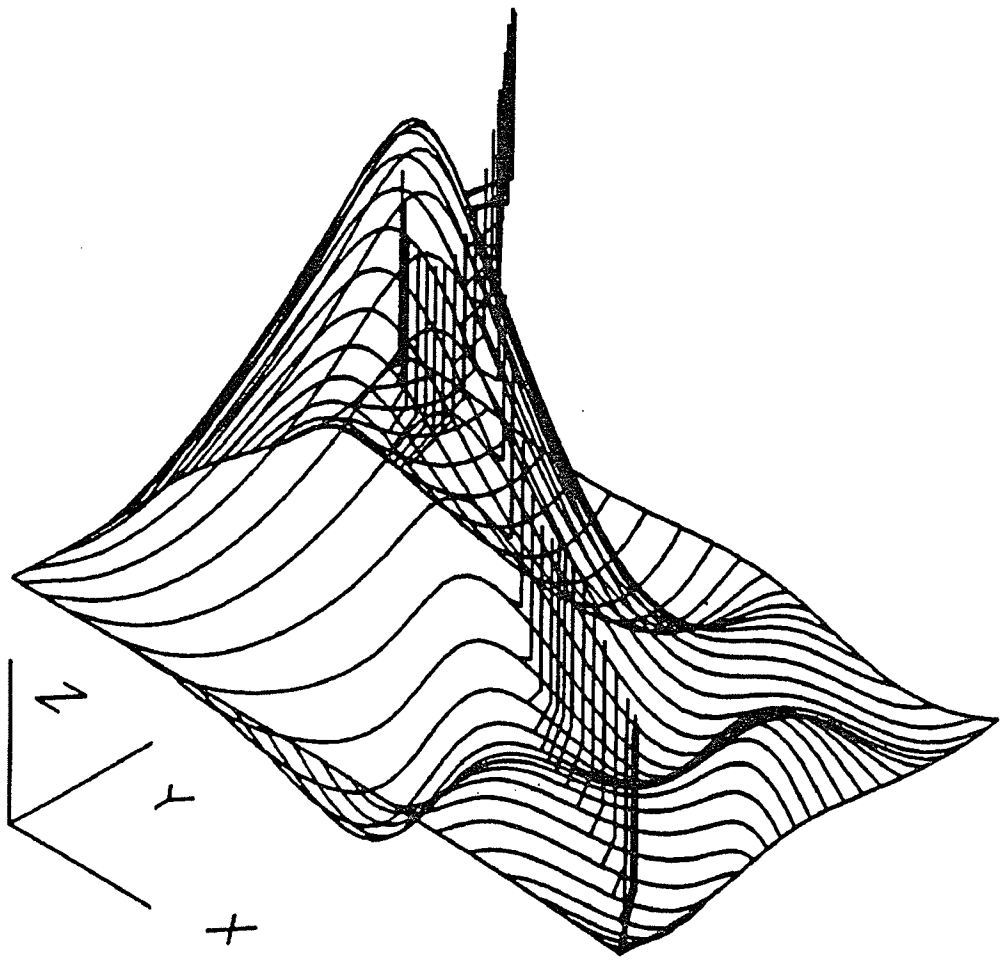

Figure 4.25. 3-axis tool path on 3D NURBS patch.

Using the above described calculations for 3-axis tool transformations, it only allows for translational part offset. The orientation of the part has to be accurately set up. In practice, general part placement is required similarly to the 5-axis case. This, again, can be introduced by the general $\mathbf{T}_p$ part transformation. With this, the final transformation can be described as follows:

$$TCP_m = T(x,y,z)\ T_p\ TCP_l \tag{4.57}$$

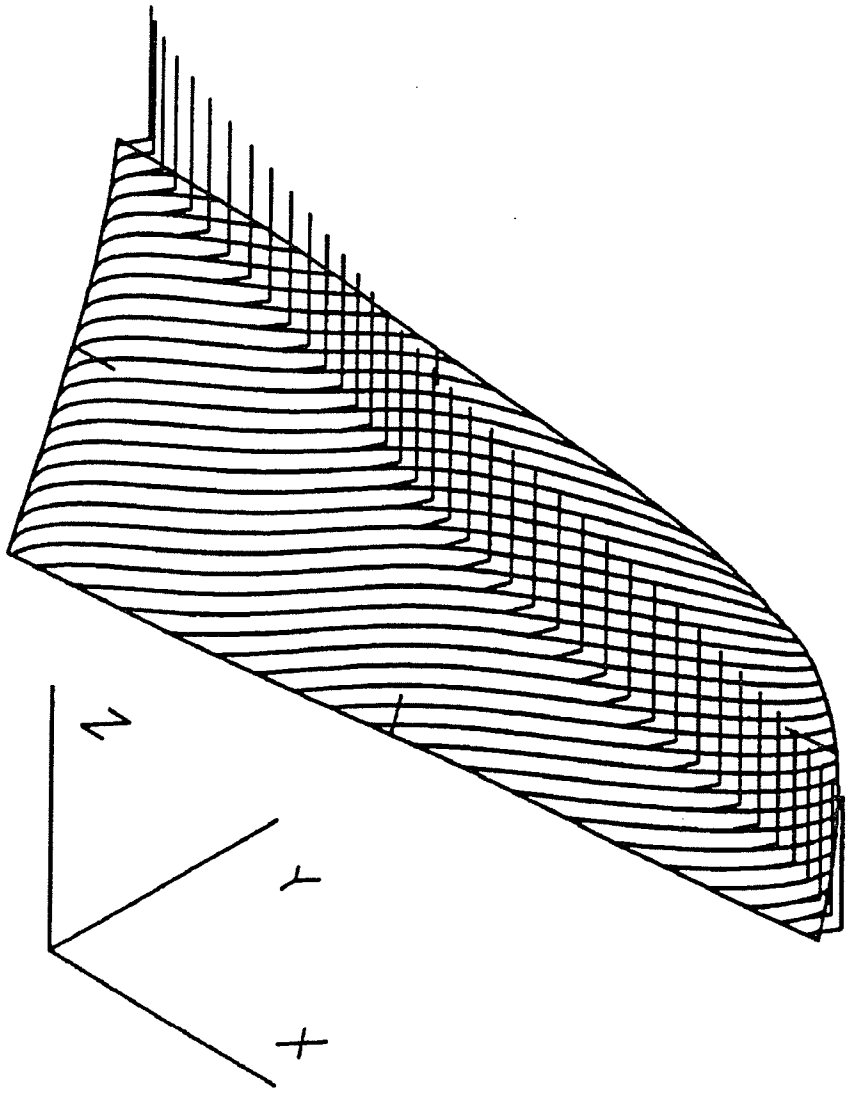

Figure 4.26. 3-axis tool path on turbine blade test surface.

The T_p part transformation matrix is defined similarly to the 5-axis case. The T_p part transformation matrix has to evaluated once before machining, while the rotational and translational part transformations have to be accomplished at every sampling period.

The same test surfaces were used for the 3-axis tool path simulation as for the 5-axis one. The only difference for the simulations was in the tool transformation, where the appropriate calculations for the 3-axis mode were carried out. The results are in Figures 4.24, 4.25, 4.26 and 4.27.

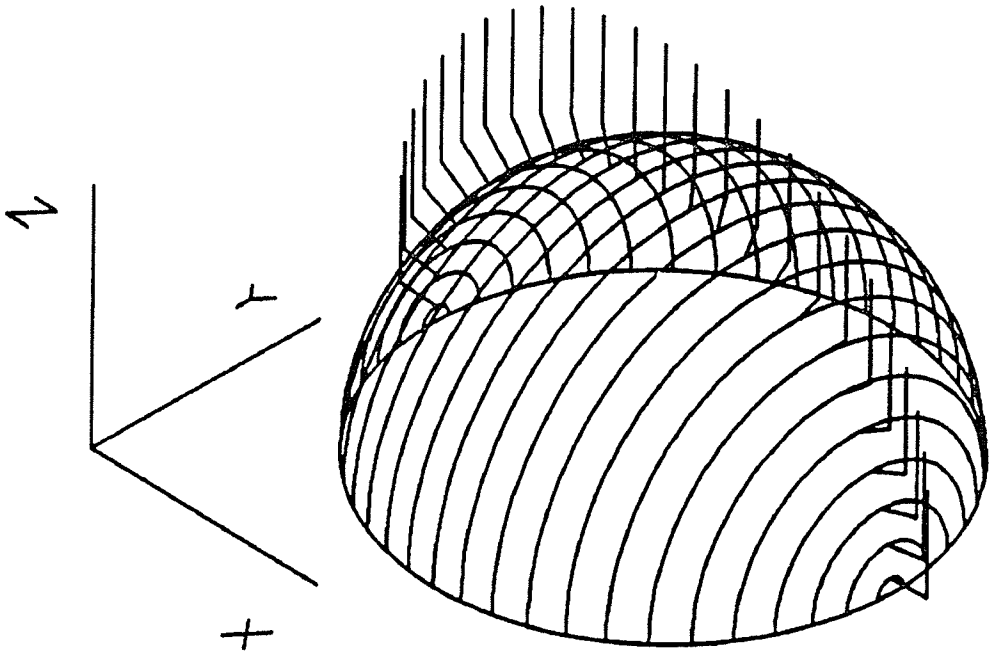

Figure 4.27. 3-axis tool path on sphere test surface.

4.3.2 Computational Considerations

As it can be seen from previous chapters, the calculation of axis coordinates to control a machine tool for sculptured surface machining is mathematically quite involved. In this section some metrics are put to the calculations to indicate the computational resources necessary to solve the problem in real-time.

The analysis is broken down into groups of functions which can be considered as the building blocks of the path generator. The values given reflect the required primitive operations to accomplish the tasks. The primitive mathematical operations - though some of them are not primitive at all - are grouped and referred to as shown below:

- **A/S** additions/subtractions
- **M/D** multiplications/divisions/square roots
- **TRIG** trigonometric functions

The values reached are based on the equations presented in this thesis which are not optimized for fast computation. Nonetheless, these values are meaningful and give good indication and guidance where optimization efforts should be concentrated for implementation purposes and where the biggest gain could be achieved.

Other functions that are not used in the advanced path generator and only solve the problem in a specialized case are included in this analysis as well. This inclusion gives a good indication about the computational price to be paid to solve the problem in the most general way.

In the tables below, 3-rd degree functions were used to get the computational efforts. This was chosen since most CAD design systems use 3-rd degree functions to represent the free form curves and surfaces.

The computational efforts for the required basic functions are given in Table 4.7. These include simple vector operations and the evaluation of B-spline basis functions.

Table 4.7. Computations for basic vector and B functions.

Function	A/S	M/D	TRIG	Other	Equations
vector unitization	2	7	0	N/A	N/A
vector cross product	3	6	0	N/A	N/A
general transformation 3X3 matrix mult.	6	9	0	N/A	N/A
rotation about a main axis	2	4	2	N/A	(4.26), (4.27)
3-rd degree B-spline basis function (B)	35	14	0	N/A	(3.33)
derivative of 3-rd degree B-spline basis function (DB)	9	7	0	N/A	(3.35)

Tables 4.8 and 4.9 contain the necessary computations for evaluating B-spline and NURBS curves and surfaces and their derivatives. The B-spline entities are included as well, as many CAD systems - even though they use the NURBS format to store the geometric entities - only generate a subclass of the NURBS objects, the B-spline entities. This fact is usually also recorded in the internal data base of the CAD system with a flag, so simpler calculations can be carried out.

Table 4.8. Computations for 3-rd degree curve functions.

Function	A/S	M/D	TRIG	Other	Equations
3-rd degree B-spline curve	9	12	0	4 B values	(3.32)
derivative of 3-rd degree B-spline curve	9	12	0	4 DB values	(3.34)
3-rd degree NURBS curve	12	31	0	4 B values	(3.40)
derivative of 3-rd degree NURBS curve	16	25	0	4 B values 4 DB values	(3.42) (3.43)

Table 4.9. Computations for 3-rd degree surface functions.

Function	A/S	M/D	TRIG	Other	Equations
3-rd degree B-spline surface	45	96	N/A	8 B values	(3.61)
partial derivative of 3-rd degree B-spline surface	48	96	N/A	4 B values 4 DB values	(3.62) (3.63)
3-rd degree NURBS surface	60	179	N/A	8 B values	(4.37)
partial derivative of 3-rd degree NURBS surface	123	314	N/A	8 B values 8 DB values	N/A

Table 4.10. Computations for the **T**, **N**, **B** vectors, and speed control calculations.

Function	A/S	M/D	TRIG	Other	Equations
T unit vector	5	13	0	2 part. derivs.	(4.19) (4.18)
N unit vector	5	13	0	2 part. derivs.	(4.8)
B unit vector	3	6	0	**T**, **N** vectors	(4.21)
TNB frame, total	13	32	0	2 part. derivs.	
speed control	7	14	0	**T** vector	(4.33) (4.42-46)

Table 4.10 lists the calculations for the **TNB** coordinate system and for the speed control. These results are used both at 3- and 5-axis tool path generation.

Tables 4.11, 4.12 and 4.13 lists the calculations for the 5- and 3-axis tool transformations respectively. As it can be seen from the tables, for the 5-axis ball nose cutter transformation more calculations are necessary than for the 5-axis tool transformation with end cutters. This is attributed to the fact that the tool orientation is continuously changing during the tool path for a ball nose cutter, while for an end cutter the tool orientation is kept constant.

Table 4.11. Computations for 5-axis tool transformation.

Function	A/S	M/D	TRIG	Other	Equations
TAX_{pp} calculation	18	18	0	**T N B** vectors	(4.50)
α & β angles	N/A	2	2	N/A	(4.51-52)
TCP_m calculation	7	8	4	N/A	(4.53)
total, 5-ax. tr.	25	28	6	**T N B** vectors	

Table 4.12. Computations for 5-axis tool transformation for ball nose cutter.

Function	A/S	M/D	TRIG	Other	Equations
TCP_l calculation	4	8	4	N/A	(4.23, 4.26-27)
TAX_l calculation	4	8	4	N/A	(4.25-27)
TAX_{pp} calculation	18	18	0	**T N B** vectors	(4.50)
α & β angles	0	2	2	N/A	(4.51-52)
TCP_m calculation	7	8	4	N/A	(4.53)
total, 5-ax. ball tr.	33	44	14	**T N B** vectors	

Table 4.13. Computations for 3-axis tool transformation.

Function	A/S	M/D	TRIG	Other	Equations
TCP_l calculation	3	3	0	**N** unit vector	(3.4)
TCP_m calculation	9	9	0	N/A	(4.57)
total, 3-ax. tr.	12	12	0	**N** unit vector	

Tables 4.14 and 4.15 summarize the calculations necessary for real-time 5- and 3-axis tool path generations on 3-rd degree NURBS surfaces. It can be clearly seen from the tables that the tasks to evaluate the NURBS surface point and the partial derivatives at the contact point need the most effort. These calculations are necessary for both 3- and 5-axis tool path generations.

These tables evidently show that optimization efforts should be concentrated on speeding up the evaluation of the B-spline basis functions, the NURBS surface points, and the partial derivatives.

Table 4.14. Computations for 5-axis tool path generation.

Function	A/S	M/D	TRIG
1 x NURBS surface, with 8 B-values	60 8 x 35	179 8 x 14	0
2 x NURBS partial derivative, with 8 B-values, and with 8 DB-values each	2 x 123 2 x 8 x 35 2 x 8 x 9	2 x 314 2 x 8 x 14 2 x 8 x 7	0
TNB frame	13	32	0
Speed control	7	14	0
5-axis tool transformation for end cutter, or	25	28	6
5-axis tool transformation for ball nose cutter	33	44	14

Table 4.15. Computations for 3-axis tool path generation.

Function	A/S	M/D	TRIG
1 x NURBS surface, with 8 B-values	60 8 x 35	179 8 x 14	0
2 x NURBS partial derivative, with 8 B-values, and with 8 DB-values each	2 x 123 2 x 8 x 35 2 x 8 x 9	2 x 314 2 x 8 x 14 2 x 8 x 7	0
T and N vectors	10	26	0
Speed control	7	14	0
3-axis tool transformation	12	12	0

Table 4.16 gives a comparison of the real-time computational efforts required for the different interpolation methods. This table only shows the calculations necessary to generate the next step along the tool path, i.e. the calculations that has to be carried out during the sampling period. Calculations which are needed to start the tool path generation and should be carried out before the block execution starts are not listed. Those calculations, depending on the implementation method, are not that time critical.

The numbers for the generalized spline interpolation are based on the results given by Huang and Yang [Huang-92a, Huang-92b].

Table 4.16. Computations for different interpolation methods.

Interpolation Method	A/S	M/D	TRIG
3-axis, linear interpolation	3	0	0
5-axis, linear interpolation	5	0	0
Generalized 3-axis 3-rd order spline interpolation	15	5	0
Advanced 3-axis tool path generation	1319	1307	0
Advanced 5-axis tool path generation for end cutter	1335	1329	6
Advanced 5-axis tool path generation for ball nose tool	1343	1345	14

The data for the first three interpolation methods in Table 4.16 are only here for the sake of completeness. The first three interpolation methods merely follow a space curve and do not accomplish any of the tasks associated with post processing. For this reason the data in Table 4.16 should only be considered for reference purposes.

4.4 Initial Implementation

The results of this research are being implemented in a practical application at the Institute for Advanced Manufacturing Technology, National Research Council of Canada. The advanced path generator is being installed in a research open architecture NC controller [Orban-94].

The practical implementation includes the advanced real-time path generator module added to the Cimprovisor Open Architecture NC Controller [Cimprovisor-95] and the NC programming module added to the UNIGRAPHICS CAD/CAM system to provide the new format NC data for the advanced path generator.

At the time of the writing of this chapter (end of April, 1995.) the 3-axis version of the advanced path generator has successfully been tested and several test pieces machined, while the operation of the 5-axis path generator has been tested in the OAC controller.

4.4.1 System Architecture

The practical implementation is based on the Cimprovisor Open Architecture NC Controller (OAC). The Cimprovisor OAC is a distributed system built around the STD32 bus hardware platform [STD-95]. The main components of the controller are the axis control modules, the PLC module, and the supervisory module. See Figure 4.28.

The architecture of the controller has been designed to minimize intertask communication. The central task of interpolation is generally the key to determining the requirements of the central processor. The approach taken is a two stage interpolation strategy, where the central processor generates the motion increments for all axes at a relatively low rate; these increments are then splined at a relatively high rate by each axis slave controller leading to acceptable contouring performance with relatively low computational load at the master. This solution considerably reduces the

need for high bandwidth in the communication between the central processor and axis slaves. The first stage interpolation sampling time is set for 32msec, while the second stage sampling time is 1msec.

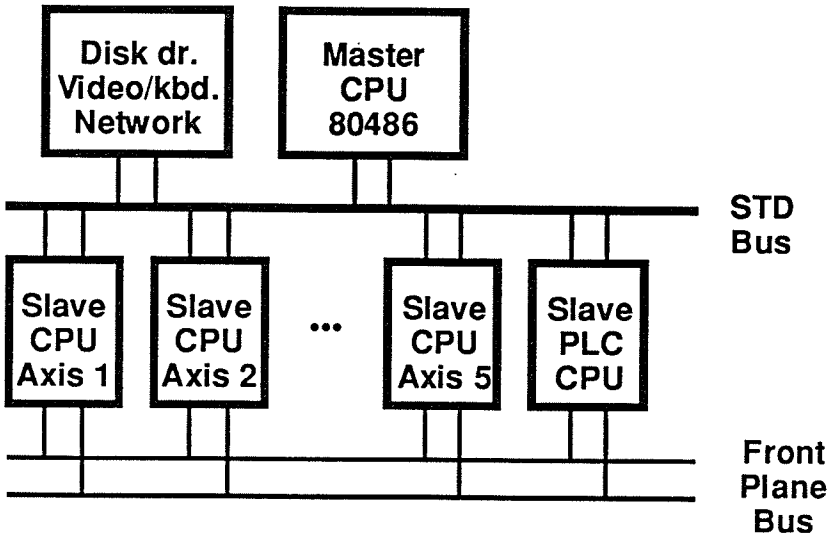

Figure 4.28. OAC system architecture.

The servo functions are realized on single board controllers. The boards read the positional input from the axis encoders and output the analog signal for the servo amplifiers. The compensating lead-lag filter on the axis boards is implemented digitally. The boards also do the low level interpolation. The axes are synchronized to each other by a high-speed front-plane bus.

The PLC or machine I/O module is implemented on another single board controller. This module is also tightly coupled to the axis controllers

through the front-plane bus. The processor interfaces to industry standard I/O modules to handle the discrete signals.

The rest of the CNC functions are provided by the supervisory module. That module is running on an Intel 80486 based system, consisting of several boards on the STD bus, and behaving like a PC clone computer, running the DOS operating system.

The advanced path generator functionality was added to the supervisory module extending the conventional linear and arc interpolation capabilities. For the more complex 5-axis machining a set of points can be calculated in real-time in less than 20msec, well below the allowable 32msec range, when machining 3-rd degree NURBS surfaces. The 486 processor was running at 50MHz speed. Initial optimization efforts have also shown that a speed advantage over a magnitude can be achieved by carefully coding the algorithms. With these optimizations fully implemented the cycle time of the first stage interpolation can be significantly reduced.

In addition to the advanced path generation the input language interpreter has been expanded to allow for the parsing of the special commands describing the machining.

The above functions were coded in the "C" programming language and integrated with the OAC controller.

4.4.2 NC Programming System

For testing the advanced path generator equipped OAC an NC programming system has been developed. The new method of tool path

generation requires the geometry of the part to be available in the controller in addition to the tool path commands.

An interactive extension was added to the UNIGRAPHICS CAD/CAM system to allow for the special programming. The operator can select the surfaces to be machined, the tool type, the machining strategy and the tolerance of the machining, very much like in any other machining system.

The programming system outputs the geometrical information in the NC program as well as the tool path on the surfaces. For the advanced path generator programming the standard G-code language has been extended. At the beginning of the NC program the geometry of the NURBS patches are described. The blocks to characterize the NURBS surfaces uses a format similar to the IGES representation. The advantage of this approach is that the data is in a textual format, and can easily be verified against the standard IGES output of the CAD system. Additional G-codes have been specified to command the various tools on the NURBS surfaces. G13 was specified for 3-axis machining and G15 for 5-axis operations. These special NC blocks also include the identifier for the NURBS surface patch, the tool path in the u,v plane and the tool angles for the 5-axis machining.

The NC programming system extension was implemented in the "C" programming language. The above described system was used to develop the NC programs for machining the test pieces with the advanced path generator equipped OAC.

4.4.3 Initial Results

Several test pieces were machined with the advanced system in 3-axis mode and with the conventional method for comparison purposes. Figure 4.29 shows a close-up of a blade machined with the advanced method, while Figure 4.30 shows the same part produced in the conventional way. Both parts were machined to the same tolerance, to 0.0015" scallop height.

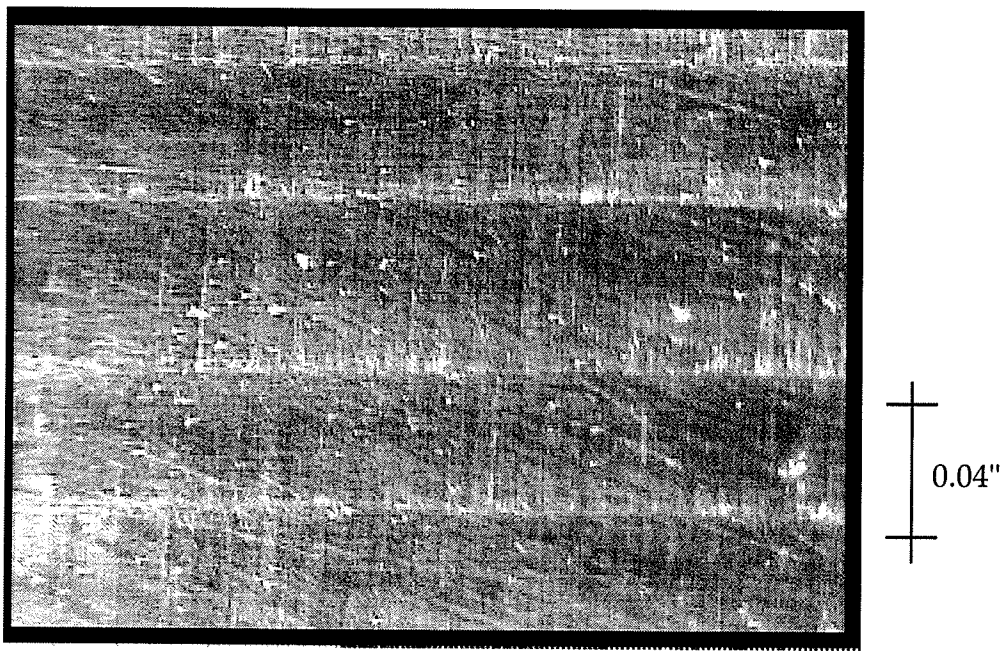

Figure 4.29. Test blade machined with advanced path generator.

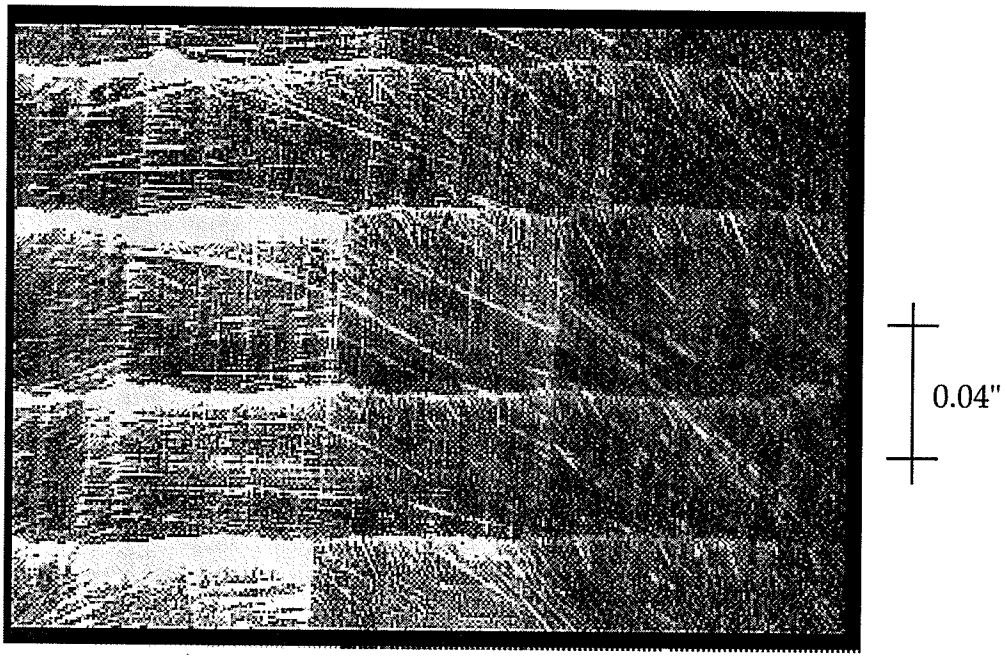

Figure 4.30. Test blade machined with line segments.

The horizontal lines on the pictures are the contours of the scallops, the result of the consecutive tool paths that moved in the horizontal direction. The fine and dense vertical lines are the actual cut marks, made by the cutting edges of the tool as it rotated. In Figure 4.30 the effect of the line segment approximation of the tool path can be clearly seen: the resultant surface is made out of facets as compared to the continuous paths of the advanced path generator in Figure 4.29.

The test conditions of the two machining were as follows:

- Wahli-51 5-axis machine tool

- NRC/UBC open architecture controller
- 6061 - T6 aluminum test piece material
- 3/8" OD HSS ball nose, four flute tool
- 20 ipm feedrate
- 4000 rpm spindle speed
- oil coolant

The comparison of the production of the same part by the two different methods also highlights the advantages of the new path generator.

Producing the NC program for the advanced interpolator was a one step operation: in the programming system the surface was selected, the tool type and nominal tool size, the machining strategy, and the NC tape was produced without any additional steps. For the conventional method the same tool path was output first in an APT format, then it translated into a Cutter Location (CL) file, and then finally postprocessed into the actual NC tape. For the post processing, the actual tool data and part setup data was required.

The comparison of the size NC data files also underlines the advantages of the advanced path generation: the advanced method resulted in a NC file of 7 KByte compared to 90 KByte of just the final tape file. If motions were generated with the same resolution in the conventional method as achieved with the advanced mode, the conventional NC tape file was over 700 KByte in size.

The actual machining also highlighted the advantages of the new method. The tool and part setup data just had to be measured and entered into the controller prior machining, while for the old method, the tool and

part had to be set up to the exact values used for the post processing. With the advanced method, the tool moved smoothly over the surface, while the line segment approximation resulted in a tangentially discontinuous motion over the part.

The surface finish also shows a considerable difference to the advantage of the new method, though no metrics have been put to the texture characterization of the two different machining yet.

The work to test the implementation of the other parts of the advanced path generator is still ongoing.

5 Summary and Conclusion

In this thesis, the state-of-the-art of sculptured surface machining was reviewed, and a new method to generate the trajectories in the NC controllers was developed. Here, the results of the research is summarized, and the possible future work is outlined.

5.1 Solution and Results

In this research, the design and simulation of a new real-time path generator module for a Computer Numerical Controller for machining sculptured surfaces has been carried out. The advanced path generator produces the motion commands directly from the most general surface geometry descriptions for 3- and 5-axis machining performing all the processing and applying all the necessary compensations in real-time.

First, the task distribution in the CAD/CAM process of sculptured surface part production was examined and evaluated. The state-of-the-art in sculptured surface machining was reviewed based on a literature survey and the shortcomings pointed out. The existing mathematical methods for surface description were presented, and the mathematics for 3-axis and 5-axis tool path generation were formulated. For the discussion of the different kinematics, general purpose matrix transformations were applied. Partial results of this work were first presented by the author in the Ph.D. candidacy paper [Orban-92a] and are now an integral parts of this thesis.

The real-time tool path generation for the most general case, for the NURBS surfaces, was developed. The requirements for the advanced path generator were drawn up, and the specification was analyzed against the known deficiencies of existing methods. It was shown that the advanced path generator, according to the given requirements, meets the expectations and corrects the known problems with sculptured surface machining.

The detailed mathematics for the contact point calculation were developed. For demonstration purposes, several test surfaces were evaluated, showing the correctness of the calculations. A speed control algorithm to direct the machining pace on the surface was presented and implemented. Simulations have been carried out to evaluate the applicability of the method and the effect of the granularity of the discretization of the problem, the required frequency of the calculations was analyzed.

Tool transformations for deriving the machine coordinates and for controlling directly the axes of the machine tool for several kind of machining strategies and tool configurations were developed. The methods allow for the run time correction of tool dimensions and part set-up coordinates. Simulations for all the test surfaces and machining methods have been carried out. The simulations proved the correctness of the calculations.

The computational aspects of the advanced path generator were also evaluated and compared. Computational load data for other interpolation methods were also included. The computational analysis also showed the areas where optimization of the algorithms would net the most gain.

The results of this research are being implemented in a practical application at the Institute for Advanced Manufacturing Technology, National Research Council of Canada. The practical implementation addresses all aspects of a production system for sculptured surface parts, including the programming system and the advanced real-time path generator module added to an open architecture NC controller.

The first test results from the implementation support the advantages claimed by the new path generation method: the planning and production is shorter easier and faster, and the parts have better surface finish.

Efforts are ongoing at the National Research Council to fully implement and test the advanced sculptured surface machining system.

5.2 Future Work

Though the foundations of an advanced path generator for sculptured surface machining has been laid down, there is still much work to be done. Most of the issues are related to the practical questions of implementation.

Though the available computing power from various processors is increasing with each newer version, optimizing the algorithms is a worthwhile undertaking. Optimizing would lead to a cheaper implementation with higher performance.

Also, a theoretical analysis on the effect of computational speed on the allowable machining speed is in order. That investigation should give precise answer on the resultant accuracy of the path generator under different

machining speeds for different surfaces. The analysis could be based on Shannon's sampling theorem.

The advanced path generator does not really know how far it is along in its path. The main difficulty is that the resultant parametric tool path curves are not parameterized by arc length but by some arbitrary parameterization method. That means that calculating the full length of the tool path or the partially covered distance could computationally be expensive. The use of that data would be invaluably helpful when calculating acceleration and deceleration strategies at the beginning and at the end of the tool path. Fortunately, sculptured surface machining do not require abrupt changes in direction and speed. Still, the availability of such a feature would make the advanced path generator more general.

A computer numerical control with the advanced path generator is part of a bigger system intended for producing parts with sculptured surfaces in an easier way. This thesis did not address the detailed issues relating to the other parts of the whole system. In the general paradigm of "design, plan, and machine" of the whole system, an advanced CNC would have the most effect on the planning stage. Beyond the fact that the functionality of the planning stage could be expanded with the integration of new features, the information to be passed to an advanced controller is different than existing standards allow for. As increased activity in the field of the development of computer numerical controllers, among others, points towards expanding the path generation capabilities of the controllers, defining and standardizing a new interface would be best accomplished within the mandate of international standard committees.

6 Appendix

6.1 Hermite Test Surface in IGES Format

```
                                                                        S      1
1H,,1H;,16H[.ugii]_herm.prt,18H[.ugii]ig_herm.igs,38HUnigraphics II on VG      1
AX/VMS Version  9.1,24HUGII/IGES Version 9.1.10,32,38,16,38,16,16H[.ugiiG      2
]_herm.prt,1.0,1,4HINCH,3,0.0D0,13H941208.080102,0.1D-7,,,,9,0,13H941204G      3
.114200;                                                                G      4
     114       1              1       1       0       0                1D      1
     114       2       3     145       0                               0D      2
114,3,0,3,3,0.0D0,0.351365697925731,0.648634302074269,1.0,0.0D0,       1P      1
0.351365697925731,0.648634302074269,1.0,0.0D0,2.70575788526025,        1P      2
-0.215964112321689,1.75089817706016,0.0D0,-0.99692252114471,           1P      3
4.85865367944203,-4.75290837113924,0.0D0,-4.52420077465957,            1P      4
22.0493340864176,-26.1075240607776,0.0D0,10.4755497921357,             1P      5
-51.0540972453288,60.4506598490845,0.0D0,0.0D0,0.0D0,0.0D0,            1P      6
2.70575788526025,-0.996931903973763,-4.52414609351699,                 1P      7
10.4754701678066,-0.215964112321689,4.85869515026799,                  1P      8
22.0490954273257,-51.0537539233677,1.75089817706016,                   1P      9
-5.75295039841009,-26.1072877414593,60.4503276933719,0.0D0,            1P     10
0.0D0,0.0D0,0.0D0,0.0D0,20.6835311859804,-18.4626583406141,            1P     11
-6.32059069913263,0.0D0,-18.4626840382772,-3.06064116990341,           1P     12
31.2769329505353,0.0D0,-6.32051756261644,31.2767248012577,             1P     13
-25.213752969196,0.0D0,2.25134274525291,1.99869531249866,              1P     14
-0.871374969730778,0.0D0,-0.296353766304929,1.44432519732889,          1P     15
-1.710159041283,0.0D0,0.996922252114471,-4.85865367944203,             1P     16
5.75290837113924,0.0D0,0.0D0,0.0D0,0.0D0,1.0,0.0D0,0.0D0,0.0D0,       1P     17
3.20247951600471,0.286684995465247,1.30099638358064,                   1P     18
-3.01240245660061,1.62965256761721,-2.89319145847637,                  1P     19
-13.1295034062585,30.4008134181778,-3.65472515400678,                  1P     20
6.48838888040509,29.4447585405465,-68.1781010931275,0.0D0,             1P     21
4.71394321183199,-5.50825651553381,0.546800517329448,0.0D0,            1P     22
5.36827086333734,-9.02939503994007,6.32018457685367,0.0D0,             1P     23
-18.0586539863959,30.374533044964,-21.2608546232337,0.0D0,0.0D0,       1P     24
0.0D0,0.0D0,0.0D0,2.25134274525291,1.99869531249866,                   1P     25
-0.871374969730778,0.0D0,0.296353766304929,-1.44432519732889,          1P     26
1.710159041283,0.0D0,6.51804581694899,-31.7666414453017,               1P     27
37.6133408030561,0.0D0,-10.4755497921357,51.0540972453288,             1P     28
-60.4506598490845,2.0,0.0D0,0.0D0,0.0D0,3.20247951600471,              1P     29
0.286684995465247,1.30099638358064,-3.01240245660062,                  1P     30
-1.62965256761721,1.20547314534044,5.47052070735146,                   1P     31
-12.6667608160946,1.75089817706016,-5.75295039841009,                  1P     32
-26.1072877414593,60.4503276933719,0.0D0,4.71394321183199,             1P     33
-5.50825651553381,0.546800517329448,0.0D0,-5.36827086333734,           1P     34
9.02939503994007,-6.32018457685367,0.0D0,-25.1251232321989,            1P     35
29.9080635459714,4.69918922248971,0.0D0,6.32051756261644,              1P     36
-31.2767248012577,25.213752969196,0.0D0,0.0D0,0.0D0,0.0D0,0.0D0,0.0D0, 1P     37
0.0D0,0.0D0,0.0D0,0.0D0,0.0D0,0.0D0,0.0D0,0.0D0,0.0D0,0.0D0,0.0D0,     1P     38
0.0D0,0.0D0,0.0D0,0.0D0,0.0D0,0.0D0,0.0D0,0.0D0,0.0D0,0.0D0,0.0D0,     1P     39
0.0D0,0.0D0,0.0D0,0.0D0,0.0D0,0.0D0,0.0D0,0.0D0,0.0D0,0.0D0,0.0D0,     1P     40
0.0D0,0.0D0,0.0D0,0.0D0,0.0D0,0.0D0,0.0D0,0.0D0,0.0D0,0.0D0,0.0D0,     1P     41
```

```
0.0D0,0.0D0,0.0D0,1.0,3.20247951600471,1.62965256761721,                1P     42
-3.65472515400678,0.0D0,0.28668080123285,-2.89316291841761,             1P     43
6.4883403356741,0.0D0,1.30102188924739,-13.1296706612907,               1P     44
29.4450325518685,0.0D0,-3.01244107369836,30.4010582598097,              1P     45
-68.1784877307286,0.0D0,0.0D0,0.0D0,0.0D0,2.25134274525291,             1P     46
-0.296354213724648,0.996898746305045,0.850407402996218D-4,              1P     47
1.99869531249866,1.44432611229536,-4.85853355234857,                    1P     48
-0.414456835659264D-3,-0.871374969730778,-1.71015802124351,             1P     49
5.75275905945254,0.490735690088151D-3,0.0D0,0.0D0,0.0D0,0.0D0,          1P     50
4.71394321183199,5.36826183406003,-18.0584783440461,                    1P     51
-0.488676606956126D-3,-5.50825651553381,-9.02934364461396,              1P     52
30.373466686282,0.300558752366129D-2,0.546800517329448,                 1P     53
6.32011144033748,-21.2592424170698,-0.459576879125072D-2,1.0,           1P     54
3.3331544415496,0.31089649595761,-0.697229131317353,0.0D0,              1P     55
0.852212016186735D-1,-0.860046502332311,1.92877987482649,0.0D0,         1P     56
-0.28668080123285,2.89316291841761,-6.4883403356741,0.0D0,0.0D0,        1P     57
0.0D0,0.0D0,1.0,0.0D0,0.0D0,0.0D0,3.3331544415496,                      1P     58
0.852217749702788D-1,-0.286675460093553,-0.244555652777494D-4,          1P     59
0.31089649595761,-0.86004818989592,2.89309522861999,                    1P     60
0.246802705732721D-3,-0.697229131317353,1.92877906354388,               1P     61
-6.48817307141387,-0.553489789567328D-3,1.0,1.04563887674291,           1P     62
-3.51748843352604,0.0D0,1.04563887674291,1.3638607513633,               1P     63
-4.58795102169578,-0.787071440161325D-4,-3.51748843352604,              1P     64
-4.58797441885862,15.4336884476482,0.264767765306304D-3,0.0D0,          1P     65
0.0D0,0.0D0,0.0D0,1.0,3.3331544415496,0.31089649595761,                 1P     66
-0.697229131317353,0.0D0,-0.852212016186735D-1,                         1P     67
0.860046502332311,-1.92877987482649,0.0D0,-1.87438349171309,            1P     68
18.9159964981259,-42.4217132232167,0.0D0,3.01244107369836,              1P     69
-30.4010582598097,68.1784877307286,2.0,0.0D0,0.0D0,0.0D0,               1P     70
3.3331544415496,0.852217749702788D-1,-0.286675460093553,                1P     71
-0.244555652777595D-4,-1.08018148931526,0.358346487797178,              1P     72
-1.20543305342078,-0.102826229075268D-3,-0.871374969730777,             1P     73
-1.71015802124351,5.75275905945254,0.490735690087961D-3,1.0,            1P     74
1.04563887674291,-3.51748843352604,0.0D0,-1.04563887674291,             1P     75
-1.3638607513633,4.58795102169578,0.787071440158676D-4,                 1P     76
-4.93187567934097,-2.36733254300623,7.96416103854389,                   1P     77
-0.183879900286802D-2,-0.546800517329448,-6.32011144033747,             1P     78
21.2592424170698,0.459576879125072D-2,0.0D0,0.0D0,0.0D0,0.0D0,          1P     79
0.0D0,0.0D0,0.0D0,0.0D0,0.0D0,0.0D0,0.0D0,0.0D0,0.0D0,0.0D0,            1P     80
0.0D0,0.0D0,0.0D0,0.0D0,0.0D0,0.0D0,0.0D0,0.0D0,0.0D0,0.0D0,            1P     81
0.0D0,0.0D0,0.0D0,0.0D0,0.0D0,0.0D0,0.0D0,0.0D0,0.0D0,0.0D0,            1P     82
0.0D0,0.0D0,0.0D0,0.0D0,0.0D0,0.0D0,0.0D0,0.0D0,0.0D0,0.0D0,            1P     83
0.0D0,0.0D0,0.0D0,0.0D0,2.0,3.20247951600471,-1.62965256761721,         1P     84
1.75089817706016,0.0D0,0.286684899866612,1.20547464155536,              1P     85
-5.7529538823518,0.0D0,1.3009950919171,5.47050286649699,                1P     86
-26.1072265033314,0.0D0,-3.01239800613529,-12.6667221595878,            1P     87
60.4501816270401,0.0D0,0.0D0,0.0D0,0.0D0,2.25134274525291,              1P     88
0.296361728657768,6.51799954276325,-10.475482588564,                    1P     89
1.99869531249866,-1.44436273727522,-31.7664352436935,                   1P     90
51.0538144587371,-0.871374969730778,1.7102013868807,                    1P     91
37.6131287631942,-60.4503993720439,0.0D0,0.0D0,0.0D0,0.0D0,             1P     92
4.71394321183199,-5.36830501773888,-25.1248237302732,                   1P     93
6.31994181713352,-5.50825651553381,9.02960924424477,                    1P     94
29.9060266715242,-31.2726628198439,0.546800517329448,                   1P     95
-6.32051756209724,4.70256029912596,25.2068559154557,2.0,                1P     96
3.3331544415496,-1.08018148931526,-0.871374969730777,0.0D0,             1P     97
0.85222420013811D-1,0.35834976403162,-1.71017257033763,0.0D0,           1P     98
-0.286684899866612,-1.20547464155536,5.7529538823518,0.0D0,             1P     99
0.0D0,0.0D0,0.0D0,1.0,0.0D0,0.0D0,0.0D0,3.3331544415496,                1P    100
-0.852239360749074D-1,-1.8743633955136,3.01240602806295,                1P    101
```

```
0.31089649595761,0.860069999511182,18.9158562595163,                    1P    102
-30.4008494609581,-0.697229131317353,-1.92882797467444,                 1P    103
-42.4214688792913,68.1781819241331,1.0,-1.04563887674291,               1P    104
-4.93187567934097,-0.546800517329448,1.04563887674291,                  1P    105
-1.36386770660524,-2.36721585904575,-6.32038719030604,                  1P    106
-3.51748843352604,4.58799781602146,7.96322190103506,                    1P    107
21.2615362069918,0.0D0,0.0D0,0.0D0,0.0D0,2.0,3.3331544415496,           1P    108
-1.08018148931526,-0.871374969730777,0.0D0,-0.85222420013811D-1,        1P    109
-0.358349764031619,1.71017257033763,0.0D0,-1.87436489165032,            1P    110
-7.8814521496077,37.613134268035,0.0D0,3.01239800613529,                1P    111
12.6667221595878,-60.4501816270401,2.0,0.0D0,0.0D0,0.0D0,               1P    112
3.3331544415496,-0.852239360749074D-1,-1.8743633955136,                 1P    113
3.01240602806295,-1.08018148931526,-0.358355574409451,                  1P    114
-7.88145447345688,12.666775837005,-0.871374969730777,                   1P    115
1.7102013868807,37.6131287631942,-60.4503993720439,1.0,                 1P    116
-1.04563887674291,-4.93187567934097,-0.546800517329448,                 1P    117
-1.04563887674291,1.36386770660524,2.36721585904575,                    1P    118
6.32038719030604,-4.93187567934097,2.36717005087035,                    1P    119
34.8629818161449,-4.70218925610165,-0.546800517329448,                  1P    120
6.32051756209724,-4.70256029912594,-25.2068559154557,0.0D0,             1P    121
0.0D0,0.0D0,0.0D0,0.0D0,0.0D0,0.0D0,0.0D0,0.0D0,0.0D0,0.0D0,            1P    122
0.0D0,0.0D0,0.0D0,0.0D0,0.0D0,0.0D0,0.0D0,0.0D0,0.0D0,0.0D0,            1P    123
0.0D0,0.0D0,0.0D0,0.0D0,0.0D0,0.0D0,0.0D0,0.0D0,0.0D0,0.0D0,            1P    124
0.0D0,0.0D0,0.0D0,0.0D0,0.0D0,0.0D0,0.0D0,0.0D0,0.0D0,0.0D0,            1P    125
0.0D0,0.0D0,0.0D0,0.0D0,0.0D0,0.0D0,0.0D0,0.0D0,0.0D0,0.0D0,            1P    126
0.0D0,0.0D0,0.0D0,0.0D0,0.0D0,0.0D0,0.0D0,0.0D0,0.0D0,0.0D0,            1P    127
0.0D0,0.0D0,0.0D0,0.0D0,0.0D0,0.0D0,0.0D0,0.0D0,0.0D0,0.0D0,            1P    128
0.0D0,0.0D0,0.0D0,0.0D0,0.0D0,0.0D0,0.0D0,0.0D0,0.0D0,0.0D0,            1P    129
0.0D0,0.0D0,0.0D0,0.0D0,0.0D0,0.0D0,0.0D0,0.0D0,0.0D0,0.0D0,            1P    130
0.0D0,0.0D0,0.0D0,0.0D0,0.0D0,0.0D0,0.0D0,0.0D0,0.0D0,0.0D0,            1P    131
0.0D0,0.0D0,0.0D0,0.0D0,0.0D0,0.0D0,0.0D0,0.0D0,0.0D0,0.0D0,            1P    132
0.0D0,0.0D0,0.0D0,0.0D0,0.0D0,0.0D0,0.0D0,0.0D0,0.0D0,0.0D0,            1P    133
0.0D0,0.0D0,0.0D0,0.0D0,0.0D0,0.0D0,0.0D0,0.0D0,0.0D0,0.0D0,            1P    134
0.0D0,0.0D0,0.0D0,0.0D0,0.0D0,0.0D0,0.0D0,0.0D0,0.0D0,0.0D0,            1P    135
0.0D0,0.0D0,0.0D0,0.0D0,0.0D0,0.0D0,0.0D0,0.0D0,0.0D0,0.0D0,            1P    136
0.0D0,0.0D0,0.0D0,0.0D0,0.0D0,0.0D0,0.0D0,0.0D0,0.0D0,0.0D0,            1P    137
0.0D0,0.0D0,0.0D0,0.0D0,0.0D0,0.0D0,0.0D0,0.0D0,0.0D0,0.0D0,            1P    138
0.0D0,0.0D0,0.0D0,0.0D0,0.0D0,0.0D0,0.0D0,0.0D0,0.0D0,0.0D0,            1P    139
0.0D0,0.0D0,0.0D0,0.0D0,0.0D0,0.0D0,0.0D0,0.0D0,0.0D0,0.0D0,            1P    140
0.0D0,0.0D0,0.0D0,0.0D0,0.0D0,0.0D0,0.0D0,0.0D0,0.0D0,0.0D0,            1P    141
0.0D0,0.0D0,0.0D0,0.0D0,0.0D0,0.0D0,0.0D0,0.0D0,0.0D0,0.0D0,            1P    142
0.0D0,0.0D0,0.0D0,0.0D0,0.0D0,0.0D0,0.0D0,0.0D0,0.0D0,0.0D0,            1P    143
0.0D0,0.0D0,0.0D0,0.0D0,0.0D0,0.0D0,0.0D0,0.0D0,0.0D0,0.0D0,            1P    144
0.0D0,0.0D0,0.0D0,0.0D0,0.0D0,0.0D0,0.0D0,0.0D0,0.0D0,0,0;              1P    145
S      1G      4D      2P    145                                        T     1
```

6.2 3D Test Surface in IGES Format

```
                                                                          S      1
1H,,1H;,20H[.ugii]ig_uvsurf.prt,20H[.ugii]ig_uvsurf.igs,38HUnigraphics IG      1
I on VAX/VMS Version  9.1,24HUGII/IGES Version 9.1.10,32,38,16,38,16,20HG      2
[.ugii]ig_uvsurf.prt,1.0,1,4HINCH,3,0.0D0,13H941207.161844,0.1D-7,,,,9, G      3
0,13H941205.153900;                                                       G      4
     128       1              1       1       0       0                 1D      1
     128       2       3      35       0                                 0D      2
128,6,4,3,3,0,0,1,0,0,0.0D0,0.0D0,0.0D0,0.0D0,0.375,0.5,0.75,             1P      1
1.0,1.0,1.0,1.0,0.0D0,0.0D0,0.0D0,0.0D0,0.5,1.0,1.0,1.0,1.0,1.0,          1P      2
1.0,1.0,1.0,1.0,1.0,1.0,1.0,1.0,1.0,1.0,1.0,1.0,1.0,1.0,1.0,1.0,          1P      3
1.0,1.0,1.0,1.0,1.0,1.0,1.0,1.0,1.0,1.0,1.0,1.0,1.0,1.0,1.0,1.0,          1P      4
1.0,1.0,0.0D0,0.0D0,0.0D0,0.284002813799965,                              1P      5
0.634297933265316D-3,0.0D0,1.23132965009852,                              1P      6
-0.109857904580179D-2,0.0D0,2.28298243642141,                             1P      7
0.204559883219474D-2,0.0D0,3.02908578271175,                              1P      8
-0.18070194829936D-1,0.0D0,4.04182447437845,                              1P      9
-0.746703834691074D-1,0.0D0,4.39842148137213,-0.108842716302616,          1P     10
0.0D0,0.172707106887345,0.711238458991976,0.118630133635135,             1P     11
-0.489138050545686,0.566822871875749,-0.497891837292401,                  1P     12
1.14483062335548,0.576153770406734,-0.849105306613958,                    1P     13
2.83469614257896,0.57256459602715,-2.96602562452424,                      1P     14
2.32320349467459,0.47622140301853,2.5385017594611,                        1P     15
4.45291579091488,0.70662719489664,-1.56572834319441,                      1P     16
4.42779741850303,0.581282412280473,0.0D0,-0.173081737357671,              1P     17
1.36902939152681,0.906230393246451D-2,2.42968081882429,                   1P     18
1.35562701799633,3.97026669293124,1.43935995539205,                       1P     19
1.42880070272356,8.46908343700451,0.814250077065053,                      1P     20
1.44006902152813,6.42063355265923,4.05732490748612,                       1P     21
1.56103637169221,-5.55311590684723,3.22384006940499,                      1P     22
1.24941240589892,3.43306919010027,4.03993040175001,                       1P     23
1.36782307345313,0.0D0,0.172889853549381,2.08263209180487,                1P     24
-0.124670950417501,-0.33573849412141,2.04975267825553,                    1P     25
-1.04909621999561,1.20660734742576,2.14664889488228,                      1P     26
-2.32862706018802,2.66866725768078,2.04303385390994,                      1P     27
-1.7009215211313,2.68826142156704,2.16112071803275,                       1P     28
1.47184641635015,4.08998135113136,2.17350687526282,                       1P     29
-0.910031582169895,4.35986749047387,2.03758989885383,0.0D0,               1P     30
-0.240158078745189D-1,2.72064401031894,0.0D0,0.317377934555666,           1P     31
2.80937857394145,0.0D0,1.15974415505114,2.54691658912529,0.0D0,           1P     32
2.32705963583752,2.74641179779269,0.0D0,2.91387104465967,                 1P     33
2.68812167103678,0.0D0,3.96860250147179,2.37338141532855,0.0D0,           1P     34
4.24642632925842,2.65189527722852,0.0D0,0.0D0,1.0,0.0D0,1.0,0,0;          1P     35
S      1G      4D      2P      35                                         T      1
```

6.3 Blade Test Surface in IGES Format

```
                                                                        S      1
1H,,1H;,19H[.ugii]ig_blade.prt,19H[.ugii]ig_blade.igs,38HUnigraphics II G      1
on VAX/VMS Version  9.1,24HUGII/IGES Version 9.1.10,32,38,16,38,16,19H[.G      2
ugii]ig_blade.prt,1.0,1,4HINCH,3,0.0D0,13H941207.161208,0.1D-7,,,,9,0,  G      3
13H941207.113700;                                                       G      4
     128       1              1      22       0       0                1D      1
     128       2       8     116       0                               0D      2
128,14,6,3,3,0,0,1,0,0,0.0D0,0.0D0,0.0D0,0.0D0,0.9375D-1,               1P      1
0.15625,0.21875,0.3125,0.40625,0.5,0.625,0.6875,0.78125,0.84375,        1P      2
0.90625,1.0,1.0,1.0,1.0,0.0D0,0.0D0,0.0D0,0.0D0,0.25,0.5,0.75,          1P      3
1.0,1.0,1.0,1.0,1.0,1.0,1.0,1.0,1.0,1.0,1.0,1.0,1.0,1.0,1.0,1.0,        1P      4
1.0,1.0,1.0,1.0,1.0,1.0,1.0,1.0,1.0,1.0,1.0,1.0,1.0,1.0,1.0,1.0,        1P      5
1.0,1.0,1.0,1.0,1.0,1.0,1.0,1.0,1.0,1.0,1.0,1.0,1.0,1.0,1.0,1.0,        1P      6
1.0,1.0,1.0,1.0,1.0,1.0,1.0,1.0,1.0,1.0,1.0,1.0,1.0,1.0,1.0,1.0,        1P      7
1.0,1.0,1.0,1.0,1.0,1.0,1.0,1.0,1.0,1.0,1.0,1.0,1.0,1.0,1.0,1.0,        1P      8
1.0,1.0,1.0,1.0,1.0,1.0,1.0,1.0,1.0,1.0,1.0,1.0,1.0,1.0,1.0,1.0,        1P      9
1.0,1.0,1.0,1.0,1.0,1.0,1.0,1.0,1.0,1.0,1.0,1.0,1.0,                    1P     10
0.418188069019652D-1,3.76725974711901,-2.51511603629027,                1P     11
0.130017594608102,3.74869368952597,-2.50362533368646,                   1P     12
0.266845662229056,3.70757475055257,-2.49886252732568,                   1P     13
0.445943054632765,3.63900371663689,-2.50827260160705,                   1P     14
0.616518558402608,3.56259846785185,-2.52900505819829,                   1P     15
0.797161066955647,3.46398402810575,-2.56973469541516,                   1P     16
0.986228561157458,3.34207885016222,-2.63218920876757,                   1P     17
1.17946140042196,3.19497963248133,-2.71989336476573,                    1P     18
1.33548099953336,3.05101622984928,-2.81742835386661,                    1P     19
1.47812064382957,2.89931123715549,-2.92790506760311,                    1P     20
1.57954298112283,2.77616849672621,-3.02265945658835,                    1P     21
1.67148811919011,2.64766771364519,-3.12644760393265,                    1P     22
1.76403534485835,2.5202973112751,-3.22882393136517,                     1P     23
1.8204111751929,2.42373453770944,-3.31131235340056,                     1P     24
1.85389480690197,2.36830374711901,-3.35826733374999,                    1P     25
0.234358445623199D-1,3.63297913267807,-2.25930154148671,                1P     26
0.974920899558423D-1,3.60633734239613,-2.26137659069018,                1P     27
0.227279154289461,3.5527596735949,-2.27231763343416,                    1P     28
0.401174288409887,3.47383109980948,-2.29455281378779,                   1P     29
0.563321590076871,3.38502601008587,-2.33141710722905,                   1P     30
0.740329255115291,3.27893980629243,-2.38135685823274,                   1P     31
0.924949312307363,3.14831238648672,-2.45463511257124,                   1P     32
1.11540607671777,2.99532954767797,-2.54956128184277,                    1P     33
1.26956655211785,2.84825619297417,-2.65105217273396,                    1P     34
1.40798095169937,2.69404447651541,-2.7656815181246,                     1P     35
1.50299443445062,2.56836026558766,-2.86539741589844,                    1P     36
1.59852189736228,2.44301075432452,-2.96457659164014,                    1P     37
1.68494152814145,2.31409691009631,-3.07075641832823,                    1P     38
1.73985191295839,2.21792850583408,-3.15334466178199,                    1P     39
1.77272284513368,2.16762539925036,-3.1950775339296,                     1P     40
-0.938428949581235D-1,2.9585965792217,-1.34311743775978,                1P     41
-0.343036651383323D-1,2.9192228725561,-1.36382926365921,                1P     42
0.719080236623461D-1,2.84862118592393,-1.40116215803433,                1P     43
0.214689556399316,2.74545618384102,-1.46010427185199,                   1P     44
0.349771754391448,2.63787946332978,-1.52644784560004,                   1P     45
0.507053743765367,2.5141324298216,-1.60209381479566,                    1P     46
0.661417565586987,2.36634730958082,-1.70426775322678,                   1P     47
```

```
0.828978289213767,2.19991547516099,-1.82155370934364,          1P     48
0.965011940315457,2.0446161201959,-1.93817839127642,           1P     49
1.09601638672877,1.88738904432181,-2.05862582236925,           1P     50
1.19283013461008,1.76521107226188,-2.15398630238257,           1P     51
1.27824964384081,1.63806487586633,-2.25864485178129,           1P     52
1.36174485819206,1.51205800379126,-2.36277530622967,           1P     53
1.41962653995512,1.41988930151655,-2.44007071297652,           1P     54
1.445230772201,1.36711945565222,-2.48698912363171,             1P     55
-0.610258147166563,1.20167170204078,0.534630096253539,         1P     56
-0.556389223748864,1.15416710421002,0.503289401879968,         1P     57
-0.467871006006337,1.06950345352256,0.444785955610447,         1P     58
-0.346296029299051,0.949142922962826,0.360107579817608,        1P     59
-0.223893465995403,0.827158320788715,0.273999211994434,        1P     60
-0.905253917574674D-1,0.684520141817307,0.16986131142798,      1P     61
0.617646470128883D-1,0.52291900209315,0.523000783691784D-1,    1P     62
0.220611796364613,0.340100749690535,-0.854470123892881D-1,     1P     63
0.357568070122476,0.174355458049145,-0.212825086943227,        1P     64
0.477979775930547,0.550772727965377D-2,-0.349343183210266,     1P     65
0.565507668613055,-0.127590132834151,-0.459568999152715,       1P     66
0.651707797284154,-0.258854772487225,-0.568319826634518,       1P     67
0.731147499823546,-0.3925431788334,-0.682031618494099,         1P     68
0.779296702560457,-0.487947457683276,-0.766199823405542,       1P     69
0.807868625434066,-0.547092220898124,-0.818830617909144,       1P     70
-0.667218917588078,0.466889731973879,1.46364695953573,         1P     71
-0.628494272182054,0.411064927802571,1.41812704283664,         1P     72
-0.559962610513213,0.319124336902084,1.3448389212446,          1P     73
-0.469822009819282,0.186424977094322,1.23595951048128,         1P     74
-0.378696734945482,0.521310025942336D-1,1.1257368903194,       1P     75
-0.277290317433791,-0.103019108528941,0.997027929543009,       1P     76
-0.174267730976267,-0.280686457012618,0.845007233930394,       1P     77
-0.650865786043987D-1,-0.478964964683846,0.673302484533539,    1P     78
0.250547050683491D-1,-0.658474000399972,0.514774156349771,     1P     79
0.119792629097468,-0.835784528369846,0.360202855553138,        1P     80
0.184556116132722,-0.97361381111349,0.23691017526993,          1P     81
0.251570311304738,-1.1107719234267,0.115125124223754,          1P     82
0.321690623613883,-1.24640015880034,-0.393906903948556D-2,     1P     83
0.365258948185188,-1.3426787474988,-0.906542045924599D-1,      1P     84
0.391662673779175,-1.40137425272959,-0.143575062545209,        1P     85
-1.0991874830869,-0.856426983309293,2.76454870019714,          1P     86
-1.04986618996331,-0.914872730312019,2.71999533455372,         1P     87
-0.982361491103376,-1.00928517705172,2.64372232773955,         1P     88
-0.885773548180398,-1.14517397249032,2.53373948933754,         1P     89
-0.798434775130918,-1.28305474726275,2.41837376242418,         1P     90
-0.708095160612397,-1.44384767049947,2.27976698986085,         1P     91
-0.610960812253862,-1.62605949382317,2.12084434423924,         1P     92
-0.510352725029923,-1.82989872088491,1.9402105250076,          1P     93
-0.421121840249106,-2.01320490820641,1.77733283473477,         1P     94
-0.341055071107416,-2.19681746404908,1.61089018741765,         1P     95
-0.274206389653379,-2.33864407745266,1.48409492526682,         1P     96
-0.208968342315209,-2.47897084866063,1.35832104084416,         1P     97
-0.144380980067372,-2.62033427806899,1.23121756243671,         1P     98
-0.103141564478549,-2.71869824734668,1.14146715309319,         1P     99
-0.761619797140337D-1,-2.78284557959258,1.08296735632434,      1P    100
-1.10001686336495,-0.867405263681746,2.78537950448866,         1P    101
-1.05479649535865,-0.926374817899375,2.73882066141491,         1P    102
-0.98214343135873,-1.02044502055577,2.66473088122018,          1P    103
-0.889042223331096,-1.15693221655032,2.55288059623735,         1P    104
-0.800824625823238,-1.29524227453288,2.43737025708759,         1P    105
-0.706725938825349,-1.45567758487151,2.30047182310275,         1P    106
-0.617284026190307,-1.63904517462812,2.13760361532591,         1P    107
```

```
-0.515128611564438,-1.84291117552015,1.95748846100815,                  1P     108
-0.429146956644075,-2.02681141150121,1.79283191074805,                  1P     109
-0.347272164951031,-2.21022652896358,1.62723791096059,                  1P     110
-0.285866449600993,-2.35238515553148,1.4981661165489,                   1P     111
-0.222892542090029,-2.49330924001404,1.37095819141313,                  1P     112
-0.164361123094227,-2.63478947105805,1.24158972689274,                  1P     113
-0.124128661645351,-2.73361804168755,1.15099052134926,                  1P     114
-0.100043863364951,-2.79626826368175,1.09305518822064,0.0D0,1.0,        1P     115
0.0D0,1.0,0,0;                                                          1P     116
S      1G      4D      2P    116                                        T      1
```

6.4 Sphere Test Surface in IGES Format

```
                                                                        S      1
1H,,1H;,20H[.ugii]ig_sphere.prt,20H[.ugii]ig_sphere.igs,38HUnigraphics IG      1
I on VAX/VMS Version  9.1,24HUGII/IGES Version 9.1.10,32,38,16,38,16,20HG      2
[.ugii]ig_sphere.prt,1.0,1,4HINCH,3,0.0D0,13H941207.161417,0.1D-7,,,,9, G      3
0,13H941204.115100;                                                     G      4
     128       1              1       1       0       0                1D      1
     128       2       7      20      0                                0D      2
128,4,4,2,2,0,0,0,0,0,0.0D0,0.0D0,0.0D0,0.5,0.5,1.0,1.0,1.0,           1P      1
0.0D0,0.0D0,0.0D0,0.5,0.5,1.0,1.0,1.0,0.34314575050762,                1P      2
0.242640687119285,0.34314575050762,0.242640687119285,                  1P      3
0.34314575050762,0.242640687119285,0.17157287525381,                   1P      4
0.242640687119285,0.17157287525381,0.242640687119285,                  1P      5
0.34314575050762,0.242640687119285,0.34314575050762,                   1P      6
0.242640687119285,0.34314575050762,0.242640687119285,                  1P      7
0.17157287525381,0.242640687119285,0.17157287525381,                   1P      8
0.242640687119285,0.34314575050762,0.242640687119285,                  1P      9
0.34314575050762,0.242640687119285,0.34314575050762,2.25,1.25,         1P     10
0.0D0,2.25,2.25,0.0D0,1.25,2.25,0.0D0,0.250000000000003,2.25,          1P     11
0.0D0,0.25,1.25,0.0D0,2.25,1.25,0.0D0,2.25,2.25,                       1P     12
0.999999999999997,1.25,2.25,0.999999999999999,0.250000000000003,       1P     13
2.25,1.0,0.25,1.25,0.0D0,2.25,1.25,0.0D0,2.25,1.25,                    1P     14
0.999999999999999,1.25,1.25,1.0,0.250000000000003,1.25,1.0,0.25,       1P     15
1.25,0.0D0,2.25,1.25,0.0D0,2.25,0.250000000000004,1.0,1.25,            1P     16
0.250000000000003,1.0,0.250000000000003,0.250000000000001,1.0,         1P     17
0.25,1.25,0.0D0,2.25,1.25,0.0D0,2.25,0.250000000000001,0.0D0,          1P     18
1.25,0.25,0.0D0,0.250000000000003,0.249999999999999,0.0D0,0.25,        1P     19
1.25,0.0D0,0.0D0,1.0,0.0D0,1.0,0,0;                                    1P     20
S      1G      4D      2P     20                                       T      1
```

6.5 Plane Test Surface in IGES Format

```
                                                                        S      1
1H,,1H;,16H[.ugii]_flat.prt,18H[.ugii]ig_flat.igs,38HUnigraphics II on VG      1
AX/VMS Version  9.1,24HUGII/IGES Version 9.1.10,32,38,16,38,16,16H[.ugiiG      2
]_flat.prt,1.0,1,4HINCH,3,0.0D0,13H941211.145930,0.1D-7,,,,9,0,13H941209G      3
.163000;                                                                G      4
     128       1              1       1       0       0              1D      1
     128       2       3      7       0                              0D      2
128,3,3,3,3,0,0,1,0,0,0.0D0,0.0D0,0.0D0,0.0D0,1.0,1.0,1.0,1.0,         1P      1
0.0D0,0.0D0,0.0D0,0.0D0,1.0,1.0,1.0,1.0,1.0,1.0,1.0,1.0,1.0,1.0,       1P      2
1.0,1.0,1.0,1.0,1.0,1.0,1.0,1.0,1.0,1.0,0.0D0,0.0D0,0.0D0,1.0,         1P      3
0.0D0,0.0D0,2.0,0.0D0,0.0D0,3.0,0.0D0,0.0D0,0.0D0,1.0,0.0D0,1.0,       1P      4
1.0,0.0D0,2.0,1.0,0.0D0,3.0,1.0,0.0D0,0.0D0,2.0,0.0D0,1.0,2.0,         1P      5
0.0D0,2.0,2.0,0.0D0,3.0,2.0,0.0D0,0.0D0,3.0,0.0D0,1.0,3.0,0.0D0,       1P      6
2.0,3.0,0.0D0,3.0,3.0,0.0D0,0.0D0,1.0,0.0D0,1.0,0,0;                   1P      7
S      1G      4D      2P      7                                       T      1
```

7 Glossary

APT - Automatically Programmed Tool, a computerized programming language/system to produce NC tapes for numerically controlled machine tools.

CAD - Computer Aided Design, a computer assisted method to design parts geometry interactively at a computer graphics workstation.

CAE - Computer Aided Engineering, a suite of computerized engineering tools, that help a designer to create an "optimal" part according to various requirements.

CAM - Computer Aided Machining, a computer assisted method to produce parts on numerically controlled machine tools.

IGES - Initial Graphics Exchange Specification, an international standard format to move geometric information between different CAD systems.

NC, CNC - Numerical Control, Computer Numerical Control, a machine tool controller, which allows for the description of machine tool actions/operations in a standard, machine tool oriented programming language.

OAC - Open Architecture computer numerical Control, a CNC that is modular, the module interfaces well defined and accessible to the user allowing for the extension and modification of the controller features.

2D machining - 2-axis machining, machining operations, where tool movement is described only in two axis. Examples are lathe machines, sheet metal operations.

3D machining - 3-axis machining, machining operations where tool axis movement is described along three axis. Example: milling operations.

5D machining - 5-axis machining, machining operations where tool axis movement is described along five axis. The extra two axis of freedom allows for ideal placement of the tool to the part, and better access for machining. Example: sculptured surface milling operations.

8 References

Allen-Bradley-91. *Series 9/240 CNC Computer Numerical Control,* Allen-Bradley, 1991.

APT-77. *American National Standard Programming Language APT* ANSI, 1977.

Barnes-91. J. Barnes, "Breaking into the Black Box." *Canadian Machinery and Metalworking,* February, 1991, pp. 23-26.

Bartels-87. R.H. Bartels, J.C. Beatty, and B.A. Barsky, *An Introduction to Splines for Use in Computer Graphics and Geometric Modeling* Morgan Kaufmann Publishers, Inc., 1987.

Bedi-92. S. Bedi and N. Quan, "Spline Interpolation Technique for NC Machines." *Computers in Industry,* Vol. 18, 1992, pp. 307-313.

Bergren-71. C. Bergren, "A Simple Algorithm for Circular Interpolation." *Control Engineering,* September, 1971, pp. 57-59.

Bézier-86. P. Bézier, *The Mathematical Bases of the UNISURF CAD System* Butterworths, 1986.

Boor-78. C. de Boor, *A Practical Guide to Splines* Springer-Verlag, 1978.

Bourne-92. D.A. Bourne, "Intelligent Manufacturing Workstations." In *Intelligent Control Systems - Winter Annual Meeting of the ASME,* 1992, pp. 77-84.

Böhm-84. W. Böhm, G. Farin, and J. Kahmann, "A Survey of Curve and Surface Methods in CAGD." *Computer Aided Geometric Design,* Vol. 1, 1984, pp. 1-60.

Bresenham-65. J.E. Bresenham, "Algorithm for Computer Control of a Digital Plotter." *IBM Systems Journal*, Vol. 4, 1965, pp. 25-30.

Briere-92. K. Briere, "InCAD/CAM, The Future Is NURBS." *Modern Machine Shop*, June, 1992, pp. 79 - 84.

Broomhead-86. P. Broomhead and M. Edkins, "Generating NC Data at the Machine Tool for the Manufacture of Free-Form Surfaces." *International Journal on Production Research*, Vol. 24, No. 1, 1986, pp. 1-14.

Chen-87. Y.J. Chen and B. Ravani, "Offset Surface Creation and Contouring in Computer-Aided Design." *Transactions of the ASME, Journal of Mechanisms, Transmissions, and Automation in Design*, Vol. 109, March, 1987, pp. 133-142.

Chen-93. Y.D. Chen, J. Ni, and S.M. Wu, "Real-time CNC Tool Path Generation for Machining IGES Surfaces." *Transactions of the ASME*, Vol. 115, November, 1993, pp. 480-486.

Chikurov-84. N.G. Chikurov, "Interpolation Algorithms for NC Microprocessor Devices." *Soviet Engineering Research*, Vol. 4, No. 6, 1984, pp. 64-65.

Chiyokura-88. H. Chiyokura, *Solid Modeling with DESIGNBASE* Addison-Weslwy Publishing Company, 1988.

Chungwatana-92. W. Chungwatana, A.C. Lin, and W.F. Lu, "Automatic Generation of Machining Data for NURBS-Based Sculptured Surfaces." In *Proceedings of the 1992 Japan - USA Symposium on Flexible Automation*, ASME, 1992, pp. 401-408.

Cimprovisor-95. *An Open Architecture Controller*, Technical Reference Manual, Document Number: 007-1000-101, Cimprovisor Hightech Industries Ltd., 1995.

Coons-64. S. Coons, "Surfaces for Computer Aided Design." Tech. Dept. M.I.T., 1964.

Danielsson-70. P.E. Danielsson, "Incremental Curve Generation." *IEEE Transactions on Computers*, Vol. C-19, 1970, pp. 783-793.

Daratech-89. *CAD/CAM/CAE systems*, Daratech CAD/CAM, CAE industry update, March 1989, .

Dean-88. S.K. Dean and R.J.F. Dow, "A Versatile Controller for 3-D Machining." *IEEE Transactions on Industrial Electronics*, Vol. 35, No. 3, August, 1988, pp. 381-386.

Duncan-83. J.P. Duncan and S.G. Mair, *Sculptured Surfaces in Engineering and Medicine* Cambridge University Press, 1983.

Edwall-82. C.W. Edwall, C.Y. Ho, and H.J. Pottinger, "Trajectory Generation and Control of a Robot Arm Using Spline Functions." In *ROBOTS VI Conference Proceedings*, Society of Manufacturing Engineers, 1982, pp. 421-444.

Eisenhart-09. L.P. Eisenhart, *A Treatise on the Differential Geometry of Curves and Surfaces* Ginn and Company, 1909.

Enlin-82. L. Enlin, "The Principles of Interpolation for Higher Order Curves." *Scientia Sinica*, Vol. XXV, No. 2, February, 1982, pp. 212-224.

EUCLID-83a. M. Engeli, "EUKLID/OZELOT - An Integrated System for Design and Milling of Complex Surfaces." In *Autofact Europe, Conference Proceedings*, CASA of SME, 1983, pp. 1-87 - 1-99.

EUCLID-83b. E. Matthias and P. Szivér, "CAD and CAM of Special Forms with the System EUCLID-OZELOT." *Reprint from Präzisions-Fertigungstechnik aus der Schweiz*, June, 1983, pp. 4, In German.

EUCLID-86. *Der direkte Weg zur komplexen dreidimensionalen Werkstückform*, Fides Trust Company Sales Brossure, 1986, In German.

Farin-93. G. Farin, *Curves and Surfaces for Computer Aided Design: a Practical Guide,* 3-rd. ed., Academic Press, Inc., 1993.

Farouki-86. R.T. Farouki, "The Approximation of Non-Degenerate Offset Surfaces." *Computer Aided Geometric Design,* Vol. 3, 1986, pp. 15-43.

Faux-79. I.D. Faux and M.J. Pratt, *Computational Geometry for Design and Manufacture* Ellis Horwood Ltd., 1979.

Gaal-81. B. Gaal, L. Monostori, and T. Varady, "A Prototype System for Computer Aided Design and Manufacturing of Sculptured Surfaces." In *CAD in Medium Sized and Small Industries,* North-Holland Publishing Company, 1981, pp. 319-329.

Giessen-86a. J.H. Giessen, "Development of Contour Surface Milling in the Machining of Presstools." *Precision Toolmaker,* July, 1986, pp. 118-122.

Giessen-86b. J.H. Giessen, "Development of Contour Surface Milling in the Machining of Presstools." *Precision Toolmaker,* September, 1986, pp. 184-186, 190.

Giessen-86c. J.H. Giessen, "Development of Contour Surface Milling in the Machining of Presstools." *Precision Toolmaker,* December, 1986, pp. 264-266.

Goldman-87. R.N. Goldman, "The Role of Surfaces in Solid Modeling." In *Geometric Modeling: Algorithms and New Trends,* Society for Industrial and Applied Mathematics, SIAM, 1987, pp. 69-90.

Greene-82. A.M. Greene, "Is it Time for a New Approach to NC Programming." *Iron Age,* 1982, pp. 83-84,89.

Grossman-86. D.D. Grossman, "Opportunities for Research on Numerical Control Machining." *Communications of the ACM,* Vol. 29, No. 6, June, 1986, pp. 515-522.

Haapaniemi-86. A. Haapaniemi, H. Nagase, M. Fujimoto, H. Hiraoka, F. Kimura, and T.T. Sata, "Development of a Real Time Numerical Controller for Machining Sculptured Surfaces." In *Software for Discrete Manufacturing*, J.P. Crestin and J.F. McWaters, IFIP, Elsevier Science Publishers B.V. (North Holland), 1986, pp. 205-214.

Heidenhain-91. *TNC 407, TNC 415 Powerful Controls for Milling Machines and Machining Centers*, Dr. Johannes Heidenhain GmbH, May, 1991.

Hermann-84a. G. Hermann, "Patch Programming: The Integration of Motion Planning into Numerical Control." *Computers in Industry*, Vol. 5, 1984, pp. 351-359.

Hermann-84b. G. Hermann, "Free-Form Shapes: An Integrated CAD/CAM System." *Computers in Industry*, Vol. 5, 1984, pp. 205-210.

Hermann-88. G. Hermann, "Algorithms for Real-Time Tool Path Generation." In *Geometric Modeling for CAD Applications*, North-Holland, 1988, pp. 295-305.

Huang-92a. J.T. Huang and D.C.H. Yang, "A Generalized Interpolator for Command Generation of Parametric Curves in Computer-Controlled Machines." In *Proceedings of the 1992 Japan - USA Symposium on Flexible Automation*, ASME.

Huang-92b. J.T. Huang and D.C.H. Yang, "Precision Command Generation for Computer Controlled Machines." *Precision Machining: Technology and Machine Development and Improvement*, Vol. 58, 1992, pp. 89-104.

ICAM-88. *CAM-APT-SURF Reference Manual*, ICAM Technologies Co., 1988.

IGES-86. *Initial Graphics Exchange Specification (IGES), Version 3.0.* National Bureau of Standards, 1986.

ISO-91. "Numerical Control of Machines - NC Processor Output - File Structure and Language Format." Tech. Dept. ISO 3592-199X(E) ISO TC 184/SC 1/ WG 4, 1991.

Khalil-87. A. Khalil and A. Powell, "5-axis Model Making Saves Time and Money." *Production Engineer*, February, 1987, pp. 15-16.

Kim-88. K. Kim and J.E. Biegel, "An Integrated Approach to Sculptured Surface Design and Manufacture." *Computers in Industrial Engineering*, Vol. 14, No. 3, 1988, pp. 271-280.

Kim-91. D.I. Kim, J.I. Song, and S. Kim, "Design of Digital Signal Processor System for CNC Systems." In *1991 International Conference on Industrial Electronics, Control and Instrumentation*, 1991, pp. 1861-1866.

Kimura-83. F. Kimura, "Design Methods of Free-Form Surfaces and their Integration into the Solid Modeling Package GEOMAP-III." In *Solid Modeling by Computers*, General Motors Research Laboratories, Plenum Press, 1983, pp. 211-236.

Kiritsis-94. D. Kiritsis, "High Precision Interpolation Algorithm for 3D Parametric Curve Generation." *Computer-Aided Design*, Vol. 26, No. 11, 1994, pp. 850-856.

Klein-84. *Solid Modeling in Computer Graphics: Technology, Application, Supply Sources*, Special Report from the S. Klein Newsletter on Computer Graphics, 1984.

Kochan-83. D. Kochan, S. Gumberidse, B. Burkhardt, and K. Zehe, "Technological and Computational Aspects of CAD/CAM System for Sculptured Surfaces." In *Advances in CAD/CAM*, North-Holland Publishing Company, 1983, pp. 289-301.

Krouse-83. J.K. Krouse, "Those Elusive Sculptured Surfaces." *Computer Aided Engineering*, Jan/Feb, 1983, pp. 30-34.

Kwangsoo-88. K. Kwangsoo and J.E. Biegel, "A Path Generation Method for Sculptured Surface Manufacture." *Computers in Industrial Engineering*, Vol. 14, No. 2, 1988, pp. 95-101.

Laflamme-85. R. Laflamme and I. Yellowley, "Dynamic Modeling and Interpolation Schemes for an Industrial Robot." In *4th Canadian CAD/CAM & Robotics Conference Proceedings*, The Canadian Institute of Metalworking, 1985, pp. 2.9-2.14.

Lee-91. Y.S. Lee and T.C. Chang, "CASCAM - An Automated System for Sculptured Surface Cavity Machining." *Computers in Industry*, Vol. 16, 1991, pp. 321-342.

Lim-92. F.S. Lim, Y.S. Wong, and M. Rahman, "Circular Interpolators for Numerical Control: A Comparison of the Modified DDA Techniques and an LSI Interpolator." *Computers in Industry*, Vol. 18, 1992, pp. 41-52.

Lin-82. C.S. Lin and P.R. Chang, "Joint Trajectory generation of Mechanical Manipulators Using Spline Functions." Tech. Dept. MS82-503 Society of Manufacturing Engineers, 1982.

Loney-87. G.C. Loney and T.M. Ozsoy, "NC Machining of Free Form Surfaces." *Computer-Aided Design*, Vol. 19, No. 2, 1987, pp. 85-90.

Masory-82. O. Masory and Y. Koren, "Reference-Word Circular Interpolators for CNC Systems." *Transactions of the ASME, Journal of Engineering for Industry*, Vol. 104, November, 1982, pp. 400-405.

Meek-93. D.S. Meek and D.J. Walton, "Approximating Quadratic NURBS Curves by Arc Splines." *Computer-Aided Design*, Vol. 25, No. 6, 1993, pp. 301-306.

Mortenson-85. M.E. Mortenson, *Geometric Modeling* John Wiley & Sons, 1985.

MOSAIC-90. S. Ashley, "A Mosaic for Machine Tools." *Mechanical Engineering*, September, 1990, pp. 38-43.

Noble-84. D.F. Noble, *Forces of Production: a Social History of Industrial Automation* Knopf, 1984.

Ogorek-85. M. Ogorek and M.H. Smith, "CNC Standard Formats." *Manufacturing Engineering*, January, 1985, pp. 43-45.

Okamoto-80. K. Okamoto and M. Isomura, "Application of Microprogramming in Numerical Machine Controllers." *EUROMICRO Journal*, Vol. 6, 1980, pp. 288-295.

Orban-80a. P. Orban and B. Korodi, "System Design and Development of the Executive Algorithm for a Position Parametric Sampled Data Path Calculation Unit ." Tech. Dept. Computer & Automation Institute of the Hungarian Academy of Sciences, 1980.

Orban-80b. P. Orban, L. Nemes, and F. Erdelyi, "Path Calculation and Sampled Data Control for Multi-Axes Machines." In *Proceedings of the Manufacont '80 IFIP/IFAC Conference* , 1980, pp. 13-17.

Orban-86. P. Orban, "Talking to Machine Tools - DNC Coupler Design." In *Proceedings of the Eight Symposium on Engineering Applications of Mechanics*, National Research Council of Canada, 1986, pp. 130-134.

Orban-92a. P. Orban, *Advanced Path Generator for Computer Numerical Control*, Ph.D. candidacy dissertation, University of Manitoba, Department of Electrical and Computer Engineering, 1992.

Orban-92b. P. Orban, "Advanced Path Generator for Sculptured Surface Machining." NRC 33579, 1992.

Orban-94. P. Orban, I. Yellowley, Y. Zhou, "Open Architecture Controllers - a Development Platform for Machine Tool Control Applications." In *Proceedings of the ASPE Spring Topical Meeting on Mechanisms and Controls for Ultraprecision Motion*, April 6-8, 1994, pp. 32-35.

Papaioannou-76. S.G. Papaioannou, "An Interpolation Algorithm for Computer Numerical Control." Tech. Dept. MR76-359 Society of Manufacturing Engineers, 1976.

Papaioannou-85. S.G. Papaioannou and D. Kiritsis, "An Application of Bertrand Curves and Surfaces to CADCAM." *Computer-Aided Design*, Vol. 17, No. 8, October, 1985, pp. 348-352.

Paul-81. R.P. Paul, *Robot Manipulators: Mathematics, Programming, and Control* MIT Press, 1981.

Pavlidis-82. T. Pavlidis, *Algorithms for Graphics and Image Processing* Computer Science Press, 1982.

Piegl-86. L. Piegl, "Curve Fitting Algorithm for Rough Cutting." *Computer-Aided Design*, Vol. 18, 1986, pp. 79-82.

Piegl-91. L. Piegl, "On NURBS: A Survey." *IEEE Computer Graphics & Applications*, Vol. 11, No. 1, January, 1991, pp. 55-71.

Pond-85. J.B. Pond, "Numerical Control: An Important Link to the Factory of the Future." *Iron Age*, May 17, 1985, pp. 32-35.

Pressman-77. R. Pressman and J. Williams, *Numerical Control and Computer-Aided Manufacturing* Wiley, 1977.

Qian-93. S. Qian, "Automatic Feed-rate Control Command Generation - A Step Towards Intelligent CNC." *Computers in Industry*, Vol. 23, 1993, pp. 199-204.

Qin-90. K. Qin and H. Bin, "Three-Point Recursion Interpolation Theory and Algorithm of Space Circular Arcs in a CNC system." *Computers in Industry*, Vol. 15, 1990, pp. 355-362.

Qiulin-87. D. Qiulin and B.J. Davies, *Surface Engineering Geometry for Computer-Aided Design and Manufacture* Ellis Horwood Ltd., 1987.

Ravani-91. B. Ravani and T.S. Ku, "Bertrand Offsets of Ruled and Developable Surfaces." *Computer-Aided Design*, Vol. 23, No. 2, 1991, pp. 145-152.

Renner-78. B. Gaal, G. Hermann, L. Horvath, G. Renner, and T. Varady, *Design and Machining of Sculptured Surfaces* Hungarian Academy of Sciences, 1978, In Hungarian.

Rogers-83. D.F. Rogers, S.G. Satterfield, and F.A. Rodriguez, "Ship Hulls, B-Splines Surfaces, and CAD/CAM." *IEEE Computer Graphics and Applications*, December, 1983, pp. 37-45.

Rogers-90. D.F. Rogers and J.A. Adams, *Mathematical Elements for Computer Graphics*, McGraw-Hill Publishing Company, 1990.

Rolls-Royce-87. C. Milacron, "Five Axes for Rolls-Royce." *Aircraft Engineering*, June, 1987, pp. 18-19.

Rüegg-92. A. Rüegg and P. Gyax, "A Genralized Kinematics Model for Three- to Five-Axis Milling Machines and Their Implementation in a CNC." *Annals of the CIRP*, Vol. 41, No. 1, 1992, pp. 547-550.

Sakamoto-93. S. Sakamoto and I. Inasaki, "Analysis of Generating Motion for Five-Axes Machining Centers." *Transaction of NAMRI/SME*, Vol. XXI, 1993, pp. 287-293.

Sakuta-91. T. Sakuta, K. Watanabe, Y. Asakura, and Y. Tagami, "Development of a High-Speed Die-sinking Method Report No. 3 -Development and Practical Applications of a High-quality CAM System-." *Toyota Technical Review*, Vol. 41, No. 1, Dec, 1991, pp. 87 - 94.

Sarraga-83. R.F. Sarraga and W.C. Waters, "Free-Form Surfaces in GMSOLID: Goals and Issues." In *Solid Modeling by Computers*, General Motors Research Laboratories, Plenum Press, 1983, pp. 187-209.

Sata-81. T. Sata, F. Kimura, N. Okada, and M. Hosaka, "A New Method of NC Interpolation for Machining the Sculptured Surface." In *Annals of the CIRP*, 1981, pp. 369-372.

Schultz-93. D. Schultz, "Why Five-Axis?." *Modern Machine Shop*, 1993, pp. 50-60.

Sharnoa-91. *Sharnoa Tiger CAD/CAM Systems*, Sharnoa Corporation, 1991.

Shpitalni-94. M. Shpitalni, Y. Koren, and C.C. Lo, "Realtime Curve Interpolators." *Computer-Aided Design*, Vol. 26, No. 11, 1994, pp. 832-838.

Siemens-94. *Sinumeric 840 D, SIA 94-MB-002B*, Siemens AG, p. 15, 1994.

Sizer-68. T.R.H. Sizer, *The Digital Differential Analyser* Chapman & Hall, 1968.

Snyder-85. W.E. Snyder, *Industrial Robots: Computer Interfacing and Control* Prentice-Hall, 1985.

STD-95. *The STD 32 Bus Specification: A Brief Overview* STD 32 Technical Data Book, Ziatech Co. 1995, pp. D-11 D-14.

Storr-89. A. Storr and J. Zirbs, "NC-Programming of Complex, Fre-Formed Surfaces." In *Software for Manufacturing*, D. Kochan and G. Olling, IFIP, Elsevier Science Publishers B.V. (North-Holland), 1989, pp. 295-303.

Stripling-81. L.B. Stripling, *Hectran: A Rotor CAD/CAM 5-Axis Numerically Controlled Milling Process*. October 1981, Presented at the Computer-Aided Manufacturing and Productivity International Conference, London, England, 21-22 October 1981.

Strohmer-86. F. Strohmer and S. Winkler, "Rechnerunterstützte Konstruktion und Fertigung von Turbinenschaufeln." *ÖZE*, Vol. 39, No. 5, May, 1986, pp. 76-84, In German.

Su-91. C.J. Su and A. Mukerjee, "Automated Machinability Checking for CAD/CAM." *IEEE Transaction on Robotics and Automation*, Vol. 7, No. 5, 1991, pp. 691-699.

Suzuk-93. H. Suzuk, H. Korcsawa, and M. Sakamoto, "Development of the Real Time CAM System Based on Parallel Processing and the Inverse Offset Method." *Transaction of NAMRI/SME*, Vol. XXI, 1993, pp. 303-309.

Suzuki-86. H. Suzuki, K. Yamazaki, and T. Hoshi, "Real Time Numerical Control System for Sculptured Surface Machining." In *14th North American Manufacturing Research Conference Proceedings*, SME, NAMRI, 1986, pp. 452-458.

Taylor-71. J. Taylor, P. Richards, and H. Halstead, "Computer Routines for Surface Generation and Display." Tech. Dept. No. 16 Marine Sciences Branch, Department of Energy Mines and Resources, 1971.

van den Berg-86. B. van den Berg, "Post Processing in a DNC Environment." In *Proceedings of the Eight Symposium on Engineering Applications of Mechanics*, National Research Council of Canada, 1986, pp. 135-141.

van den Berg-88. B. van den Berg and P. Orban, "Automated Part Set-Up for NC Machining of Sculptured Surfaces." In *Proceedings of the Ninth Symposium on Engineering Applications of Mechanics*, 1988, pp. 558-566.

Varady-82. T. Varady, "An Experimental System for Interactive Design and Manufacture of Sculptured Surfaces." *Computers in Industry*, Vol. 1, No. 2, 1982, pp. 125-136.

Venjara-93. Y. Venjara, "Reducing Setup Time on CNC Machines." Tech. Dept. TE93-150 Society of Manufacturing Engineers, 1993.

Wildish-86. M. Wildish, "Cutting Times Cut by Five Axis Units." *Machinery and Production Engineering*, 19 February, 1986, pp. 22-23.

Willmore-59. T.J. Willmore, *An Introduction to Differential Geometry* Oxford University Press, 1959.

Wilson-87. P.R. Wilson, "Modeling Abstractions." In *Solid Modeling: Breaking Through the Technological Barriers*, CAM-I and CAD/CIM ALERT, 1987, pp. 64-76.

Yang-94. D.C.H. Yang and T. Kong, "Parametric Interpolator Versus Linear Interpolator for Precision CNC Machining." *Computer-Aided Design*, Vol. 26, No. 3, 1994, pp. 225-234.

Yellowley-94. I. Yellowley and P.R. Pottier, "The Integration of Process and Geometry within an Open Architecture Machine Tool Controller." *Int. J. Mach. Tools Manufact.*, Vol. 34, No. 2, 1994, pp. 277-293.

Yeung-94. M.K. Yeung and D.J. Walton, "Curve Fitting with Arc Splines for NC Toolpath Generation." *Computer-Aided Design*, Vol. 26, No. 11, 1994, pp. 845-849.